DETERMINATION OF CELL VIABILITY OF SUPEROXIDE DISMUTASE KNOCKOUT *ESCHERICHIA COLI* STRAINS USING OXIDATIVE STRESS ASSAYS

A thesis presented to the faculty of the Graduate School of Western Carolina University in partial fulfillment of the requirements for the degree of Master of Science in Biology.

By
Christopher Mark Beyer

Director: Dr. Lori Seischab
Assistant Professor of Biology
Biology Department

Committee Members: Dr. Seań O'Connell, Biology
Dr. Jack Summers, Chemistry

March 2012

ACKNOWLEDGEMENTS

I would like to thank Dr. Lori Seischab for her guidance and support during this project. I would also like to thank Dr. Jack Summers and Dr. Seań O'Connell for serving on my thesis committee, and Dr. Sabine Rundle for serving as my thesis reader.

TABLE OF CONTENTS

LIST OF TABLES

LIST OF FIGURES

Appendix A Figures

LIST OF EQUATIONS

ABSTRACT

Cell viability of superoxide dismutase knockout *Escherichia coli* strains using oxidative stress assays was determined for three strains: Periplasmic knockout (AS393), cytoplasmic knockout (PN134), and periplasmic/cytoplasmic knockout (AS391). The cytoplasmic or endogenous superoxide was generated using the redox-cycling agent paraquat, while the periplasmic or exogenous superoxide was generated using the xanthine/xanthine oxidase enzyme. It was hypothesized that exogenous superoxide produced in the xanthine/xanthine oxidase assay would have the largest effect on the periplasmic knockout (AS393) while endogenous superoxide produced in the paraquat assay would effect the growth of the cytoplasmic knockouts (AS391, PN134). Cell growth was determined using optical density for the three knockout strains along with four additional strains: ATCC4157, DH10B, MG1655, and W3110. Using total cell counts obtained with a hemacytometer, the relationship between optical density and cell number was determined for all seven strains. Fluorescence assays using the nucleic acid dyes SYTO9 and PI were used to obtain the percentage of live cells for each strain, which was essential for the xanthine/xanthine oxidase assay. Each strain had a different optimal concentration of nucleic acid dyes necessary to obtain the highest fluorescence intensity. Using fluorescence dyes required the investigation of the inner filter effect. It was determined that inner filter effects are present and need to be accounted for. The paraquat assay inhibited the growth of the three knockout strains with the periplasmic knockout (AS393) being more affected than the others. The total time of aeration altered the effectiveness of paraquat. Specifically, as aeration time increased, growth inhibition increased. The xanthine/xanthine oxidase assay showed little to no effect on the cell viability of the knockout strains. Alteration of pH from

7.5 to 6.5 showed similar results. Other alterations to the xanthine/xanthine oxidase assay obtained similar results as well.

INTRODUCTION

1. Cellular Production of Reactive Oxygen Species

Reactive oxygen species (ROS) are reactive molecules that contain an oxygen atom. They are a natural byproduct of several metabolic processes such as the metabolism of oxygen, which can be used as signaling molecules; however, increased levels of the species lead to cell damage (Miao and St. Clair 2009). Examples of reactive oxygen species produced are peroxides, compounds containing a peroxide anion (O_2^-) such as hydrogen peroxide (O_2^{2-}), hydroxyl radicals (OH·), and superoxides ($O_2^- \cdot$). Hydrogen peroxide can cause damage to cells so it is converted by an enzyme known as catalase to water and oxygen shown in Equation 1:

$$H_2O_2 \rightarrow 2H_2O + O_2 \qquad (1)$$

2. Cellular Damage by Reactive Oxygen Species

The hydroxyl radical ($OH \cdot$) is a powerful oxidant that can damage DNA, proteins, and membranes (Keyer et al. 1995). Superoxide causes cell damage in several different ways. It can cause DNA damage, membrane lipid peroxidation where the radicals take electrons from the lipids in the cell membrane causing damage, and the oxidation of amino acids in proteins. The DNA damage and oxidation of amino acids are caused by the hydroxyl radical. The peroxidation proceeds from a free radical initiated chain oxidation of unsaturated lipids. This consists of three steps. The first is initiation in this step the radical is produced and combines with hydrogen to form water and a radical. The second is propagation in this step the radical reacts with oxygen and creates an acid radical (Figure 1) (Wilhelm 1990). The last step is termination which is when two radicals react to form a non-radical.

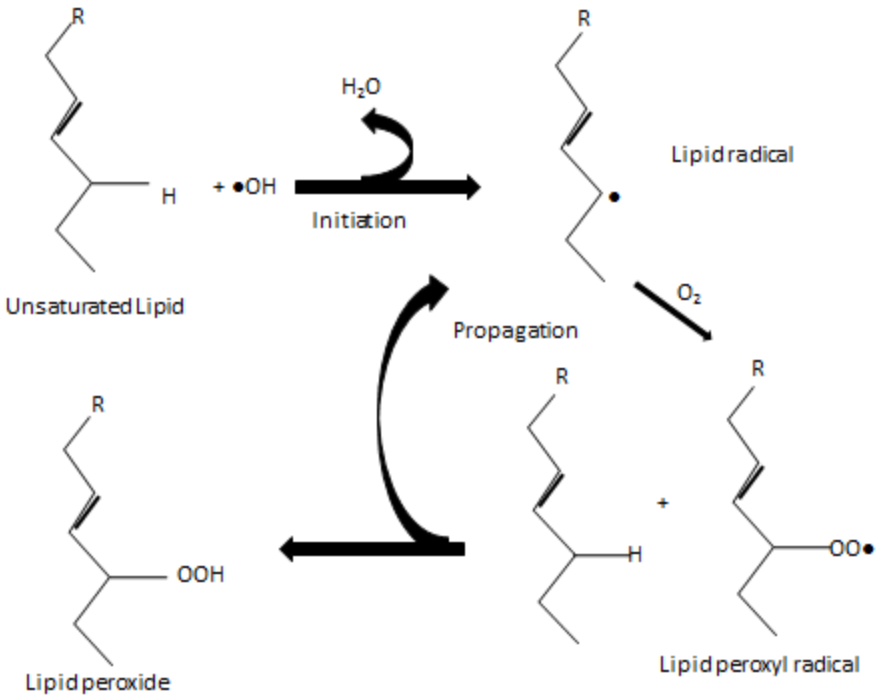

Figure 1. Membrane lipid peroxidation caused by free radicals

An organism reaches oxidative stress when there are more reactive oxygen species than the organism can detoxify. This occurs from either the increased production of oxidizing species or decreased antioxidant defenses. This results in membrane, protein, and nucleic acid damage caused by free radicals and peroxides. The level of damage may increase with different conditions of oxidative stress from physical or chemical interactions (Zaremba and Olinski 2010). Severe imbalances can cause cell death and even moderate stress can lead to programmed cell death, apoptosis (Xie L et al. 2008). Three knockout superoxide dismutase strains were selected because they lack the superoxide dismutase so they cannot combat superoxide with SOD.

3. Superoxide Dismutase

Human phagocytes use superoxide to kill invading microbes. Phagocytes produce superoxide through an oxygen-dependent mechanism (Link and Riley 1988). The injury caused by oxidative stress can cause an increase in superoxide. Aerobic organisms have enzymes such as superoxide dismutase (SOD) to neutralize the toxic superoxide. The superoxide dismutase family of enzymes specializes in eliminating the toxic superoxide anion radicals as by-products of oxygen (Miao and St. Clair 2009). For example, by dismutating the superoxide into oxygen and hydrogen peroxide shown in Equation 2 (McCord and Fridovich 1968).

$$2O_2 \bullet^- + 2H^+ \rightarrow O_2 + H_2O_2 \qquad (2)$$

SOD comes in various classified by the metal cofactor present. Examples are manganese superoxide dismutase (Mn-SOD), and copper-zinc superoxide dismutase (Cu/Zn-SOD), or iron superoxide dismutase (Fe-SOD) (Miao and St. Clair 2009; Fridovich and Yost 1973). *Escherichia coli* contains Mn-SOD, Fe-SOD, and Cu/Zn-SOD (Friodvich, Keele, and McCord 1970; Benov and Fridovich 1994; Fridovich and Yost 1973). Mn-SOD and Fe-SOD also known as the endogenous superoxide dismutases are located within the cytoplasm of the cell. The endogenous superoxide dismutases are expressed during the log phase of *E. coli* growth, and they protect against O_2 formed due to aerobic metabolism. Cu/Zn-SOD, the exogenous superoxide dismutase, is located within the periplasm of the cell. Exogenous superoxide dismutase is expressed during stationary phase of *E. coli* growth and is hypothesized to protect against respiratory bursts from host immune cells and to reduce the reactive oxygen species produced by the host cells to combat the pathogens (Langford 2002).

4. *Escherichia coli* Strains

Escherichia coli was selected as a model system for studying bacterial SOD enzymes. The three *E. coli* strains, DH10B, MG1655, and W3110, were selected because their genomes have been completely sequenced, they have been studied extensively and they are well characterized.

DH10B is typically used for propagation of large insert genomic DNA libraries. The genome is circular with a length of 4,686,137 base pairs. DH10B is largely collinear with the K-12 strain known as MG1655, meaning they are conserved between the two strains. DH10B is more closely related to MG1655 than W3110 because it does not contain W3110's inversion, which is a piece of DNA that has been clipped out and reinserted upside down. It has a 13.5 fold higher mutation rate then MG1655, and has 226 mutated genes relative to MG1655. Which cannot grow on synthetic minimal medium unless leucine is present (Durfee et.al. 2008). MG1655 and W3110 are two closely related K-12 strains of *Escherichia coli*. There are differences between the two at 267 sites, with 251 being short single-nucleotide changes such as insertions or deletions. Thirteen of the sites have insertion sequence elements and 2 sites have W3110 inversions (Koji et.al. 2006). MG1655 is grown on LB medium (Baev et.al. 2006). Both strains require pyrimidine to grow on minimal medium because of the pyrE gene (Jensen 1993).

The three knockout superoxide dismutase strains used in this study, which were selected because they lack superoxide dismutase so they cannot combat superoxide with SOD, were AS391, AS393, and PN134. This is important because superoxide is very toxic to cells; it has been shown to have a 10 fold more sensitive effect on *E. coli* cells lacking cytosolic SOD than wild type cells (Carlioz and Touati 1986). AS393 lacks the periplasmic CuZn superoxide dismutase, which is normally expressed during stationary phase of *E. coli* growth. PN134 is the SOD knockout, which lacks Fe-SOD and Mn-SOD which are normally

expressed during the log phase of *E. coli* growth. AS391 is the triple knockout which lacks CuZn-SOD, Fe-SOD, and Mn-SOD. Since CuZn-SOD is found in the periplasm during stationary phase of *E. coli* growth, we hypothesized that xanthine/xanthine oxidase should have the largest effect on AS391 and AS393, which lack the periplasmic CuZn-SOD. Paraquat is a source for the production of cytoplasmic superoxide, so we hypothesized that the knockouts missing both Fe-SOD and Mn-SOD (AS391 and PN134) would have their growth affected in the presence of paraquat.

5. Determination of Cell Viability

We decided to assess the effects of superoxide-generating agents, such as paraquat, on bacterial cells by measuring their effects on growth rates. Bacterial cultures are grown in a liquid medium and their concentration is determined from their absorbance, measured using a spectrophotometer (Fridovich, Kitzler, and Minakami, 1990). These absorbances are plotted over time to produce a growth curve. This method does not distinguish between live and dead cells for stationary phase but measures only the scattering of light throughout the liquid bacterial sample.

One method to distinguish between live and dead cells is to use a hemacytometer and stain the cells with trypan blue. The hemacytometer is a microscope slide that is covered with a coverslip. Using capillary action two areas of the hemacytometer are filled with a known volume of cells. These two areas can be viewed under a microscope to assess whether the cells are alive or dead. The two areas are divided into 9 squares with grids for an easier ability to count cells. To distinguish whether a cell is alive or dead the stain trypan blue is used because it is membrane impermeable. Cells that have compromised membranes will stain while cells with intact membranes will not. Even though the hemacytometer has a small area, the number of bacterial cells that can fit in the area is extremely large. Cell numbers must be decreased by dilution with phosphate buffer saline (PBS), so they are

within the range of 20 to 100 cells per square. This method has several disadvantages however. Sometime it is hard to distinguish between live and dead cells. Also, while this method is normally fast, each sample must be diluted and then stained for a 5 to 15 minute period which will continuously increase for each additional dilution that is needed do to this staining length of time needed for each dilution.

Fluorescence assays are more rapid techniques that would be amenable to high throughput applications. The live/dead fluorescence assay employs two dyes which bind to DNA. These fluorophores bind to DNA and when bound they exhibit a large increase in fluorescence intensity. The first fluorophore is SYTO9 which has an excitation/emission maxima around 480/500 nm, and will stain all bacteria in a population, both those with intact membranes and damaged membranes. The second fluorophore is propidium iodide (PI), which has an excitation/emission maxima around 490/635. PI cannot pass through the membrane of a healthy cell, so it only stains bacteria with damaged membranes. PI displaces SYTO9 within cells with damaged membranes. In an ideal assay bacteria with intact membranes only containing SYTO9 and bacteria with damaged membranes only containing PI.

The concentrations of these dyes must be optimized for each *E. coli* strain that is used. The SYTO9 dye concentration is optimized 1) to ensure that the amount of dye is enough to stain all of the cells present, 2) to minimize the waste, and 3) to prevent fluorescence quenching at high dye concentrations. The optimization of the second dye, PI, is undertaken by holding the SYTO9 concentration constant and varying the propidium iodide concentrations. When optimized, the assay should have a linear correlation between a fluorescence parameter and the ratio of live/dead cells. Comparing the fluorescence intensities of the unknown samples to a standard curve will give the ratio of live to dead cells. The standard curve is prepared from mixtures with known live/dead ratios and fluorescence

intensities. This assay can be used to determine the viability of *E. coli* after oxidative stress tests.

6. Paraquat Assay for Intracellular Oxidative Stress

A common source for the production of intracellular or cytoplasmic superoxide is the herbicide paraquat. Paraquat, or 1'-dimethyl-4, 4'-bipyridinium dichloride, is highly toxic due to its ability to increase intracellular production of O_2^- (Hassan and Friodvich 1978). Paraquat catalyzes superoxide production by redox cycling, being reduced by Nicotinamide adenine dinucleotide phosphate (reduced) and re-oxidized by oxygen (Bus and Gibson 1984) (Figure 2).

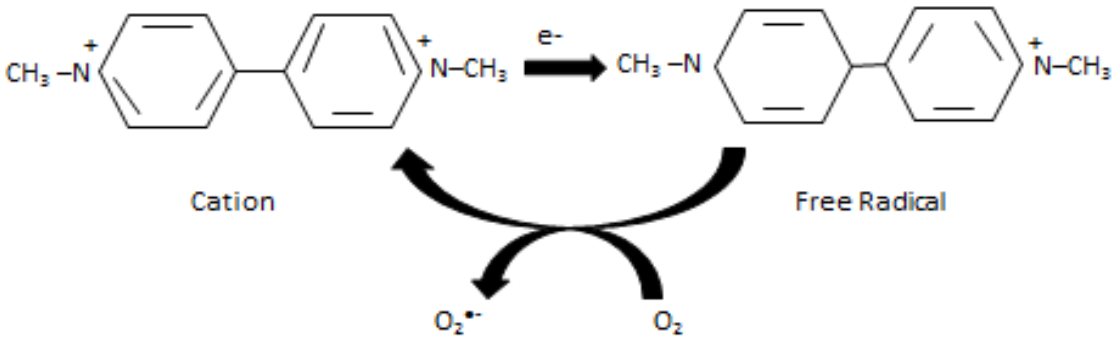

Figure 2. Paraquat reduction-oxidation reaction to produce superoxide (modified from Bus and Gibson 1984)

Paraquat was discovered to be more toxic to *E. coli* in the presence of oxygen than in its absence (Fridovich, Kitzler, and Minakami 1990). Paraquat's toxicity can be increased by preventing the induction of the superoxide dismutase by an inhibitor. Paraquat can be used to explore biological effects of increased intracellular O_2^- in *E. coli*.

7. Xanthine/Xanthine Oxidase Assay for Extracellular Oxidative Stress

The enzyme xanthine oxidase is a good source for periplasmic or extracellular superoxide. Xanthine oxidase consists of 2 flavin molecules which are bound as flavin adenine dinucleotide (FAD), 2 molybdenum atoms contained as a molybdopterin cofactor, and ferredoxin iron-sulfur clusters (Figure 2). In mammals the enzyme exists in another form, xanthine dehydrogenase. The two forms of the enzyme can be converted reversibly by sulfide reagents or irreversibly by proteolysis. Reduction substrates act upon the molybdenum sites and donate electrons to FAD while oxidizing urate and xanthine to form superoxide and hydrogen peroxide (Harrison 2002).

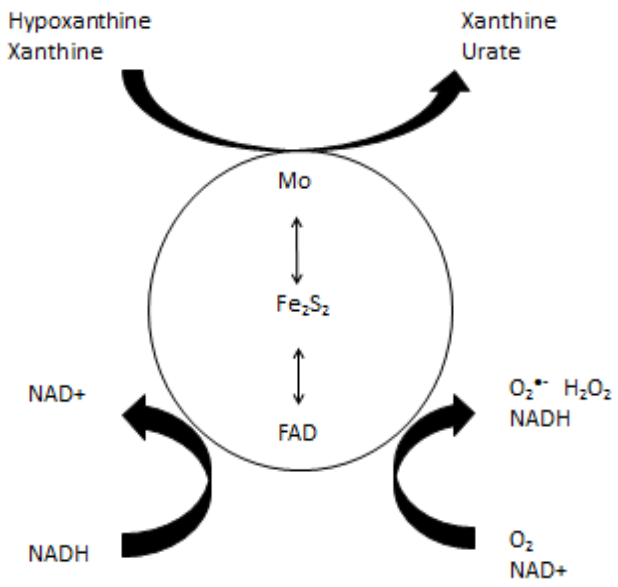

Figure 3. Production of superoxide by xanthine oxidase

8. Inner Filter Effect

Fluorescence assays are an easy and convenient approach to study the changes between different substrates. Fluorescence assays are affected by the inner filter effect. Fluorescence intensity and the concentration of fluorophore form a linear relationship when the absorbance of the fluorophore is low. There are two types of inner filter effects. The first is absorption, in which the fluorophore absorbs the excitation light, thus changing the overall intensity of the excitation light. The excitation intensity will not be constant throughout the solution because the fluorophores around the edge of the solution will absorb some amount of the excitation light. This means that the fluorophores at the center will receive less excitation light. Normally the flurophores at the center of the solution are the ones that will be detected by the fluorescence microplate reader or other spectrophotometer, so this must be accounted for. The second is reabsorption, which occurs when a macromolecule absorbs at the

wavelength which the fluorophore emits. The fluorophore emission will not be detected because it will be reabsorbed by a macromolecule. The fluorescence assay I used relies on the intensity of light emitted by the fluorophore to determine the percentage of live and dead cells, so the inner filter effect must be considered. The inner filter effect will affect the fluorescence emissions when the sum of the absorbance values for the excitation and emission wavelengths exceed 0.08. The inner filter effect is more prevalent when the concentrations of the substrates are increased, more specifically when the substrate concentration values exceed 20 μM (Palmier and Doren 2007). The fluorescence measurements will lose their linearity in these higher concentrations (Palmier and Doren 2007). The inner filter effect must be accounted for in these assays because they assume linearity of the two nucleic acid dyes.

SIGNIFICANCE

The three knockout *E. coli* strains, AS391, AS393, and PN134, were used to determine whether the differences between the strains lead to differences in the various assays and tests. One example of how differences in strains of the same species lead to different results is in the paraquat assay. The toxicity of paraquat is different in different strains. Some strains show a loss of viability when briefly exposed to paraquat, whereas others show no such loss (Fridovich, Kitzler, and Minakami 1990). Other differences when briefly exposed to paraquat include growth inhibition and cyanide-resistant respiration (Fridovich, Kitzler, and Minakami 1990). These differences occurred because the strains have two different retentions for paraquat (Fridovich, Kitzler, and Minakami 1990). Characterizing the various *E. coli* strains would help see the differences between the similar strains.

Various studies have shown that the fluorescence assays can be used for cytotoxicity assays. These tests are rapid methods to assess various things like antibiotic potency (Hoerr et al. 2007). If these can produce results for various strains of *E. coli* then it would save time, be easier to use, and be less expensive than other techniques.

The lethality of the three major classes of bactericidal antibiotics, aminoglycoside, quinolone, and β-lactams is due to the production of superoxide. The antibiotics cause in increase in NADH consumption which in turn causes an increase in the amount of superoxide produced. So superoxide is the key to lethality in bactericidal antibiotics (Kohanski et al. 2007). Most bacterial pathogens are aided by the enzymes known as superoxide dismutases (SOD). We hypothesized that without these enzymes, bacteria become more vulnerable to antibiotics, which increase the bacteria's oxidative stress by increasing reactive oxygen

species. The testing of these various effects could provide valuable information for combating pathogens in the future.

SPECIFIC AIMS

1. Characterization of Growth for the *E. coli* Strains

Growth curves for *E. coli* strains of ATCC4175, DH10B, MG1655, W3110, AS391, AS393, and PN134 were examined using either a UV/Vis microplate reader or Spectronic 20+ spectrophotometer. The effects of paraquat are dependent on growth curves. The differences between the phases of growth assist in determining the effects of paraquat on the *E. coli* strains.

2. Determine Whether use of the Fluorescence Assay was Valid for each *E. coli* Strain

This part of my study was done by using a consistent protocol for all the listed *E. coli* strains. For two nucleic acid dyes SYTO9 and propidium iodide, the optimum concentrations were determined with this protocol and the validity of the fluorescence assay was assessed. The absorbances at the emission and excitation wavelengths using the optimal concentrations of SYTO9 and PI dye were measured using a UV/Vis microplate reader in order to assess whether an inner filter effect was occurring. Cell counts were also gathered using a hemacytometer and compared to cell counts gathered using the fluorescence assay. Both the cell counts and inner filter effect help determine the validity of the assay.

3. Test the Effects of Reactive Oxygen Species on a SOD Knockout *E. coli* Strain

Three strains of *E. coli* were used; one was a strain with the cytoplasmic superoxide dismutase (SOD) gene knocked out, the second was a strain with the periplasmic superoxide dismutase (SOD) gene knocked out, while the third was a double mutant with both the periplasmic and cytoplasmic superoxide dismutase genes knocked out. The paraquat and xanthine/xanthine oxidase assays were used in these comparisons to measure the effects of superoxide endogenously and exogenously. Cells were grown in the presence of paraquat and their growth was monitored using an absorbance of 670 nm. The xanthine/xanthine

oxidase assay treated cells that were harvested and resuspended with a xanthine solution. The fluorescence assay was used at various time points to estimate cell viability.

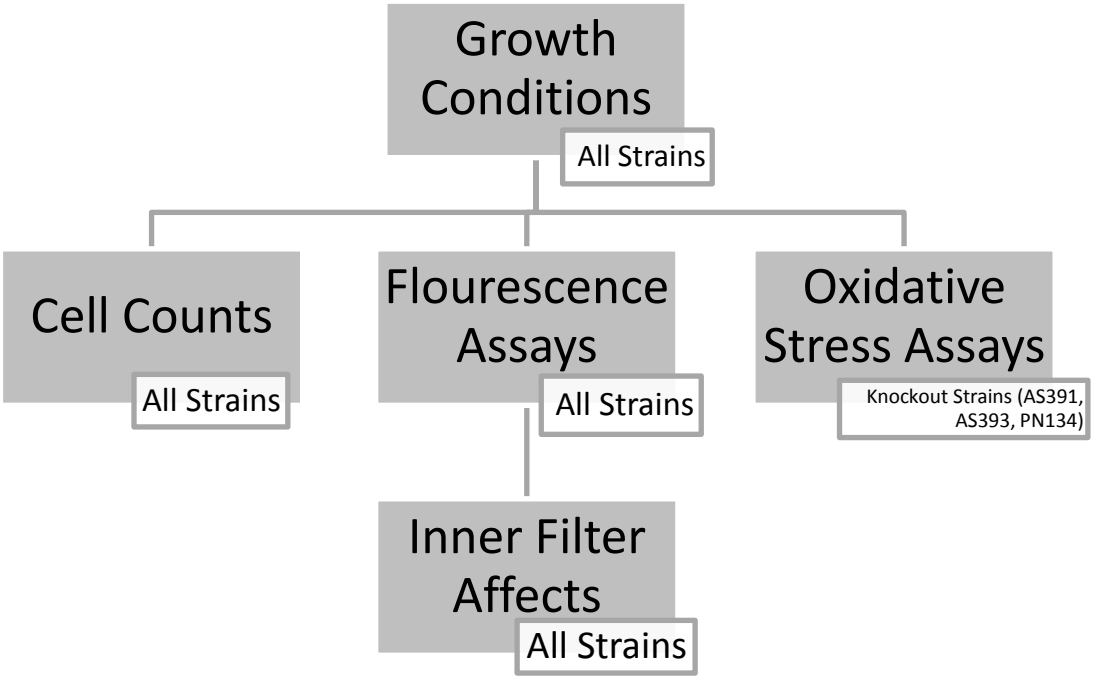

Figure 4. Flow chart for the experiments divided by strains.

MATERIALS AND METHODS

1. Cell Maintenance

The cell lines: DH10B, MG1655, and W3110 were received freeze dried from American Type Culture Collection. These cell lines were rehydrated and grown on LB plates. After the strains recovered from the rehydration process, the cell lines were stored as both glycerol stocks and stab agar tubes. The cell lines: AS391, AS393, and PN134 were received from the lab of James Imlay (University of Illinois at Urbana-Champaign, Department of Microbiology) in stab agar. Cultures from these samples were plated onto LB media agar plates. After the cells were grown, glycerol stocks and stabs were created of these cell lines. Glycerol stocks were prepared by adding 0.15 mL of glycerol to a 2 mL screw-top vial and after autoclaving then 0.85 mL of log-phase *E. coli* were added to the vials. The vials were vortexed and frozen in dry ice at -70°C and stored in a -80°C freezer. Stab cultures were also prepared. 1 mL of stab agar was added to a 2 mL vial and after solidification several single colonies were added to the vial using a straight wire. The vials were incubated for 8 hours at 37°C, then sealed and stored in the dark at 4°C. Before experiments were conducted, bacterial cultures were grown on LB media plates for 32 hours at 37°C. Individual colonies were added to 5 mL of LB media broth in a 15 mL tube that was incubated at 37°C, while shaking at 200 rpm, until log-phase was reached.

2. Growth Curves

Bacterial cultures were grown on LB media plates for 18 hours at 37°C. An individual colony was removed from a plate and added to a 15 mL tube containing 15 mL of LB broth. The tube was incubated at 37°C and shaken at 200 rpm. Measurements were taken every 20 minutes using a Spectronic 20+ spectrophotometer at a wavelength of 670 nm. For the absorbance measurements, 4 mL of the broth was added to a 10 mL tube prior to

each reading. The Spectronic 20+ spectrophotometer was zeroed with LB blanks after every 3 measurements.

3. Hemacytometer Counts

A mixture of 100 µL of the cell culture was combined with 150 µL of phosphate buffered saline (PBS) and 250 µL of trypan blue stain in a 2 mL microcentrifuge tube. The mixture was then incubated for 5-15 minutes at room temperature. A hemacytometer and coverslip were prepared by cleaning them with 70% isopropanol. The chambers of the hemacytometer were then filled by capillary action by placing a pipette tip filled with the solution at the loading grove for the chamber by the rear of the coverslip. The hemacytometer was then placed under a microscope and viewed at 100X magnification, one grid at a time. The microscope was then focused to 400X magnification so a single square could be counted at a time. The four corner squares along with the center were used for a total count of five squares out of the nine on the hemacytometer. Both grids were counted and an average number of cells per square was calculated by dividing the number of cells by the number of squares and then multiplying that by 10^4 and the dilution factor of 5.

4. Fluorescence Assays for Cell Viability

SYTO9 Saturation

The fluorescence assay consists of the two nucleic acid dyes: SYTO9 and propidium iodide. The protocol requires the concentration of SYTO9 to be determined first. Cells were taken at the end of log-phase and it was assumed they were 100% alive. The cells were centrifuged at 4300 rpm for 9 minutes and then were resuspended by gentle inversion using 2 mL of 0.85% NaCl solution (gentle), or by vortexing (rough). The concentrations of the cells were adjusted to an optical density of 0.05 using a 0.85% NaCl solution with a Spectronic 20+ spectrophotometer at a wavelength of 670 nm. Serial dilutions of various SYTO9 dye concentrations were prepared from a stock solution. The wells of a ninety six well plate were

filled with 100 μL of cells and 100 μL of dye. The concentrations of the dye were diluted 2:1 so the correct concentration was contained in the well. Wells were prepared in triplicate for each of the concentrations. The well plate was incubated at room temperature for 15 minutes in the dark before measures were taken in a BMG Labtech FLUOstar fluorescence microplate reader at an excitation wavelength of 485 nm and an emission wavelength of 520 nm. The saturation curve was created using a plot of the dye concentration versus fluorescence.

Propidium Iodide

Cells were taken at the end of log-phase and were split between two 15 mL tubes. Seventy percent ethanol was added to tube and incubated for 30 minutes at 37°C with shaking at 200 rpm. The cells were assumed 100% dead. The other tube was incubated for 30 minutes at 37°C with shaking at 200 rpm. The cells were assumed 100% alive. The cells were then centrifuged at 4300 rpm for 9 minutes and resuspended by gentle inversion using 2mL of 0.85% NaCl solution (gentle), or by vortexing (rough). The concentrations of the cells, 100% live and 100% dead, were adjusted to an optical density of 0.05 using a 0.85% NaCl solution with a Spectronic 20+ spectrophotometer at a wavelength of 670 nm. Different ratios of live to dead cells were created by mixing different proportions of each. These ratios were: 0:100 (100% dead), 10:90 (90% dead), 30:70 (70% dead), 50:50 (50% dead), 70:30 (30% dead), 90:10 (10% dead), and 100:0 (0% dead). One hundred μL of these different ratios were added the 96 well plate wells, with another 100 μL added to the well which was comprised of 50 μL SYTO9 and 50 μL PI for a total of 200 μL in the wells. Wells were prepared in triplicate for each of the concentrations. The SYTO9 concentration used was the appropriate concentration obtained from the SYTO9 saturation curve. Various PI concentrations were created using a 20 mM stock solution. Solutions of SYTO9 and PI dyes were prepared at four times the appropriate concentration values so that when the dyes were transferred to the 96 well plate, the wells in the plate would have the appropriate

concentrations when all substances were added to the wells. The well plate was incubated at room temperature for 15 minutes in the dark before measures were taken in a fluorescence microplate reader with the excitation wavelength set to 485 nm and the emission wavelength set to 520 nm and 612 nm. A plot of SYTO9 fluorescence versus PI fluorescence was created to determine the best PI concentration via linearity.

5. Paraquat Assay

Cultures were prepared by inoculating 3 mL of LB media broth supplemented with 0.2% glucose in a 10 mL tube with a colony from the desired strain. The tubes were next aerated by shaking at 200 rpm for 15 minutes at 37°C. 200 µL aliquots were removed from the 10 mL tubes and added to a 96 well plate in triplicate. These were the untreated samples. Twenty four µL of 100X concentrated paraquat solution (50µM) were added to the 10 mL tubes for a ratio of 100:1 and mixed for one minute. Two hundred µL aliquots were removed from the 10mL tubes treated with paraquat and were added to the 96 well plate in triplicate. These were the treated samples. The 96 well plate was inserted into a Molecular Devices UV/Vis platereader which was read at 670 nm wavelength and at a constant temperature of 37°C. Samples were mixed before each reading.

6. Xanthine/Xanthine Oxidase Assay

Cell Preparation

Two sets of cells were grown. The first was started immediately while the second set was started 1 ½ hours later. When the cells reached stationary phase, they were collected by centrifugation for 5 minutes at 4300 rpm using a Marathon 6K Fisher Science centrifuge. The cells were resuspended in 2 mL of 50 mM of potassium phosphate buffer (PPB) and the optical density adjusted to 0.05 at 670 nm as measured using a Spectrometer 20+. The pH of PPB buffer was adjusted to 6.5 with 1 M HCl or 7.5 with 1 M KOH.

Xanthine and Xanthine Oxidase Preparation

A 0.15 mM xanthine solution was prepared by dissolving the solid in 1 mL 1 M NaOH followed by the addition of sterile H_2O and the pH adjusted to the desired amount with 1 M HCl for a total volume of 100 mL. One hundred μL of xanthine oxidase enzyme solution (XO) with 0.2 units/mL was prepared by diluting the stock xanthine oxidase suspension in cold PPB.

Cell Treatment

A 3 mL reaction mix was prepared for treated and untreated cultures by adding 1.90 of the cell suspension and 1 mL of the xanthine solution in a culture tube. Untreated cultures received 100 μL of sterile H_2O, while treated received 100 μL of XO. The culture tubes were placed in a Nutrator mixer. 100 μL aliquots were removed at 0, 15, 30, 60, and 90 minute intervals for the Live/Dead assay. These cells were harvested by centrifugation followed by resuspension in a 0.85% NaCl solution and the optical density was adjusted to 0.05 at 670 nm.

SYTO9/PI Calibration Curve

Cells from the untreated set were used in the standardization graph for the Live/Dead assay. These cells were centrifuged in an Eppendorf 5415C centrifuge, resuspended in 2 mL

of 50 mM of potassium phosphate buffer (PPB) and the optical density adjusted to 0.05 at 670 nm with a Spectrometer 20+. Different ratios of live to dead cells were created as described on page 16.

Fluorescence Measurements

One hundred μL of the aliquots from the treated cell set and 100 μL of the different ratios from untreated set were added to the 96 well plate wells, with the other 100 μL comprised of 50 μL SYTO9 and 50 μL PI at their appropriate concentrations for a total of 200 μL in the wells. Wells were prepared in triplicate for each aliquot. The 96 well plate was incubated at room temperature for 15 minutes in the dark before measurements were taken in a fluorescence microplate reader with the excitation wavelength set to 485 nm and the emission wavelength set to 520 nm and 612 nm.

7. Inner Filter Effect

For each *E. coli* strain, the optimal concentrations of PI and SYTO9 had already been determined. These concentrations of dye were pipetted into wells of a clear 96 well plate. The well plate was incubated the in the dark, at room temperature, for 15 minutes. Absorbance measurements were obtained using a UV/Vis microplate reader at the dyes' excitation wavelength (485 nm) and emission wavelengths (520 nm and 612 nm).

RESULTS

1. Optical Density Measurements using a Spectrophotometer

Determination of Growth Curves using Cell Density as a Measurement of Growth

ATCC4157, DH10B, MG1655, W3110, AS391, AS393, and PN134 exhibited similar growth patterns. When grown under the same conditions, the strains ATCC4157, AS391, AS393, and PN134 entered stationary phase at approximately 6 hours of growth (Figure 5 & 6), while the strains DH10B, MG1655, and W3110 entered stationary phase at 7 to 9 hours of growth (Figure 7). Once the growth characteristics were determined for each strain, repeatable results could be obtained for each experiment.

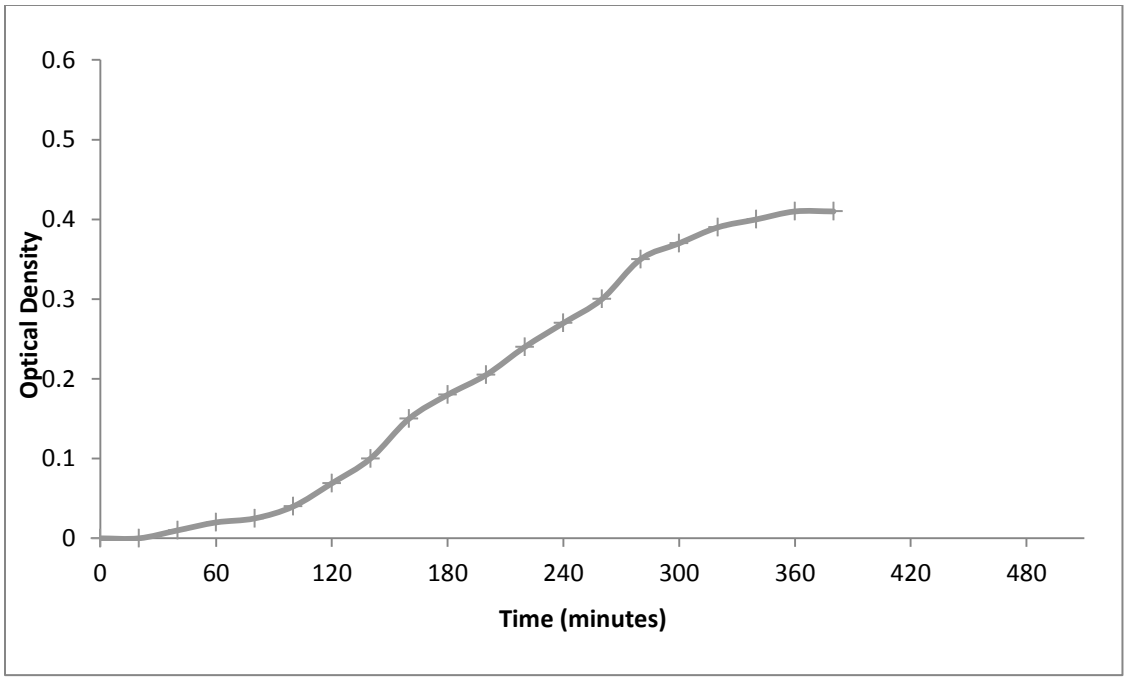

Figure 5. Complete growth curves for the *E. coli* strain: ATCC4157. Cells were grown in LB broth and aerated for 15 minutes before first absorbance measurement. Measurements were taken using a Spec 20, at 670 nm wavelength, at a constant temperature of 37°C and samples were mixed for 5 seconds before each reading.

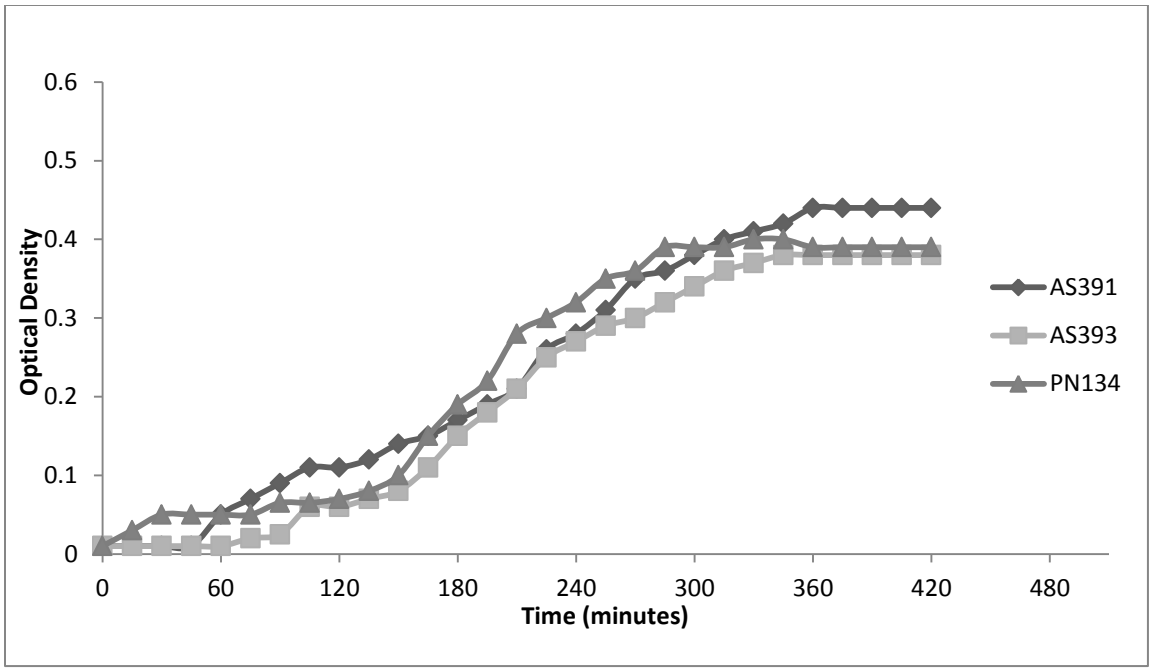

Figure 6. Complete growth curves for the three *E. coli* strains: AS391, AS393, and PN134. Cells were grown in LB broth and aerated for 15 minutes before first absorbance measurement. Measurements were taken using a Spec 20, at 670 nm wavelength, at a constant temperature of 37°C and samples were mixed for 5 seconds before each reading.

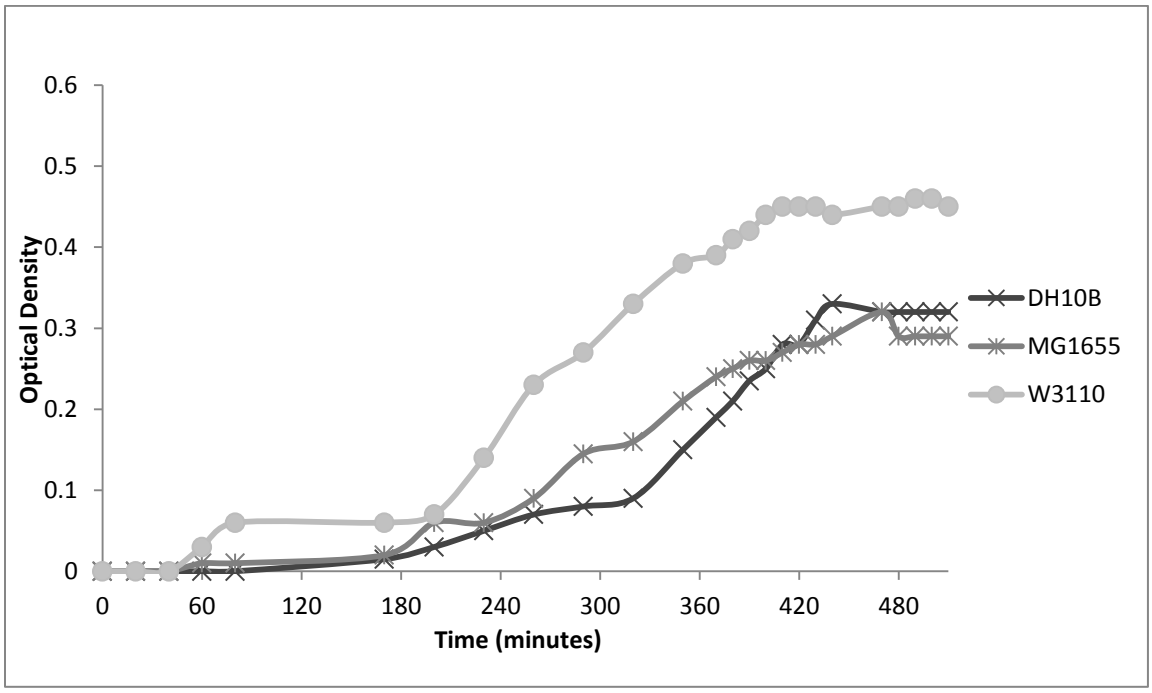

Figure 7. Complete growth curves for the three *E. coli* strains: DH10B, MG1655, and W3110. Cells were grown in LB broth and aerated for 15 minutes first absorbance measurement. Measurements were taken using a Spec 20, at 670 nm wavelength, at a constant temperature of 37°C and samples were mixed for 5 seconds before each reading.

Relationship between Optical Density and the Number of Cells

Live and dead cells can be distinguished using trypan blue, a stain that is membrane impermeable. Cells that have compromised membranes will be stained while cells with intact membranes will not. Once stained, live and dead cells in a particular volume can be counted using a hemacytometer. By this method, the total number of cells was determined for cell solutions that had a range of optical density at 670 nm. Measurements were done for each *E. coli* strain at both log and stationary phases. A different relationship between the optical density measurements and cell count was obtained for each strain; however each strain similarly had a positive correlation between cells per mL and optical density (Appendix A). At a given OD_{670} DH10B, MG1655, and W3110 all shared similar cell numbers. AS391, AS393, and PN134 were all derived from the same strain and have similar numbers as well, but they are different from DH10B, MG1655, and W3110. OD_{670} to cells per mL conversion factors obtained from these relationships are shown in Table 1.

Table 1. OD_{670} to cells/mL conversion factors. The number of cells per ml (n) can be determined by a given optical density (o) using the equation; n = A(o) +B. The A and B values are shown for each strain at log and stationary phase. The strains were grown in LB broth at 37ºC until the proper phase was reached. Cells were diluted to various concentrations, resuspended in a PBS buffer with trypan blue, and added to a hemacytometer to be counted. Conversion factors were obtained from a linear fit line created from standard curve made from the various concentrations and cell counts.

Strain	**Growth Phase**	**A**	**B**
AS391	Log Phase	$3x10^6$	$5x10^6$
	Stationary Phase	$1x10^7$	$-8x10^6$
AS393	Log Phase	$3x10^6$	$1x10^7$
	Stationary Phase	$1x10^7$	$-4x10^6$
DH10B	Log Phase	$4x10^5$	$3x10^5$
	Stationary Phase	$7x10^5$	$-4x10^5$
MG1655	Log Phase	$8x10^5$	$-7x10^4$
	Stationary Phase	$5x10^5$	$7x10^5$
PN134	Log Phase	$6x10^6$	$3x10^6$
	Stationary Phase	$7x10^6$	$-4x10^6$
W3110	Log Phase	$9x10^5$	$-1x10^5$
	Stationary Phase	$4x10^5$	$8x10^5$

2. Fluorescence Assays for Cell Viability

SYTO9/PI Calibration for ATCC4157

When bound to DNA SYTO9 and PI exhibit a large increase in fluorescence intensity. SYTO9 is membrane permeable and will stain all bacteria in a population. Propidium iodide (PI) stains bacteria only with damaged membranes because it cannot pass through the membrane. PI displaces SYTO9 from DNA. Therefore, a mixture containing the

proper concentrations of the two dyes will have bacteria with intact membranes only containing SYTO9 and bacteria with damaged membranes only containing PI bound to DNA. SYTO9 concentrations were selected in a range of 0.1 to 6 μM for calibration of the dye. Optical density was adjusted to 0.05 at 670 nm to maintain a consistency between all experiments. As shown in Figure 8, the fluorescence intensity measured at 520 nm peaked at a SYTO9 concentration of 4 μM, meaning that the cells were saturated at this concentration.

Using the pre-determined concentration of SYTO9, the proper concentration of propidium iodide was determined using a range of live to dead cell ratios to create a linear relationship between the percentage of live cells and ratio of SYTO9 to PI (Figure 9). The live and dead cell suspension optical densities were adjusted to 0.05 at a wavelength of 670 nm. The concentration of SYTO9 was held constant and a range of propidium iodide concentrations between 1 to 20 μM was tested for each live to dead ratio. The optimal concentration of propidium iodide was selected based upon the relationship between the fluorescence intensities and ratios of live to dead cells. The optimal dye concentration of propidium iodide for ATCC4157 was 20 μM (Table 2).

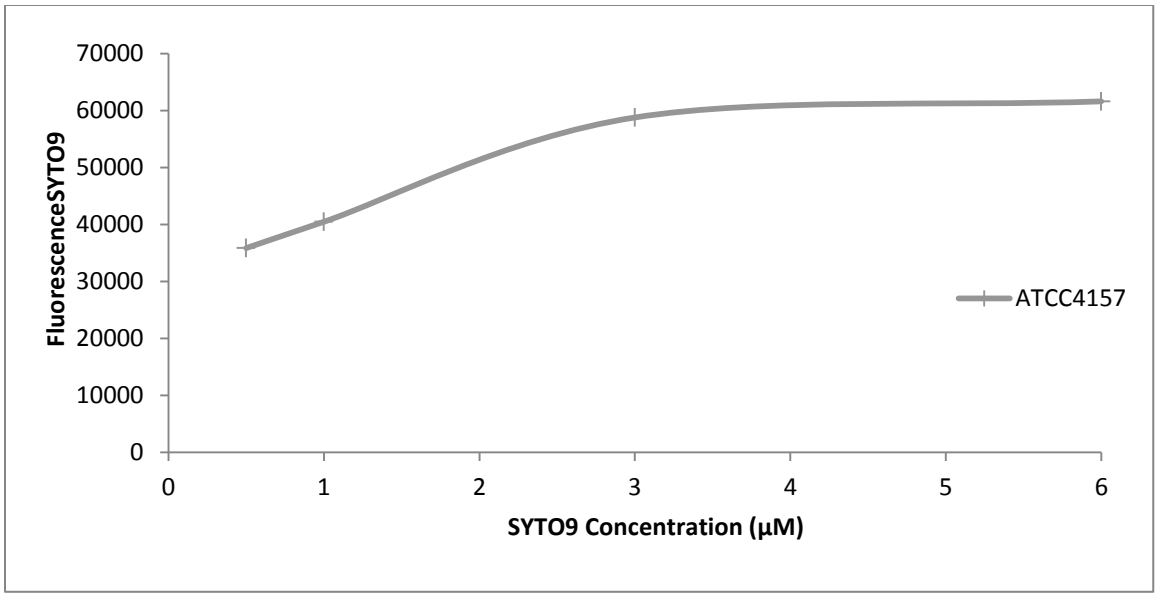

Figure 8. SYTO9 saturation curve for the *E. coli* strain: ATCC4157. Readings were taken using a fluorescence microplate reader using an excitation wavelength of 480 nm and emission of 520 nm. Strains were grown at 37°C in LB broth prior to the start.

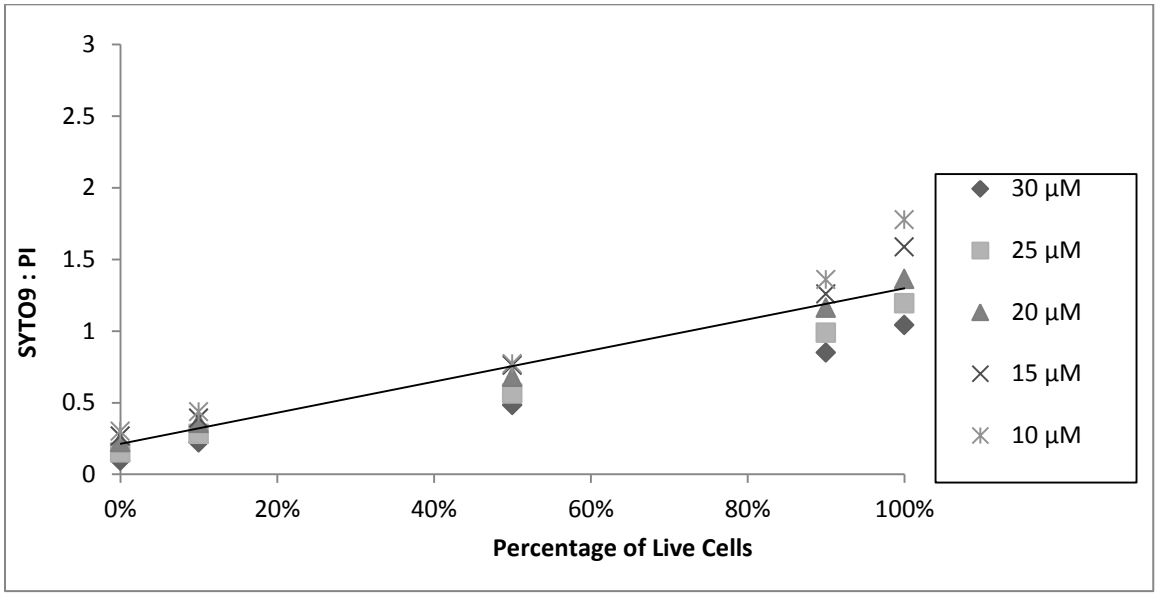

Figure 9. A live: dead assay for the adequate concentration of propidium iodide fluorophore for ATCC4157. The SYTO9 fluorophore was used at a different concentration for each strain. The strains were grown until they reached stationary phase in LB broth at 37°C before use. The measurements were recorded using a fluorescence microplate reader, at an excitation wavelength of 480 nm and emission of 520 nm for SYTO9 and emission of 612 nm for PI.

SYTO9/PI Calibration for DH10B, MG1655, and W3110

SYTO9 and PI were calibrated for the *E. coli* strains DH10B, MG1655, and W3110 because each strain has slight differences in membrane permeability. The same range of SYTO9 dye concentrations were tested for these three strains as for ATCC4157. As shown in Figure 10, the fluorescence intensity reached saturation at 2 μM. Two methods of mixing were used, simple inversion and vortexing. Simple inversion was deemed the better method and a comparison between both methods can be found in Appendix A. The range of dye used for the propidium iodide had to be expanded to a wider range, 10 to 40 μM, than for ATCC4157 because linearity between the two fluorophores and live to dead ratios was not found. Using this wider range, the propidium iodide concentration was determined for each of the three strains (Figure 11-13). Figures 11-13 are representative of the graphs created for the calibration. Additional figures are in Appendix A. The optimal dye concentration of propidium iodide for DH10B, MG1655, and W3110 ranged between 25 to 30 μM (Table 2).

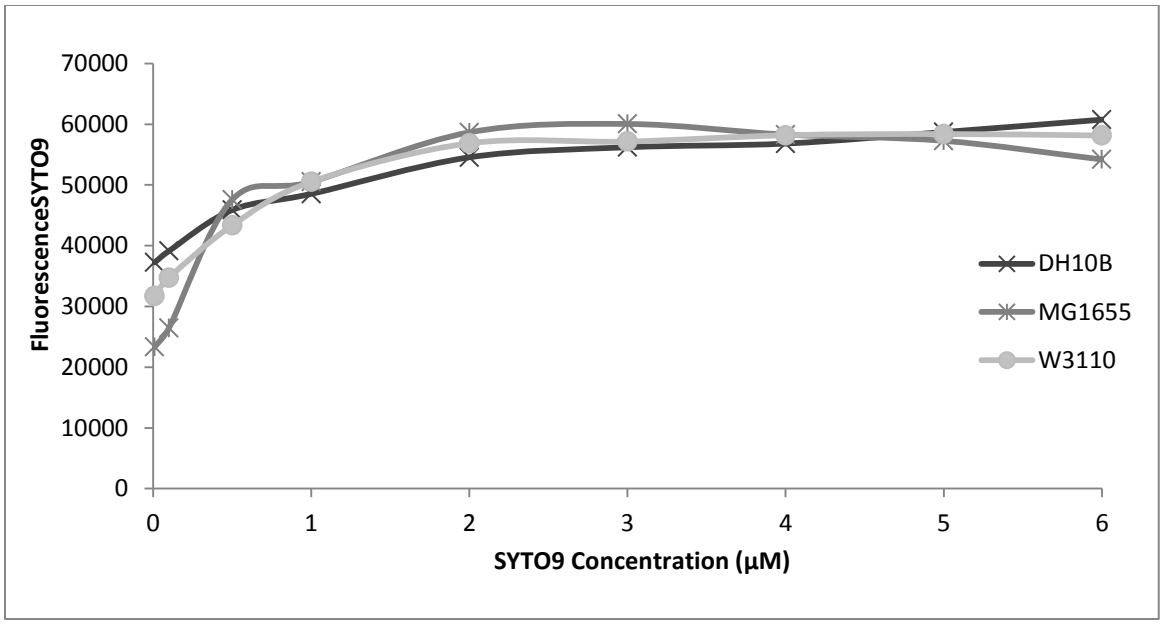

Figure 10. SYTO9 saturation curve for the three *E. coli* strains: DH10B, MG1655, and W3110. Measurements were taken using a fluorescence microplate reader at an excitation wavelength of 480 nm and emission of 520 nm. Strains were grown at 37°C in LB broth prior to the start.

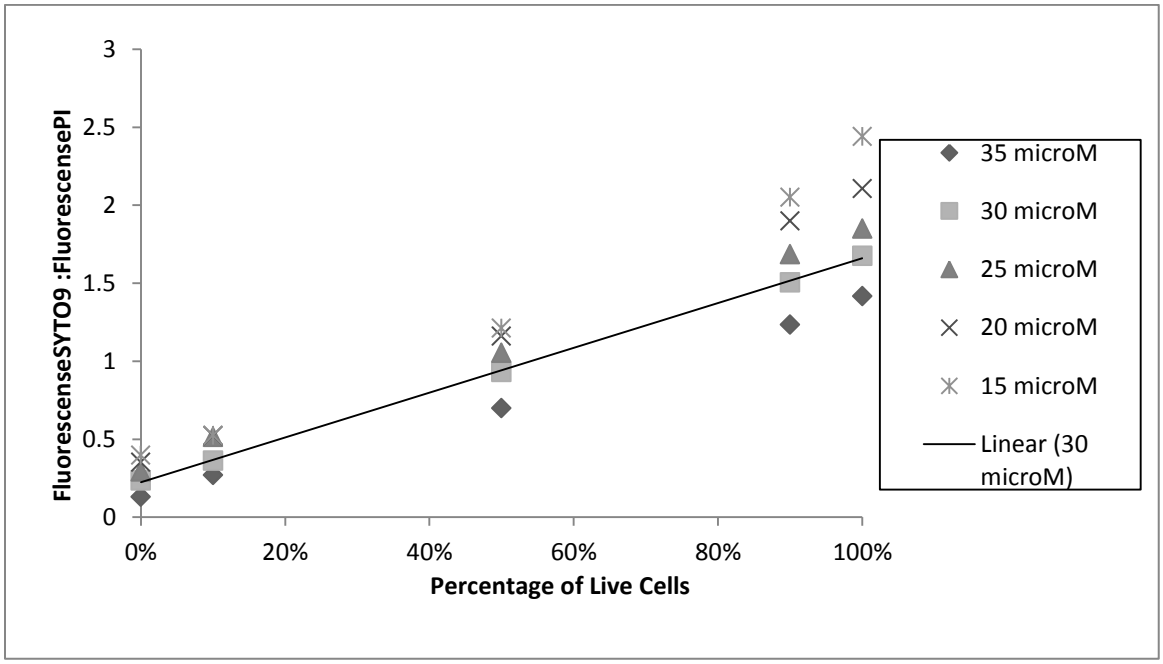

Figure 11. A live: dead assay for the adequate concentration of propidium iodide fluorophore for DH10B. The SYTO9 fluorophore was used at a different concentration for each strain. The strains were grown until they reached stationary phase in LB broth at 37°C before use. The measurements were recorded using a fluorescence microplate reader, at an excitation wavelength of 480 nm and emission of 520 nm for SYTO9 and emission of 612 nm for PI.

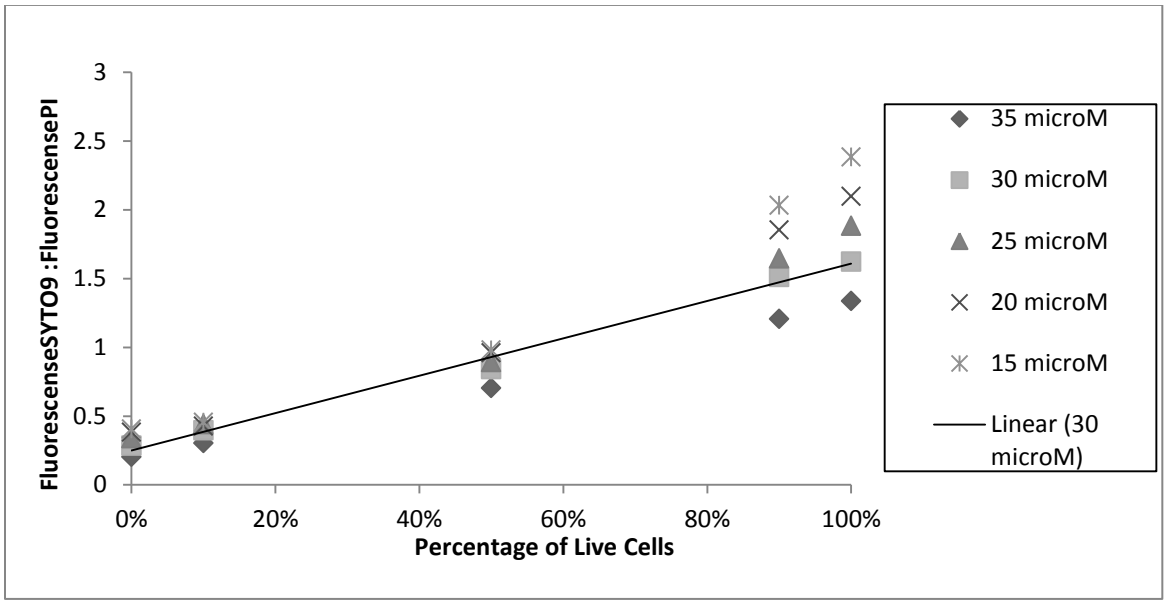

Figure 12. A live: dead assay for the adequate concentration of propidium iodide fluorophore for MG1655. The SYTO9 fluorophore was used at a different concentration for each strain. The strains were grown until they reached stationary phase in LB broth at 37°C before use. The measurements were recorded using a fluorescence microplate reader, at an excitation wavelength of 480 nm and emission of 520 nm for SYTO9 and emission of 612 nm for PI.

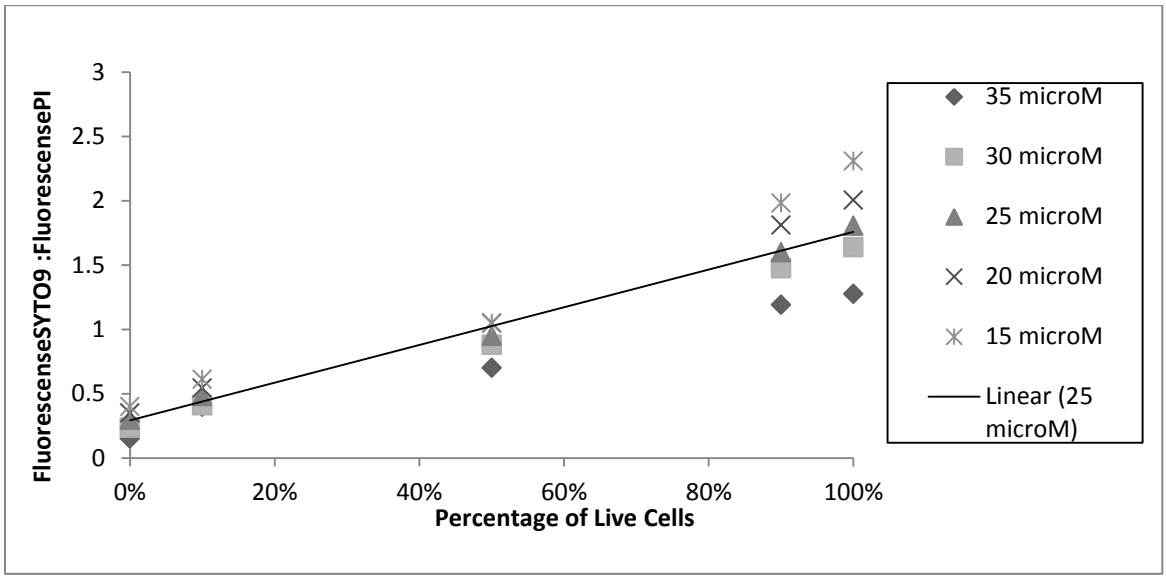

Figure 13. A live: dead assay for the adequate concentration of propidium iodide fluorophore for W3110. The SYTO9 fluorophore was used at a different concentration for each strain. The strains were grown until they reached stationary phase in LB broth at 37°C before use. The measurements were recorded using a fluorescence microplate reader, at an excitation wavelength of 480 nm and emission of 520 nm for SYTO9 and emission of 612 nm for PI.

SYTO9/PI Calibration for AS391, AS393, and PN134

As with the previous experiments, SYTO9 and PI were calibrated for the *E. coli* strains AS391, AS393, and PN134 because each strain has slight differences in membrane permeability. As with the previous strains, the same range of SYTO9 dye concentrations were tested for these three strains. As shown in Figure 14, the fluorescence intensity reached saturation at 3 μM. The range of dye used for the propidium iodide for these strains was also was varied, between 10 to 40 μM. The propidium iodide concentration that was used to create a linear relationship between the percentage of live cells and ratio of SYTO9 to PI, varied for the three strains (Figure 15-17). Figures with wider ranges are located in Appendix A. The optimal dye concentration of propidium iodide for DH10B, MG1655, and W3110 was 30 μM (Table 2).

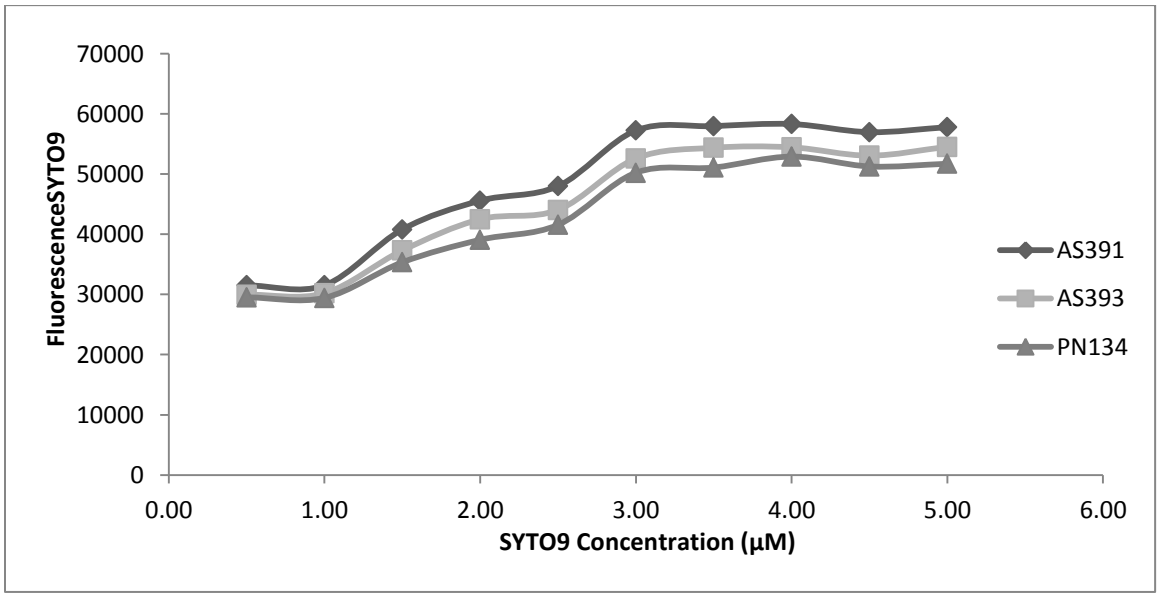

Figure 14. SYTO9 Saturation Curve for the three *E. coli* strains: AS391, AS393, and PN134. Readings were taken using a fluorescence microplate reader using an excitation wavelength of 480 nm and emission of 520 nm. Strains were grown at 37°C in LB broth supplemented with 0.2% glucose prior to the start.

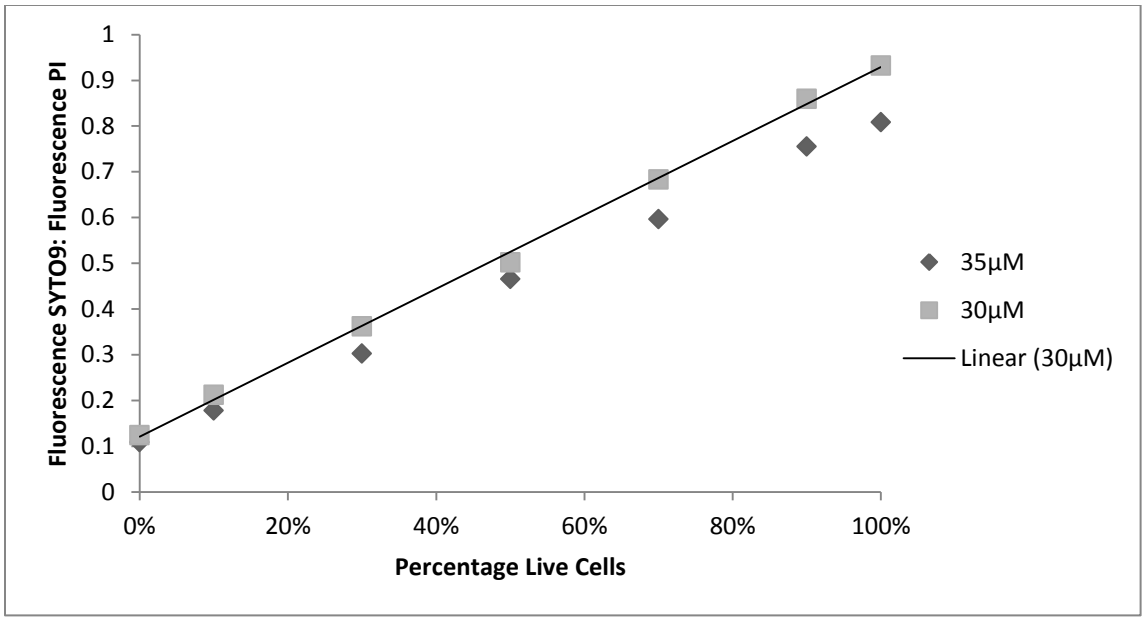

Figure 15. A live: dead assay for the adequate concentration of propidium iodide fluorophore for AS391. The SYTO9 fluorophore was used at a different concentration for each strain. The strains were grown until they reached stationary phase in LB broth at 37°C before use. The measurements were recorded using a fluorescence microplate reader, at an excitation wavelength of 480 nm and emission of 520 nm for SYTO9 and emission of 612 nm for PI.

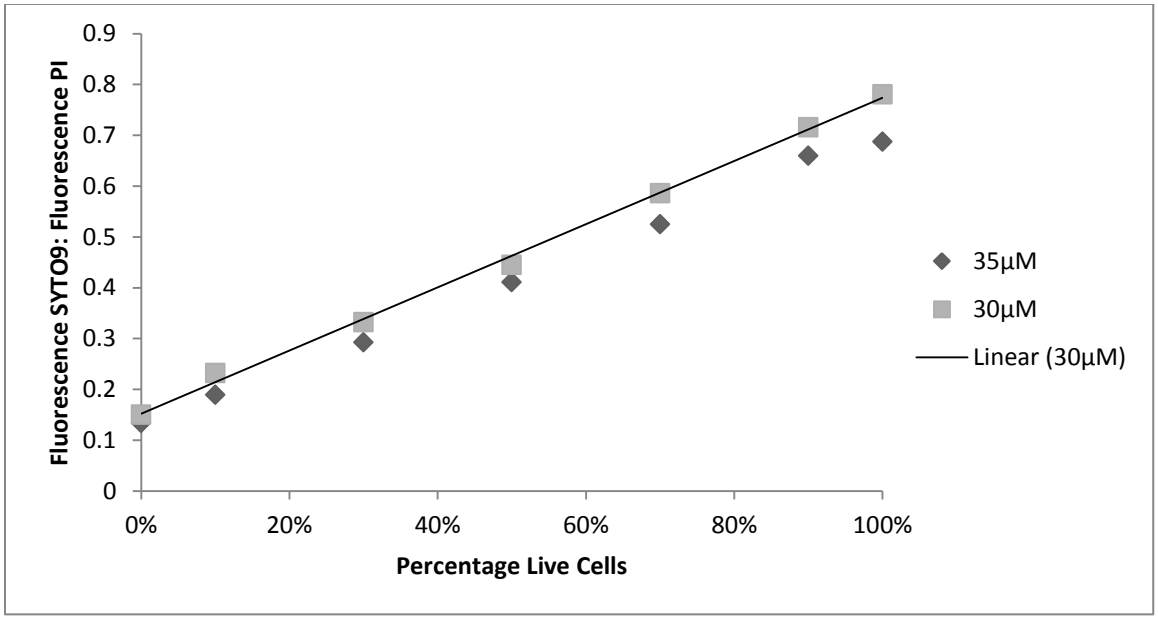

Figure 16. A live: dead assay for the adequate concentration of propidium iodide fluorophore for AS393. The SYTO9 fluorophore was used at a different concentration for each strain. The strains were grown until they reached stationary phase in LB broth at 37°C before use. The measurements were recorded using a fluorescence microplate reader, at an excitation wavelength of 480 nm and emission of 520 nm for SYTO9 and emission of 612 nm for PI.

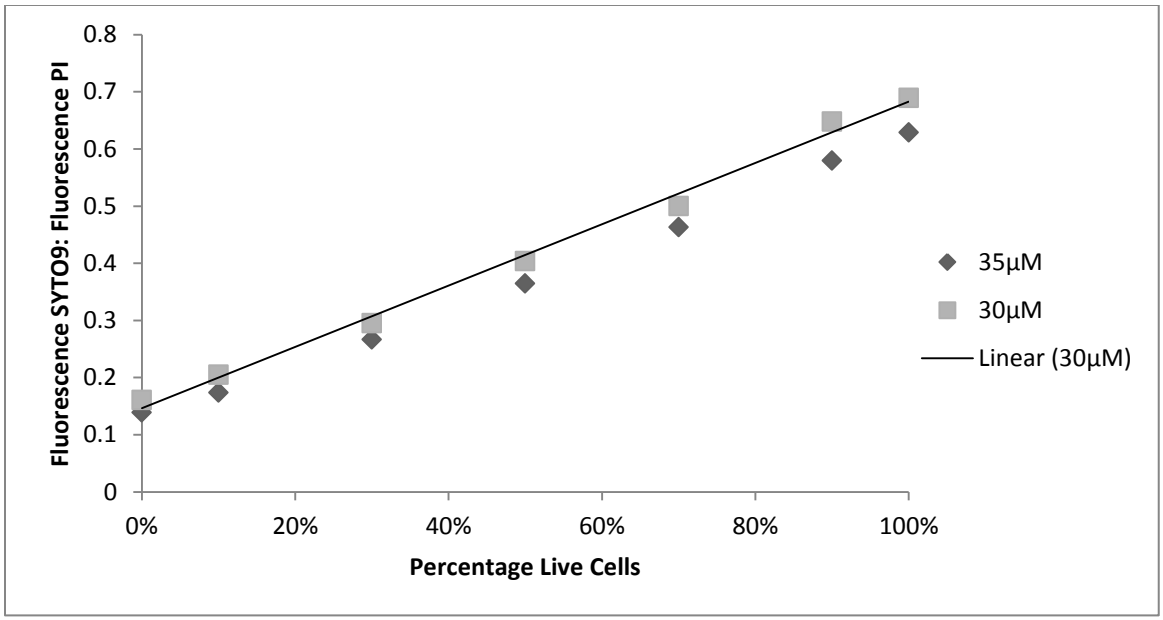

Figure 17. A live: dead assay for the adequate concentration of propidium iodide fluorophore for PN134. The SYTO9 fluorophore was used at a different concentration for each strain. The strains were grown until they reached stationary phase in LB broth at 37°C before use. The measurements were recorded using a fluorescence microplate reader, at an excitation wavelength of 480 nm and emission of 520 nm for SYTO9 and emission of 612 nm for PI.

Table 2. Optimal Dye Concentration for all *E. coli* strains. The concentration of dyes that provide the best fluorescence intensity for each *E. coli* strain while maintaining linearity between the two nucleic acid dyes. Concentrations were determined from the SYTO9:PI standardization curves obtained using the fluorescence nucleic acid dyes.

	Nucleic Acid Dyes	
***E.coli* Strain**	**SYTO9**	**PI**
ATCC4157	4 µM	20 µM
AS391	3 µM	30 µM
AS393	3 µM	30 µM
DH10B	2 µM	30 µM
MG1655	2 µM	25 µM
PN134	3 µM	30 µM
W3110	2 µM	25 µM

Inner Filter Effect

When using fluorescence assays, the inner filter effect must be accounted for because it changes the intensity of the emitted light. The absorbance for the appropriate concentration of each dye (Table 2), was measured using a microplate spectrophotometer at the excitation

wavelength (485 nm) and emission wavelengths (520 nm and 612 nm). When the sum of the absorbances at the excitation and emission wavelengths exceeds 0.08, inner filter effects cause a decrease in fluorescence (Palmier and Doren 2007). The emission/excitation values are shown in Table 3.

Table 3. Absorbance values at the excitation and emission wavelengths to test the inner filter effect. Measurements were taken at the excitation and emission wavelengths for the desired concentrations of dye with a microplate reader. The absorbances at the excitation and emission wavelengths of each dye, at the desired concentration, were added for each of the *E. coli* strains. The absorbance of both dyes was obtained by creating a mixture of PI and SYTO9 dyes each at their appropriate concentration. Optimal dye concentrations were prepared following the protocol for the fluorescence nucleic acid dyes. The concentrations varied from 20 µM to 35 µM for PI and 1 µM to 3 µM for SYTO9.

***E. coli* Strain**	**Wavelength (Excitation/ Emission)**	**Sum of Absorbances of PI at λ_{ex} and λ_{em}**	**Sum of Absorbances of SYTO9 at λ_{ex} and λ_{em}**	**Sum of Absorbances of a PI and SYTO9 mixture at λ_{ex} and λ_{em}**
AS391, AS393, PN134	485/520 nm	0.218	0.056	0.307
	485/612 nm	0.119	0.055	0.201
ATCC4157	485/520 nm	0.101	0.116	0.195
	485/612 nm	0.057	0.114	0.148
DH10B	485/520 nm	0.174	0.010	0.191
	485/612 nm	0.096	0.011	0.122
MG1655, W3110	485/520 nm	0.134	0.010	0.154
	485/612 nm	0.076	0.011	0.102

3. Paraquat Assay

The effects of 50 µM paraquat on the three SOD knockout *E. coli* strains were assessed using Luria-Bertani broth as a growth medium. Samples were aerated (via shaking at 200 rpm) for 15 minutes prior to the addition of paraquat. Growth curves were determined by measuring the absorbance at 670 nm using a UV/Vis platereader reader at a constant temperature of 37°. Paraquat significantly reduced the growth of AS391 and PN134, while it only slightly decreased the growth rate of AS393 (Figure 18-20). Samples were mixed by the

UV/Vis platereader for 1 minute prior to measurements taken every 5 minute (Figure 18-20).

Additional experiments using various mixing and reader times are reported in Appendix A.

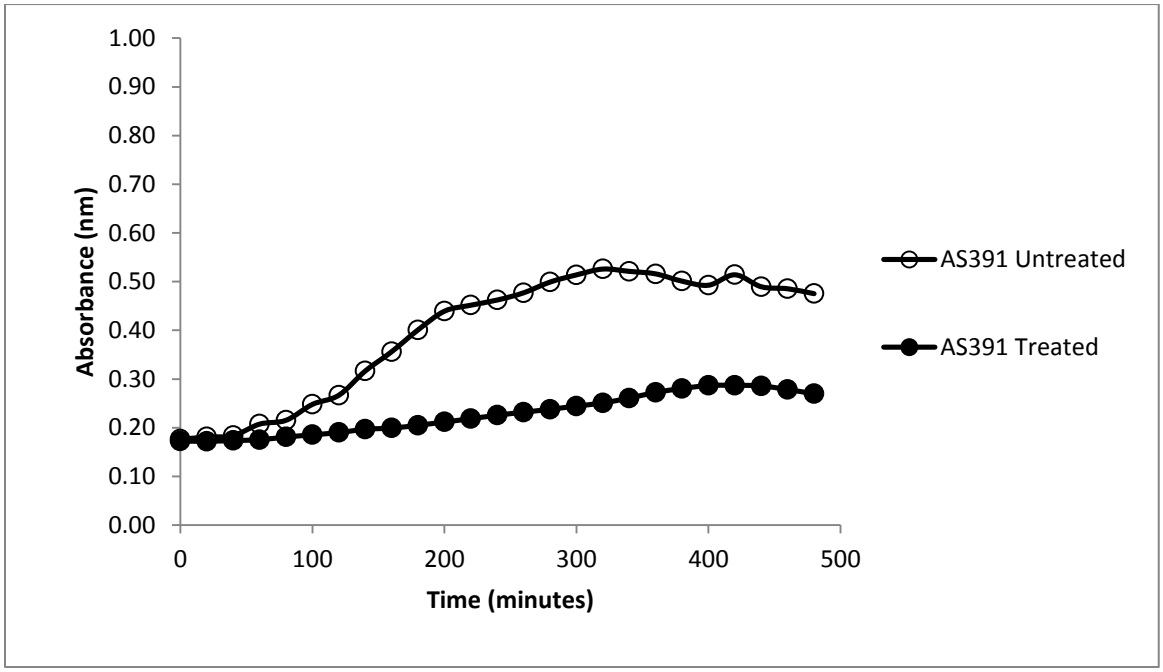

Figure 18. Growth curve with paraquat treatment for the *E. coli* strain: AS391. The strain was grown in LB broth and aerated for 15 minutes before starting. Treated cells received paraquat after the 15 minutes of aeration. Measurements were taken using a UV/Vis platereader, at 670 nm wavelength, and at a constant temperature of 37°C. Samples were mixed for 1 minute before each 5 minute reading.

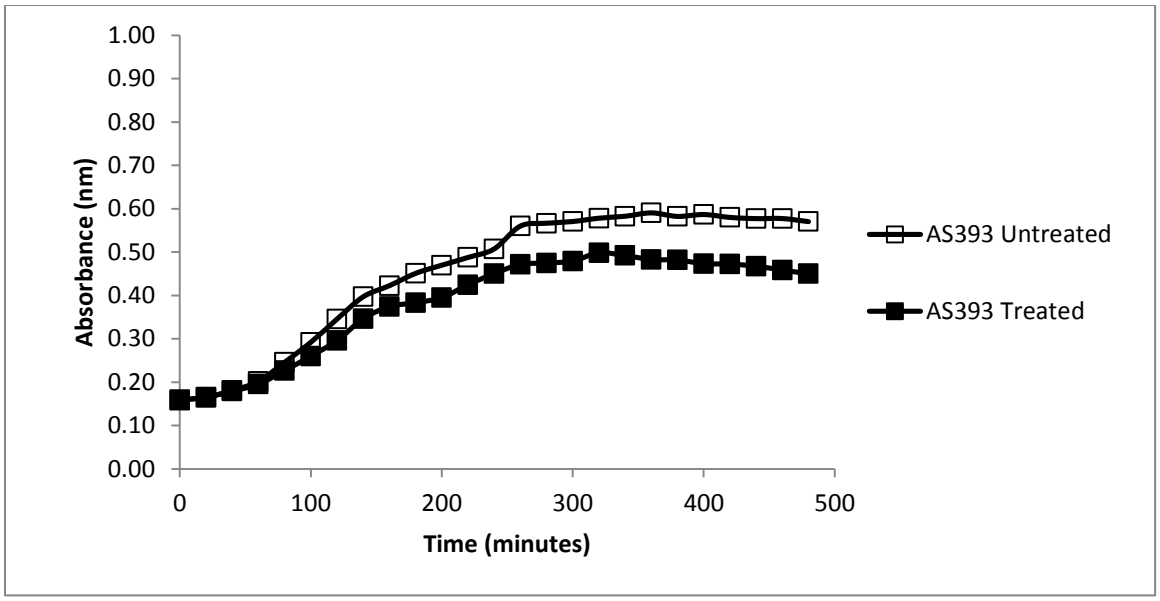

Figure 19. Growth curve with paraquat treatment for the *E. coli* strain: AS393. The strain was grown in LB broth and aerated for 15 minutes before starting. Treated cells received paraquat after the 15 minutes of aeration. Measurements were taken using a UV/Vis platereader, at 670 nm wavelength, and at a constant temperature of 37°C. Samples were mixed for 1 minute before each 5 minute reading.

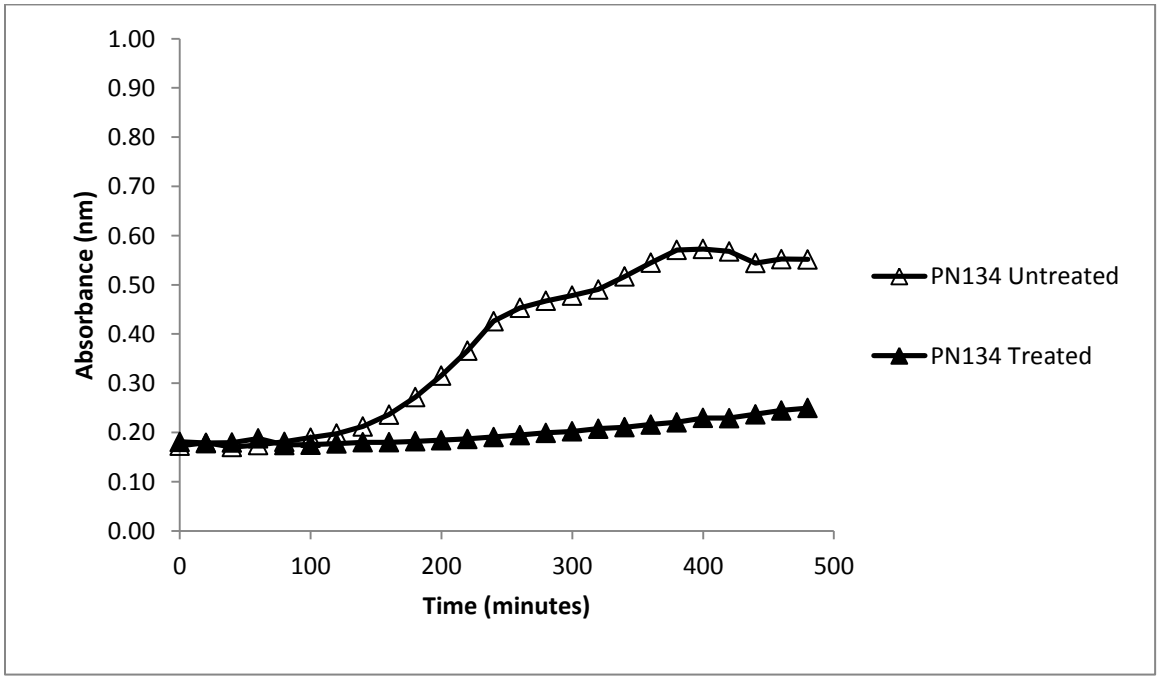

Figure 20. Growth curve with paraquat treatment for the *E. coli* strain: PN134. The strain was grown in LB broth and aerated for 15 minutes before starting. Treated cells received paraquat after the 15 minutes of aeration. Measurements were taken using a UV/Vis platereader, at 670 nm wavelength, and at a constant temperature of 37°C. Samples were mixed for 1 minute before each 5 minute reading.

4. Xanthine/Xanthine Oxidase Assay

Cell Viability using Xanthine/Xanthine Oxidase at pH 7.5

To determine cell viability using the xanthine xanthine oxidase assay, a SYTO9/PI fluorescence assay was used. Fluorophore emissions were measured using a microplate reader. A calibration curve control was created for each reading to maintain the linear relationship between the percentage of live cells and ratio of SYTO9 to PI (Figure 21). Treatment with xanthine had little to no effect on the cell viability for any of the three knockout strains (Figures 22-24). Since there appeared to be an increase in cell viability (Figures 22-24) we assessed if the cells were growing, by measuring the absorbance for each sample before the fluorophore emissions were measured. There was no change in the optical density for each of the time periods except for the initial decrease after the cells are added to the xanthine solution (Figures 25-27).

To optimize the assay, we changed certain variables to see the effects on cell viability. Temperature was increased from 4°C to 27°C during centrifuging. The xanthine solution storage temperature was increased from 4°C to 27°C. Treated cell aliquot sizes were increased from 100 µL to 400 µL. Centrifuging times were decreased from 9 to 5 minutes. These data can be found in Appendix A.

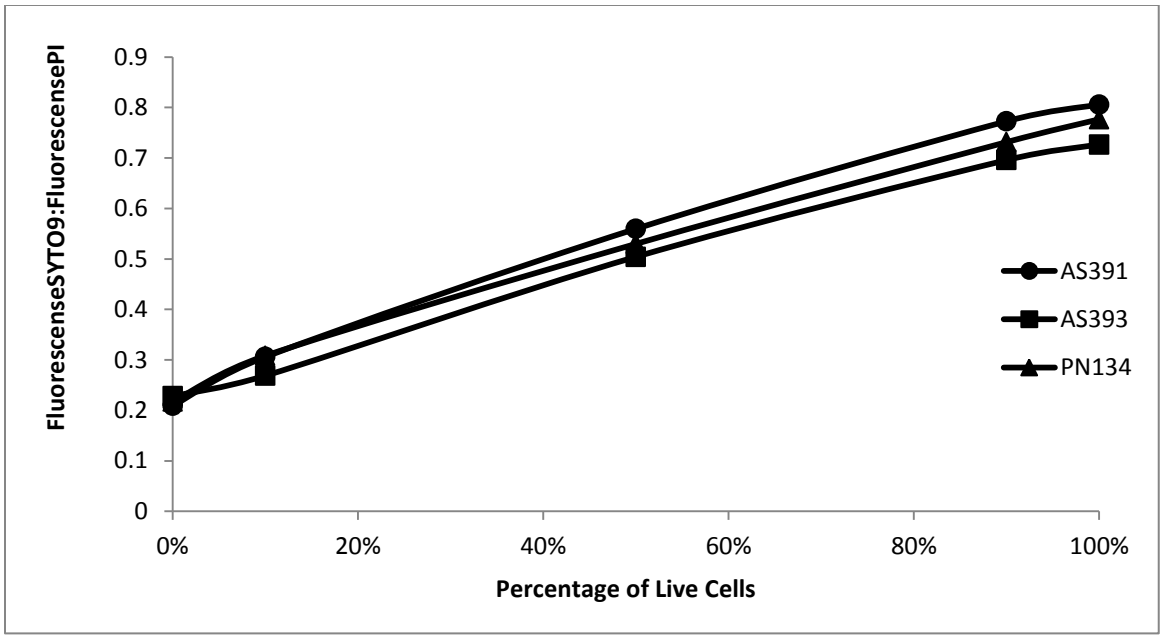

Figure 21. Calibration curve for the *E. coli* strains: AS391, AS393, PN134 prior to xanthine oxidase assay start. The strains were started 1.5 hours after the start of the first strains and were grown for the appropriate time frame in LB broth at 37°C before use. The concentrations used for propidium iodide and SYTO9 were 30 μM and 3 μM respectively. The measurements were recorded using a fluorescence microplate reader, using an excitation wavelength of 480 nm and emission of 520 nm for SYTO9 and emission of 612 nm for PI, and the strain was prepared using the fluorescence nucleic acid dyes.

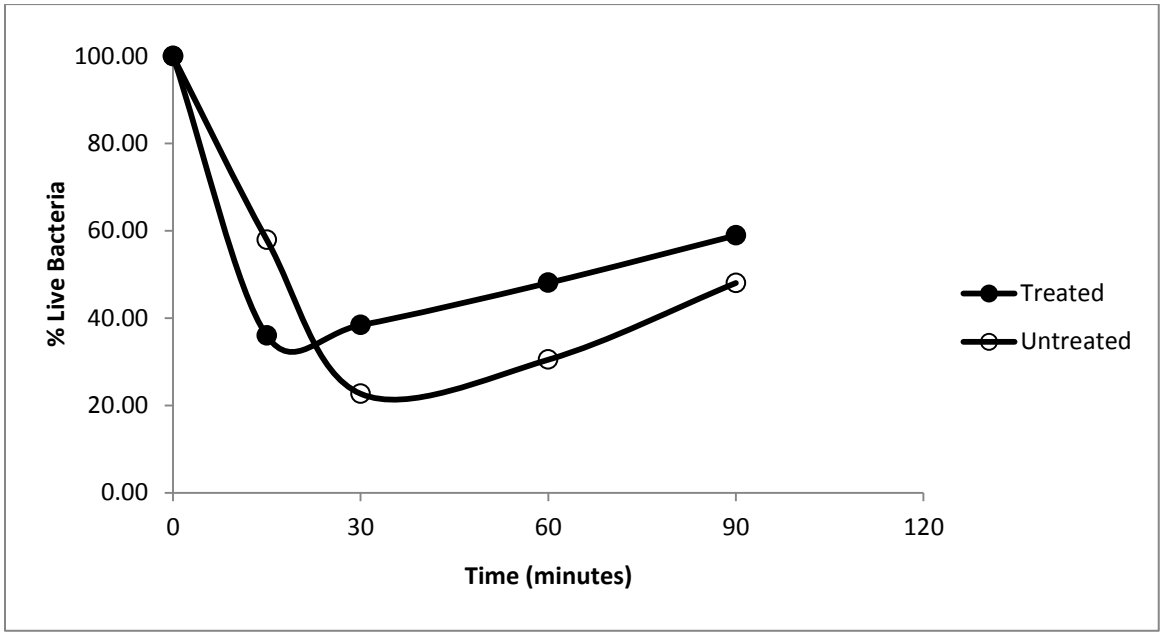

Figure 22. Effect of xanthine/xanthine oxidase treatment on the viability of AS391 at pH 7.5. Cells were harvested at stationary phase and resuspended in a potassium phosphate buffer which was adjusted to a pH of 7.5. Untreated and treated cells received 1 mL of xanthine solution. Treated cells received 100 μL xanthine oxidase while untreated received 100 μL H_2O. Viability was tested with the fluorescence nucleic acid dyes.

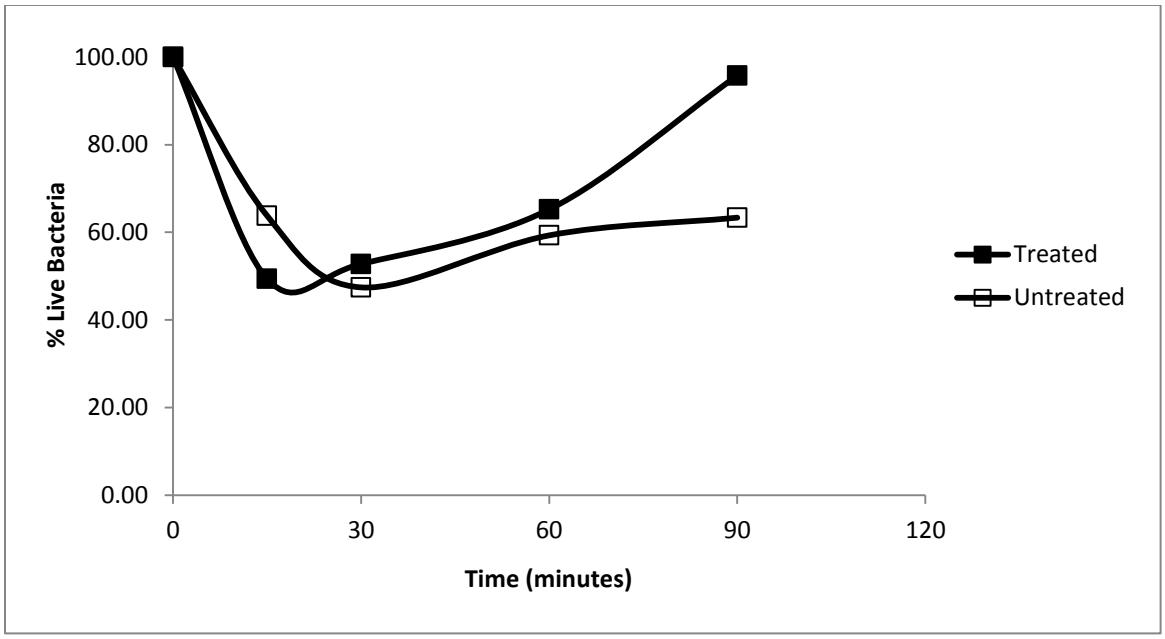

Figure 23. Effect of xanthine/xanthine oxidase treatment on the viability of AS393 at pH 7.5. Cells were harvested at stationary phase and resuspended in a potassium phosphate buffer which was adjusted to a pH of 7.5. Untreated and treated cells received 1 mL of xanthine solution. Treated cells received 100 µL xanthine oxidase while untreated received 100 µL H_2O. Viability was tested with the fluorescence nucleic acid dyes.

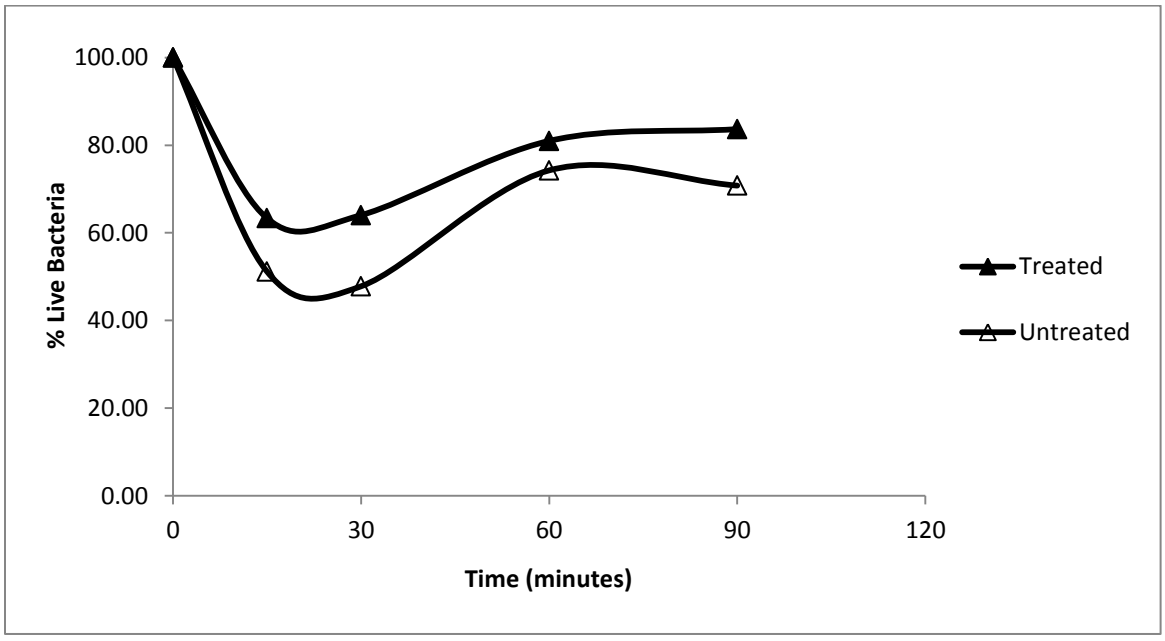

Figure 24. Effect of xanthine/xanthine oxidase treatment on the viability of PN134 at pH 7.5. Cells were harvested at stationary phase and resuspended in a potassium phosphate buffer which was adjusted to a pH of 7.5. Untreated and treated cells received 1 mL of xanthine solution. Treated cells received 100 µL xanthine oxidase while untreated received 100 µL H_2O. Viability was tested with the fluorescence nucleic acid dyes.

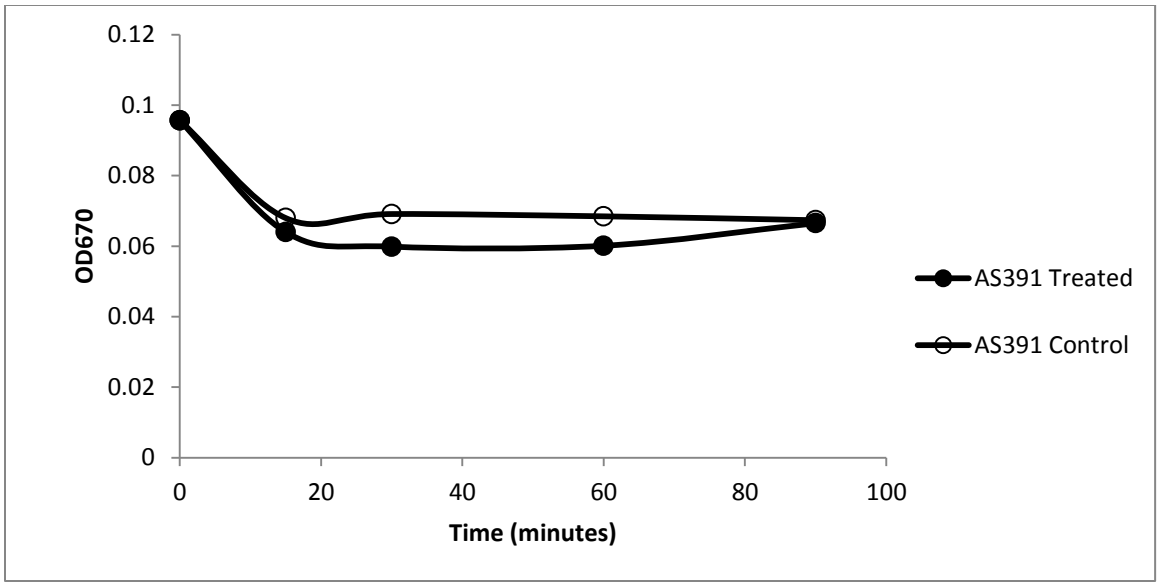

Figure 25. Optical density for the *E. coli* strain AS391, prior to xanthine oxidase assay measurements, at pH 7.5. The strains were started 1.5 hours after the start of the first strains and were grown for the appropriate time frame in an LB media broth at 37°C before use. The measurements were taken using a UV Vis microplate reader at the wavelength of 670 nm. Samples were taken from the xanthine oxidase reaction tubes and measured before undergoing centrifugation for the fluorescence nucleic acid dyes.

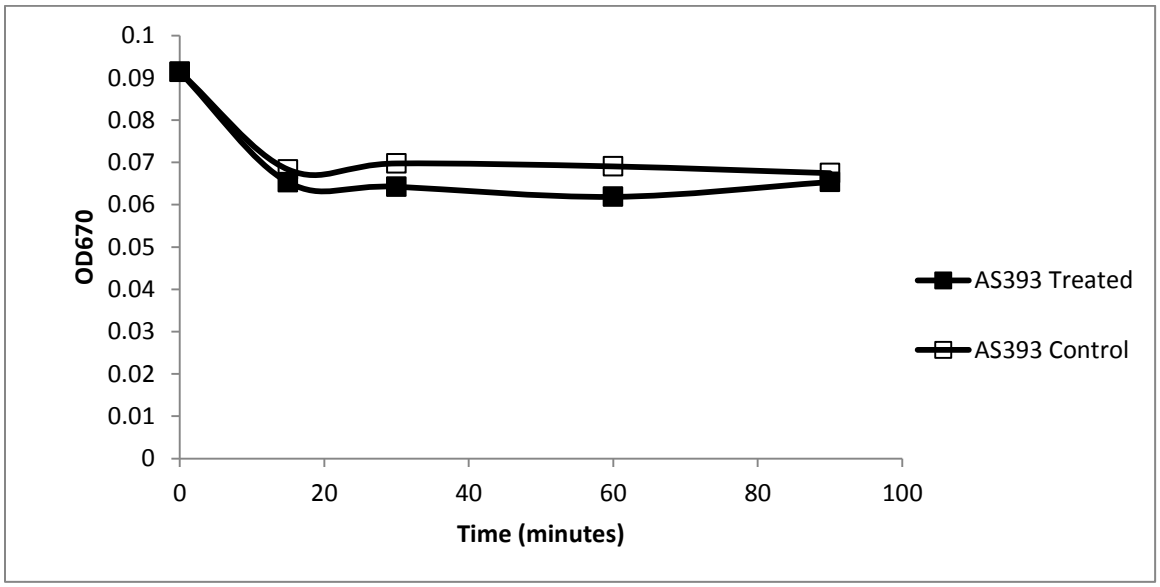

Figure 26. Optical density for the *E. coli* strain AS393, prior to xanthine oxidase assay measurements, at pH 7.5. The strains were started 1.5 hours after the start of the first strains and were grown for the appropriate time frame in an LB media broth at 37°C before use. The measurements were taken using a UV Vis microplate reader at the wavelength of 670 nm. Samples were taken from the xanthine oxidase reaction tubes and measured before undergoing centrifugation for the fluorescence nucleic acid dyes.

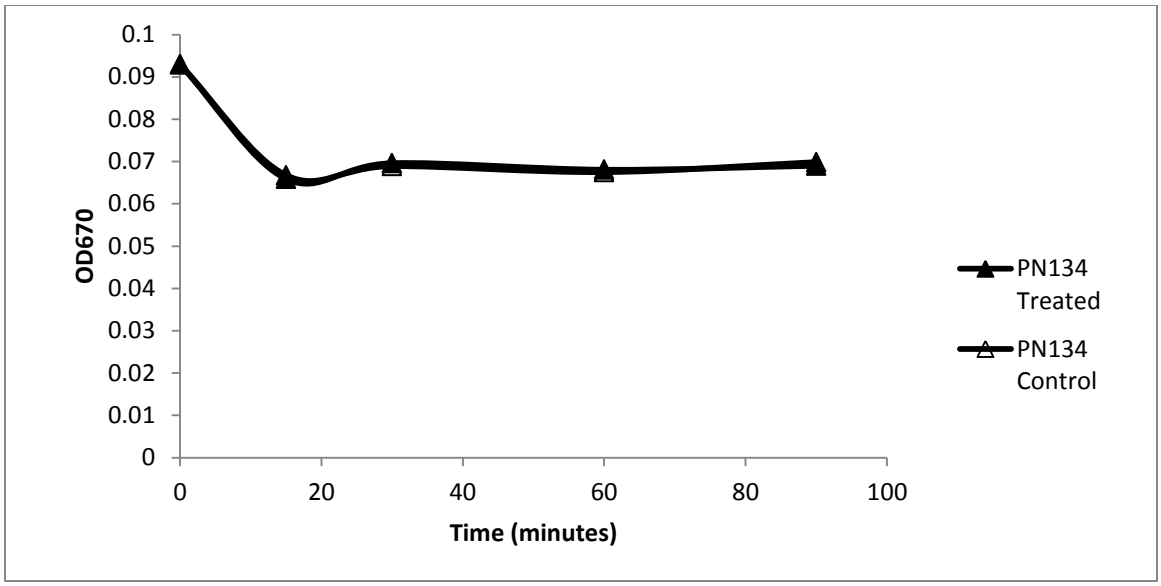

Figure 27. Optical density for the *E. coli* strain PN134, prior to xanthine oxidase assay measurements, at pH 7.5. The strains were started 1.5 hours after the start of the first strains and were grown for the appropriate time frame in LB broth at 37°C before use. The measurements were taken using a UV Vis microplate reader at the wavelength of 670 nm. Samples were taken from the xanthine oxidase reaction tubes and measured before undergoing centrifugation for the fluorescence nucleic acid dyes.

Cell Viability using Xanthine/Xanthine Oxidase at pH 6.5

Since the cell viability did not vary at pH 7.5, the pH of the buffer solution was decreased to 6.5. A calibration curve control was created for each reading to maintain the linear relationship between the percentage of live cells and ratio of SYTO9 to PI again (Figure 28). Treatment with xanthine had little to no effect on the cell viability for any of the three knockout strains (Figures 29-31). The decrease in cell viability had the same trend at pH 6.5 as at pH 7.5. Specially the absorbance measurements also showed that there was no change in optical density for each of the time periods expect for the initial decrease after the cells were added to the xanthine solution, the same as for pH 7.5 (Figures 32-34). For example, the optical density starts at 0.85 and initially drops to 0.6 for the treated cells and 0.7 for untreated cells at the 15 minute time point however the ODs are unchanged after the 15 minute time point (Figure 32). Certain assay variables changes from pH 7.5 were also

assessed at pH of 6.5, such as temperature changes for xanthine solution, temperature changes for centrifuging, decreased centrifuging times, and increased treated cells aliquot sized. These figures are found in Appendix A.

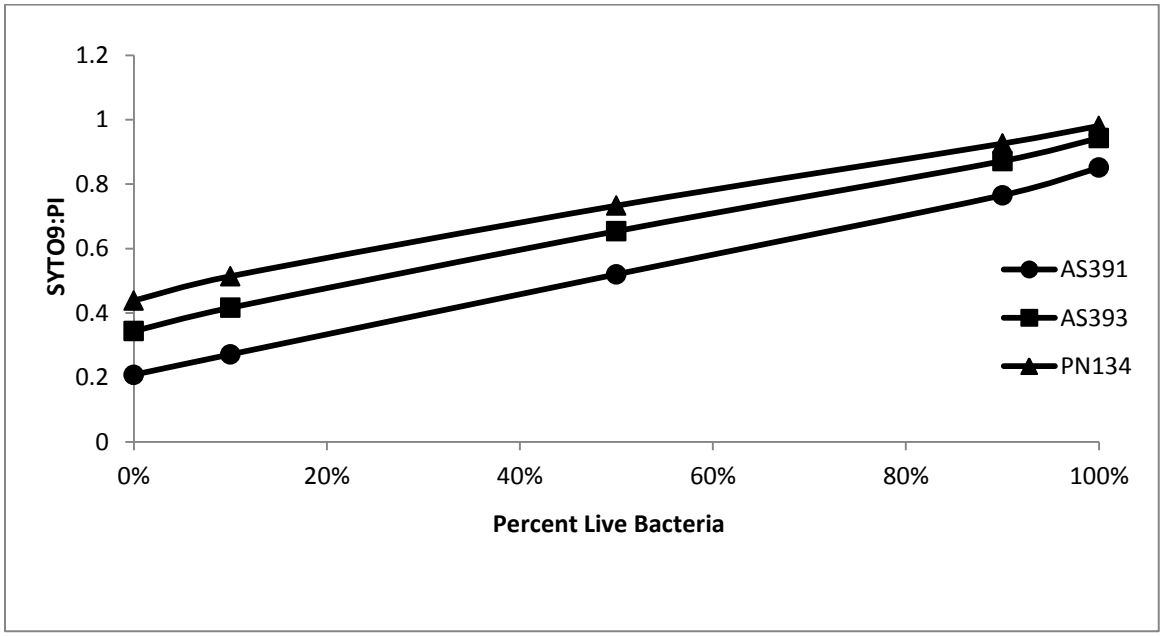

Figure 28. Calibration curve for the *E. coli* strains: AS391, AS393, PN134 prior to xanthine oxidase assay start. The strains were started 1.5 hours after the start of the first strains and were grown for the appropriate time frame in LB broth at 37°C before use. The concentrations used for propidium iodide and SYTO9 were 30 μM and 3 μM respectively. The measurements were recorded using a fluorescence microplate reader, using an excitation wavelength of 480 nm and emission of 520 nm for SYTO9 and emission of 612 nm for PI, and the strain was prepared using the fluorescence nucleic acid dyes.

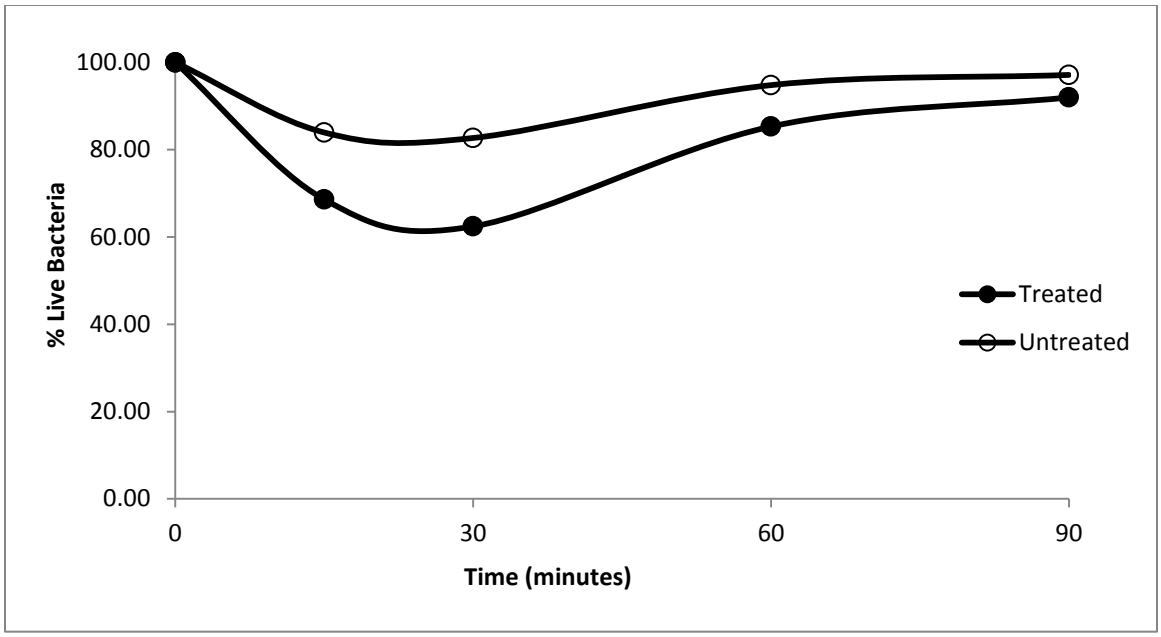

Figure 29. Effect of xanthine/xanthine oxidase treatment on the viability of AS391 at pH 6.5. Cells were harvested at stationary phase and resuspended in a potassium phosphate buffer which was adjusted to a pH of 6.5. Untreated and treated cells received 1 mL of xanthine solution. Treated cells received 100 µL xanthine oxidase while untreated received 100 µL H_2O. Viability was tested with the two nucleic acid dyes.

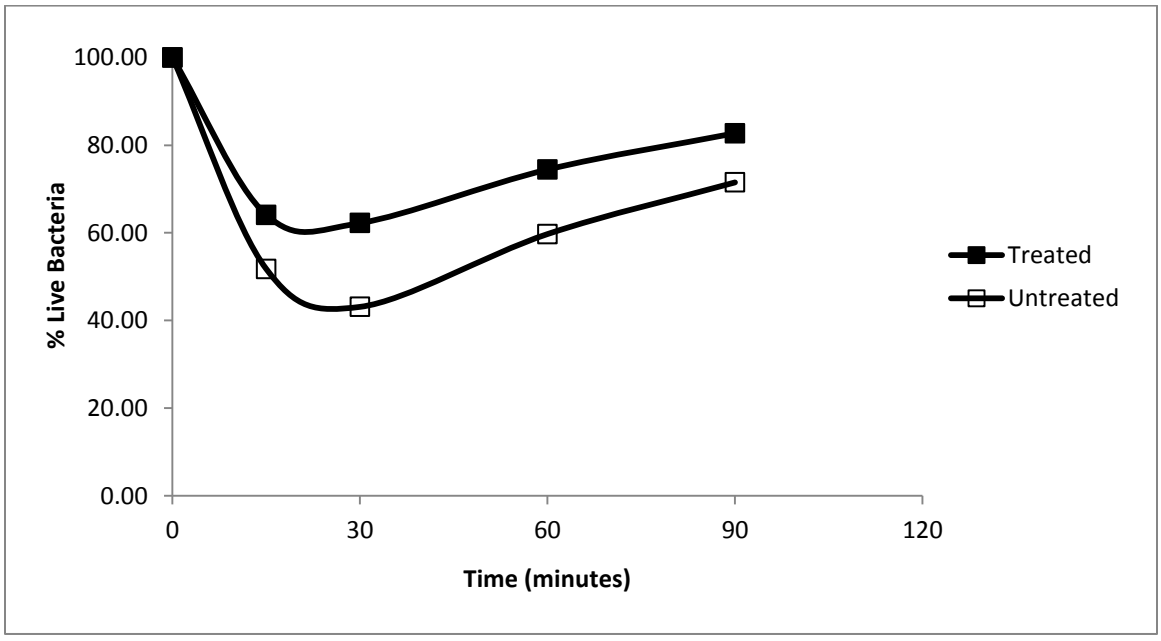

Figure 30. Effect of xanthine/xanthine oxidase treatment on the viability of AS393 at pH 6.5. Cells were harvested at stationary phase and resuspended in a potassium phosphate buffer which was adjusted to a pH of 6.5. Untreated and treated cells received 1 mL of xanthine solution. Treated cells received 100 µL xanthine oxidase while untreated received 100 µL H_2O. Viability was tested with two nucleic acid dyes.

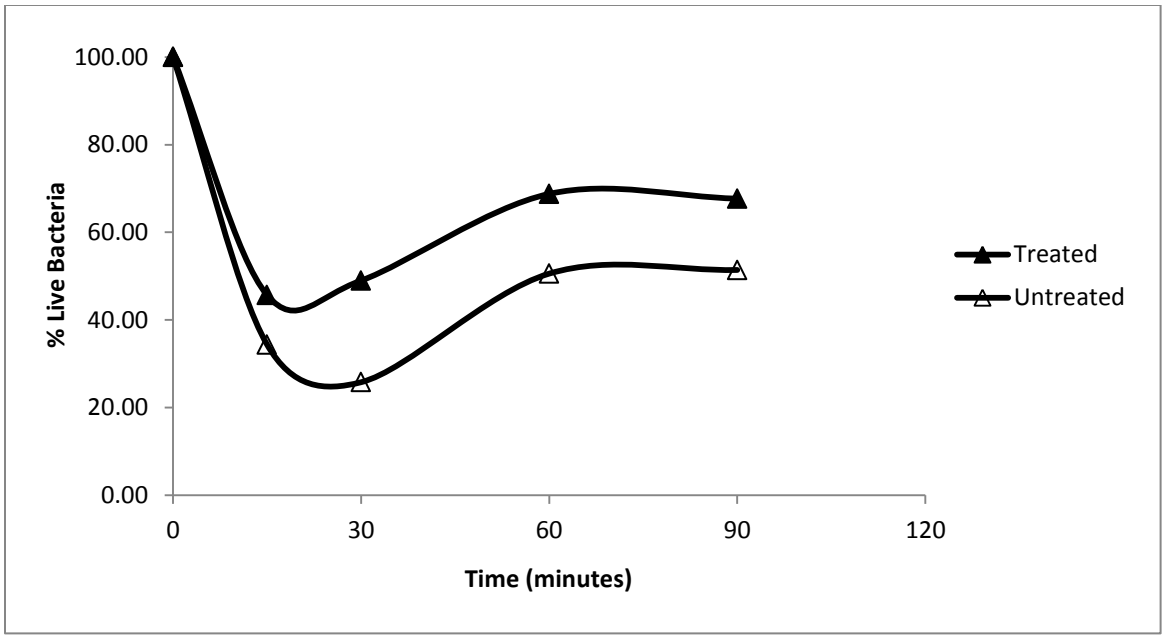

Figure 31. Effect of xanthine/xanthine oxidase treatment on the viability of PN134 at pH 6.5. Cells were harvested at stationary phase and resuspended in a potassium phosphate buffer which was adjusted to a pH of 6.5. Untreated and treated cells received 1 mL of xanthine solution. Treated cells received 100 µL xanthine oxidase while untreated received 100 µL H_2O. Viability was tested with the two nucleic acid dyes.

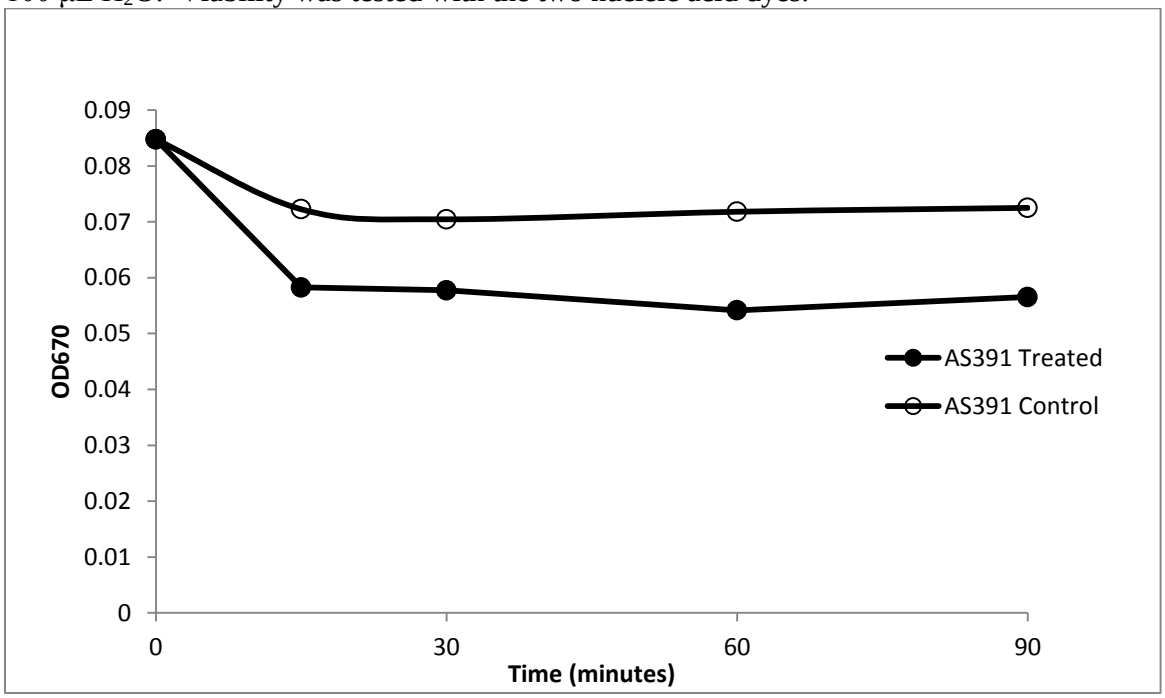

Figure 32. Optical density for the *E. coli* strain AS391, prior to xanthine oxidase assay measurements at pH 6.5. The strains were started 1.5 hours after the start of the first strains and were grown for the appropriate time frame in LB broth at 37°C before use. The measurements were taken using a UV Vis microplate reader at the wavelength of 670 nm. Samples were taken from the xanthine oxidase reaction tubes and measured before undergoing centrifugation.

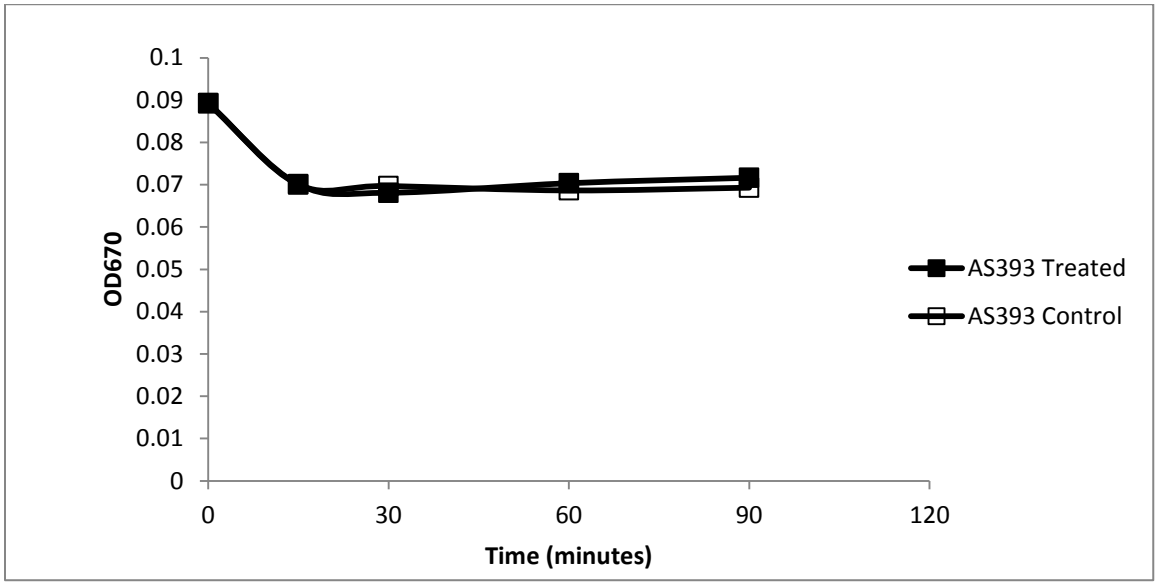

Figure 33. Optical density for the *E. coli* strain AS391, prior to xanthine oxidase assay measurements at pH 6.5. The strains were started 1.5 hours after the start of the first strains and were grown for the appropriate time frame in LB broth at 37°C before use. The measurements were taken using a UV Vis microplate reader at the wavelength of 670 nm. Samples were taken from the xanthine oxidase reaction tubes and measured before undergoing centrifugation.

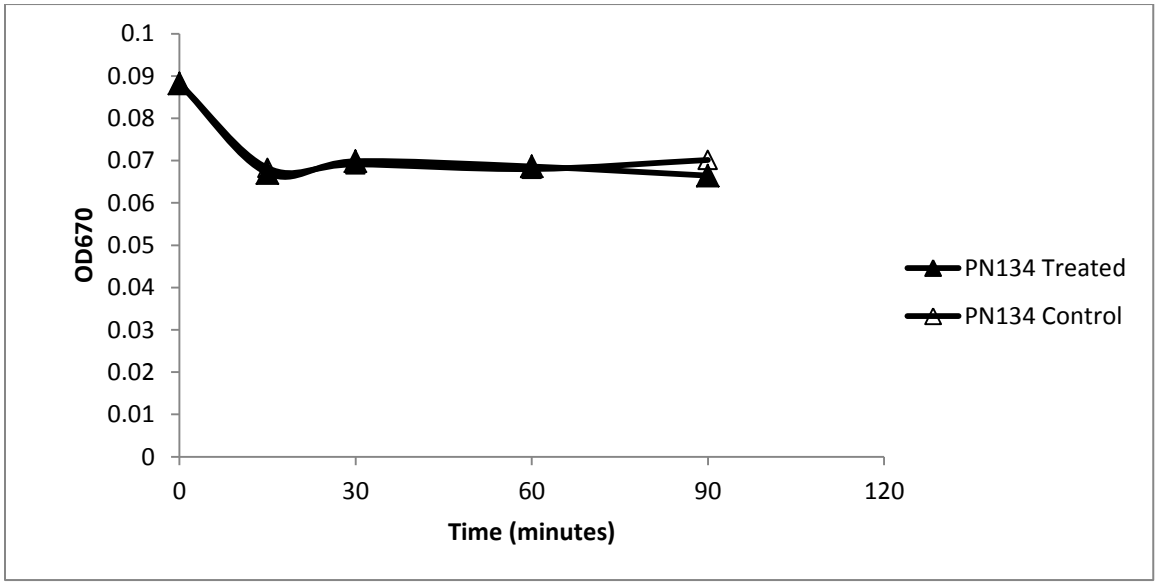

Figure 34. Optical density for the *E. coli* strain AS391, prior to xanthine oxidase assay measurements at pH 6.5. The strains were started 1.5 hours after the start of the first strains and were grown for the appropriate time frame in LB broth at 37°C before use. The measurements were taken using a UV Vis microplate reader at the wavelength of 670 nm. Samples were taken from the xanthine oxidase reaction tubes and measured before undergoing centrifugation.

DISCUSSION

The Purpose of Determining Growth Curves

E. coli growth has 4 phases: lag, log, stationary, and death. The focus of these experiments requires the log and stationary phases to be known. The timing of these phases needs to be consistently replicated for each experiment. Since each *E. coli* strain may have different timing for their phases, the phases needed to be determined for each sub strain. The knockout strains (AS391, AS393, PN134) and ATCC4157 reached stationary phase at 6 hours. Whereas DH10B reached stationary phase at 7 hours and MG1655/W3110 reached stationary phase at 9 hours.

Relationship between Optical Density and the Number of Cells

The optical density is a measure of the turbidity of the cell suspension. Different strains of *E. coli* have different characteristics that affect the optical density. For example, different strains can exhibit different light scattering due to lipopolysaccharides in the outer membrane of the bacteria. Samples of two different strains might give similar optical density measurements, but have different total number of cells. This was true for the strains in these experiments. DH10B, MG1655, and W3110 all shared similar low cell numbers at an OD of 0.1 during log phase of $7x10^5$ cells/mL, $1.2x10^6$ cells/mL, and $1.2x10^6$ cells/mL. Whereas AS391, AS391, and PN134 had similar high cell numbers of $8x10^6$ cells/mL, $1.3x10^7$ cells/mL, and $9x10^6$ cells/mL. A large disparity occurred during stationary phase with DH10B, MG1655, and W3110 having $3x10^7$ cells/mL, $7.3x10^5$ cells/mL, and $8x10^5$ cells/mL respectively, while AS391, AS393, and PN134 had cell numbers of $2x10^6$ cells/mL, $6x10^6$ cells/mL, and $3x10^6$ cells/mL respectively. AS391, AS393, and PN134 were all derived from the same strain and have similar numbers. These differences should be taken into account when comparing the 6 strains.

Assessing Cell Viability with the SYTO9 and PI Nucleic Acid Dyes

When using fluorescence assays to assess cell viability it is essential to calibrate the dye concentrations for each strain. The fluorescence increases as dye concentration increases until a plateau is reached when all cells are stained. The fluorescence measurements may decrease at higher dye concentrations due to dye quenching. Previous experiments narrowed the concentration range for SYTO9 to 0.1 to 10 µM (Patterson 2010). These experiments also observed a high concentration of SYTO9 (16 µM) was required for saturation which differs from results obtained in this study (Patterson 2010). For the experiments in this study, the optimal concentration determined for each strain ranged from 2 to 4 µM. ATCC4157 had the largest optimal SYTO9 concentration (4 µM), while the other strains had lower amounts with AS391, AS393, and PN134 at 3 µM, and DH10B, MG1655, and W3110 at 2 µM. All optimal dye concentrations are for a particular number of cells as determined by optical density. The previous experiments used a cell suspension that had an OD_{670} of 0.05 (Patterson 2010). A cell density of 0.05 was used in these experiments as well. Larger cell densities may cause disproportionality between cell and dye concentrations.

The concentration range for the nucleic acid dye propidium iodine (PI) in previous experiments was 1 to 100 µM (Patterson 2010). The optimal dye concentration for the strains used in these experiments ranged from 20 to 30 µM. The PI concentration was 30 µM which was the optimal PI concentration for AS391, AS393, PN134, and DH10B. MG1655 and W3110 had an optimal PI concentration of 25 µM, whereas ATCC4157 was at 20 µM. These concentrations were relatively high.

Normally, at low concentration the fluorescence intensity will be proportional to the concentration of the fluorophore. However at higher concentrations, the inner filter effects need to be accounted for. There are two types of inner filter effects, the first is absorption.

Fluorophores may absorb some of the excitation light which lowers the intensity of the excitation light. When the fluorophores at the edge of the sample will absorb the excitation light, a smaller amount of the light reaches the fluorophores in the center of the solution. These fluorophores at the center are normally the ones that are measured by the spectrophotometer. The second inner filter effect is reabsorption. This occurs when a molecule absorbs the wavelengths at which the fluorophore emits. A fluorophore will be emitting light; however a molecule will absorb this light and prevent the light from being detected. Since the inner filter effects change the intensity of the emitted light, they need to be considered when the experiments are based on the amount of emitted light to determine the percentage of live to dead cells. When the sum of the absorbance at the excitation and emission wavelengths exceeds 0.08, the inner filter effects cause a decrease in fluorescence (Palmier and Doren 2007). Table 3 shows that when SYTO9 and PI are combined in solution, the sum of the absorbance at the excitation and emission wavelengths does exceed 0.08. This means that inner filter effects are occurring. The use of a standard curve can work around this problem to a certain degree. However, inner filter effects should be considered when interpreting the data.

Assessing Paraquat Toxicity with Optical Density

The growth of the three knockout *E. coli* strains were reduced in the presence of paraquat. This is different as compared to results obtained previously. Previous studies indicated that optical density increased, but a plateau of CFUs was reached when treated with paraquat (Patterson 2010). However, the results relied upon CFUs and not absorbance values, which may account for the discrepancies. AS391 and PN134 were effected more than AS393, with PN134 being the most effected. This makes sense considering which SODs are knocked out. AS393 is the periplasmic knockout, which is also known as the exogenous SOD knockout. AS393 is missing Cu/Zn-SOD, which is normally expressed during

stationary phase of *E. coli* growth. PN134 is the cytoplasmic or endogenous SOD knockout. PN134 lacks Mn-SOD and Fe-SOD, which are normally expressed during the log phase of *E. coli* growth. AS391 is the triple knockout (lacking periplasmic and cytoplasmic SODs). Since paraquat is a source for the production of intracellular superoxide and since PN134 and AS391 are cytoplasmic SOD knockouts, it makes sense that PN134 and AS391 would be affected in the presence of paraquat. PN134 is the cytoplasmic knockout which lacks the Fe-SOD and Mn-SOD during log phase, which is the phase that paraquat is effective. AS391 is the triple knockout, which lacks both periplasmic and cytoplasmic SOD, so paraquat would affect it during log phase. Whereas AS393 is the periplasmic knockout, which lacks CuZn-SOD expressed during stationary phase so paraquat is not as effective against inhibiting growth because it mainly effects growth during log phase.

Aeration of the mixtures (specifically, shaking between readings) also affected the growth of the three strains in the presence of paraquat. For example the greater the aeration the more the growth was inhibited. When samples were only mixed for 5 seconds between 5 minute readings, the growth was only slightly inhibited for the endogenous knockouts or not inhibited at all for the exogenous knockout. However as the aeration was increased, a greater decrease in optical density occurred. Mixing the samples continuously provided that greatest growth inhibition, affecting all three knockout strains. Other mixing and reading times were assessed such as 5 minute readings with 2 minute mixing between the reading, and 5 minute readings with a 1 minute mixing between readings. The effect of paraquat on the strains depends upon which knockout it is and the amount of aeration that occurs.

Assessing Effects of Extracellular Superoxide with Xanthine/Xanthine Oxidase

The xanthine/xanthine oxidase assay is a source for exogenous superoxide. Since AS393 is missing Cu/Zn-SOD and AS391 is the triple knockout which is missing Cu/Zn-COD as well, these strain should be affected by superoxide produced by the xanthine/xanthine oxidase assay because Cu/Zn-SOD is in the periplasm of the cell. However, the xanthine/xanthine oxidase assay had puzzling effects upon the three knockout *E. coli* strains. After the initial addition of xanthine to the strains, there is a large decrease in percentage of live cells. However, as time passes it appears that the strains are recovering and growing, as determined using the fluorescence assay for cell viability. This seems very unlikely however, since the cells are removed from the growth media and then exposed to only a PPB buffer solution and the xanthine solution. Previous studies showed a decrease in 24.2% of cell viability using the xanthine/xanthine oxidase assay along with the fluorescence assay for cell viability (Patterson 2010). Thus to determine if the cells were really growing, the absorbance was measured. Since the absorbance did not increase, it was concluded that the cells were not growing in the presence of xanthine.

The protocol was changed in several ways in an attempt to see any effects of superoxide produced by xanthine/xanthine oxidase. The temperature was increased from 4°C to 27°C during centrifuging to avoid any shock to the cells, and the temperature for xanthine was increased from 4°C to 27°C to again avoid any temperature shock to the cells. The aliquot size of the treated cells was increased from 100 µM to 400 µM to gather additional treated cells for the fluorescence assay. Additionally, centrifuging times were decreased from 9 to 5 minutes to ensure cells could be resuspended more effectively and faster. These changes did not provide any different results however.

The pH of 7.5 was used first because previous experiments determined that the xanthine/xanthine oxidase assay should be more effective at that pH. Since no effects were

seen at pH 7.5, the pH was lowered to 6.5. The alteration of the pH had no decisive effect upon the knockout strains, however. Previous finding report that superoxide must be protonated before it can enter the cell (Korshunov and Imlay 2002). These researchers used similar knockout strain along with oxygen starved cells in order to detect the superoxide generated from xanthine oxidase. Oxygen was in good supply for the xanthine/xanthine oxidase which may explain why the results were different. This does however show the limitations of the xanthine/xanthine oxidase assay because superoxide is protonated at a pH of 4-5 within a phyagolysosome, however this cannot be tested because xanthine oxidase is inactive at this low of pH. It is speculated that these lack of effects are due to some factor that cannot be measured using these methods. One such idea is changes in the membrane of the bacterial cells. Changes in the membrane can occur during this assay, but cannot be detected with this assay.

REFERENCES

Baev MV, Baev D, Radek AJ, Campbell JW. Growth of *Escherichia coli* MG1655 on LB Medium: Monitoring Utilization of Amino Acids, Peptides, and Nucleotides with Transcriptional Microarrays. Applied Microbiology and Biotechnology. 2006. 71(3): 317-22.

Benov LT, Fridovich I. *Escherichia coli* Expresses a Copper- and Zinc-Containing Superoxide Dismutase. Journal of Biological Chemistry. 1994. 269(41): 25310-25314.

Bus JS, Gibson JE. Paraquat: Model for Oxidant-Initiated Toxicity. Environmental Health Perspectives. 1984. 55: 37-46.

Carlioz A, Touati D. Isolation of Superoxide Dismutase Mutants in *Escherichia coli*: is Superoxide Dismutase Necessary for Aerobic Life? The EMBO Journal. 1986. 5(3): 623-30.

Durfee T, Nelson R, Baldwin S, Plunkett G 3rd, Burland V, Mau B, Petrosino JF, Qin X, Muzny DM, Ayele M, Gibbs RA, Csorgo B, Posfai G, Weinstock GM, Blattner FR. The Complete Genome Sequence of *Escherichia coli* DH10B: Insights into the Biology of a Laboratory Workhorse. Journal of Bacteriology. 2008. 190(7): 2597-2606.

Fridovich I, Keele BB Jr, McCord JM. Superoxide Dismutase from *Escherichia coli* B. A New Manganese-Containing Enzyme. Journal of Biological Chemistry. 1970. 245(22): 6178-6181.

Fridovich I, Kitzler J, Minakami H. Effects of Paraquat on *Escherichia coli*: Differences between B and K-12 strains. Journal of Bacteriology. 1990. 172(2): 686-690.

Fridovich I, Yost FJ Jr. An Iron-Containing Superoxide Dismutase from *Escherichia coli*. Journal of Biological Chemistry. 1973. 248(14): 4905-4908.

Harrison R. Structure and Function of Xanthine Oxidoreductase: Where are we now? Free Radical Biology and Medicine. 2002. September 33(6): 774-797.

Hassan HM, Fridovich I. 1978. Superoxide Radical and the Oxygen Enhancement of the Toxicity of Paraquat in *Escherichia coli*. The Journal of Biological Chemistry. 253(22): 8143-8148.

Hassan HM, Fridovich I. Paraquat and *Escherichia coli*. Mechanism of Production of Extracellular Superoxide Radical. Journal of Biological Chemistry. 1979. 254(21): 10846-10852.

Hoerr V, Ziebuhr W, Kozitskaya S, Katzowitsch E, Holzgrabe U. Laser-Induced Fluorescence-Capillary Electrophoresis and Fluorescence Microplate Reader Measurement: Two Methods to Quantify the Effect of Antibiotics. Analytical Chemistry. 2007. 79(19): 7510-7518.

Jensen KF. The *Escherichia coli* K-12 "Wild Types" W3110 and MG1655 have an rph Frameshift Mutation that Leads to Pyrimidine Starvation due to Low pyrE Expression Levels. Journal of Bacteriology. 1993. 175(11): 3401-3407.

Keyer K. Gort A., Imlay J. Superoxide and the Production of Oxidative DNA Damage. Journal of Bacteriology. 1995. 177(23): 6782-6790.

Kohanski M, Dwyer D, Hayete B, Lawrence C, Collins J. A Common Mechanism of Cellular Death Induced by Bactericidal Antibiotics. Cell. 2007. 130: 797-810.

Koji Hayashi, Naoki Morooka, Yoshihiro Yamamoto, Katsutoshi Fujita, Katsumi Isono, Sunju Choi, Eiichi Ohtsubo, Tomoya Baba, Barry L Wanner, Hirotada Mori, and Takashi Horiuchi. Highly Accurate Genome Sequences of *Escherichia coli* K-12 Strains MG1655 and W3110. Molecular Systems Biology. 2006. 2. 2006 0007

Korshunov SS, Imlay JA. A Potential Role for Periplasmic Superoxide Dismutase in Blocking the Penetration of External Superoxide into the Cytosol of Gram-negative Bacteria. 2007. 43(1): 95-106.

Langford PR, Sansone A, Valenti P, Battistoni A, Kroll JS. Bacterial Superoxide Dismutase and Virulence. Methods in Enzymology. 2002. 349: 155-166.

Link E., Riley P. Role of Hydrogen Peroxide in the Cytotoxicity of the Xanthine/xanthine Oxidase System. Biochemical Journal. 1988. 249: 391-399.

Miao Lu, St. Clair DK. Regulation of Superoxide Dismutase Genes: Implications in Disease. Free Radical Biology & Medicine. 2009. 47: 344-356.

McCord JM, Fridovich I. The Reduction of Cytochrome c by Milk Xanthine Oxidase. Journal of Biological Chemistry. 1968. 243(21): 5753-5760.

Palmier M., Doren S. Rapid Determination of Enzyme Kinetics from Fluorescence: Overcoming the Inner Filter Effect. Journal of Analytical Biochemistry. 2007. 371(1): 43-51.

Patterson J. Assessment of the Effects of Supoeroxide-generating Agents on the Growth and Viability of *Escherichia coli* using Traditional Microbiological Methods and the Baclight Viability Stain. M.S. Thesis. Western Carolina University. 2010.

Wilhelm J. Metabolic Aspects of Membrane Lipid Peroxidation. ACTA Universitatis Carolinae Medica Monographia. 1990. 137:1-53.

Xie L, Zhu X, Hu Y, Li T, Gao Y, Shi Y, Tang S. Mitochondrial DNA Oxidative Damage Triggering Mitochondrial Dysfunction and Apoptosis in High Glucose-induced HRECs. Investigative Ophthalmology and Visual Science. 2008. 49(9): 4203-4209.

Zaremba T., Olinski R. Oxidative DNA Damage--Analysis and Clinical Significance. Postepy Biochemii. 2010. 56(2): 124-38.

APPENDIX A

Optical Density Measurements and Cell Counts

Cell counts were measured for each *E. coli* strain at both log and stationary phases. A different relationship between the optical density measurements and cell count was found for each strain; however each strain had a positive correlation between cells per mL and optical density (Figure 1-12).

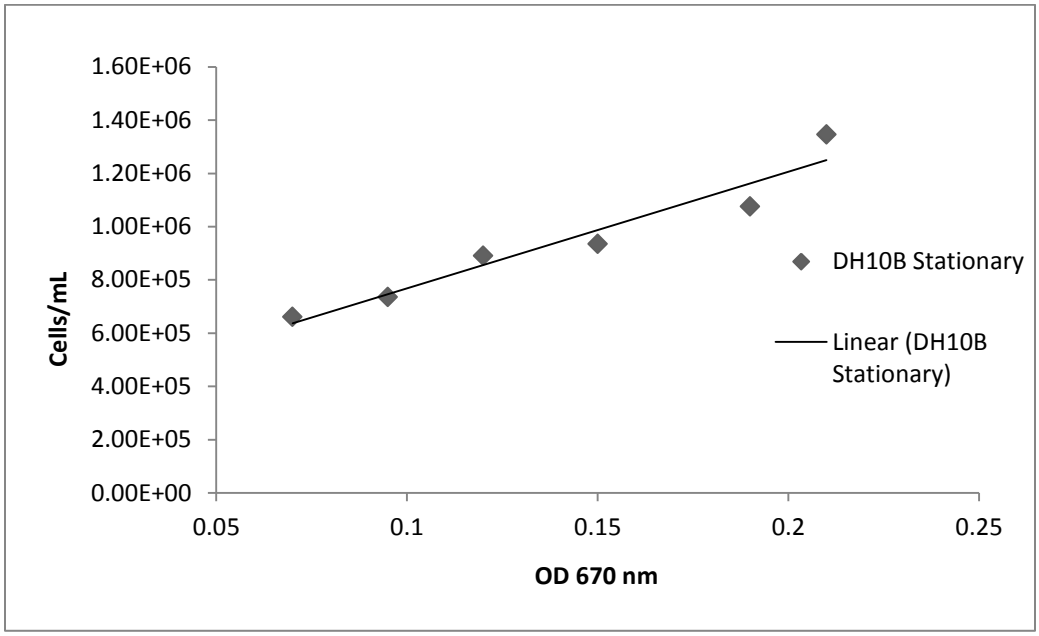

Figure 1. Relationship between the total cell count and optical density at 670 nm for the stationary phase *E. coli* strain DH10B. Measurements were taken using a Spec 20, at 670 nm wavelength, at a constant temperature of 37°C. Strains were grown at 37°C in LB prior to the start.

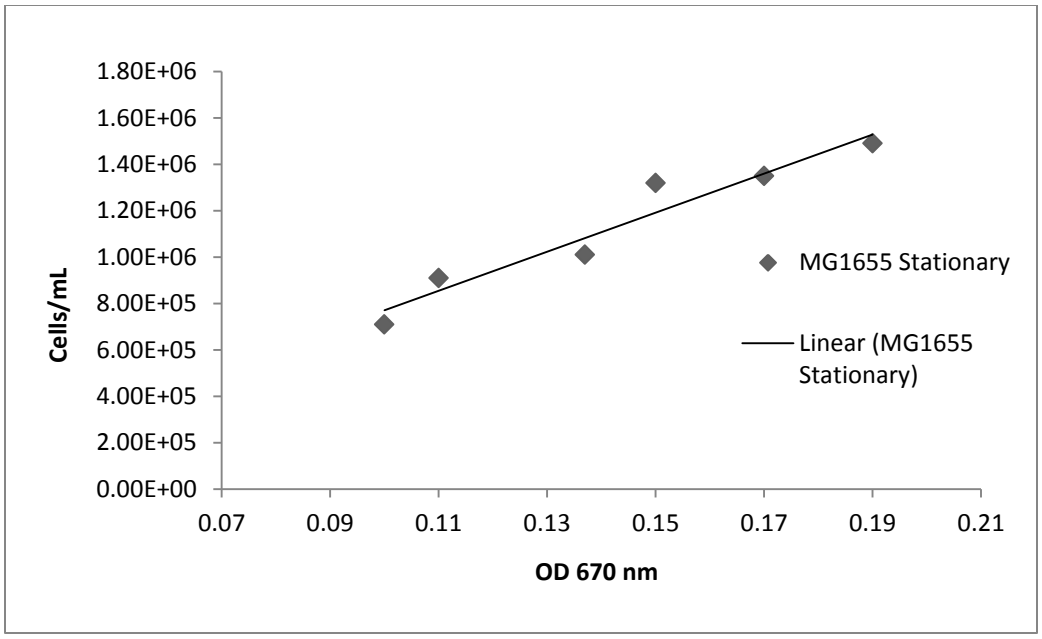

Figure 2. Relationship between the total cell count and optical density at 670 nm for the stationary phase *E. coli* strain MG1655. Measurements were taken using a Spec 20, at 670 nm wavelength, at a constant temperature of 37°C. Strains were grown at 37°C in LB broth prior to the start.

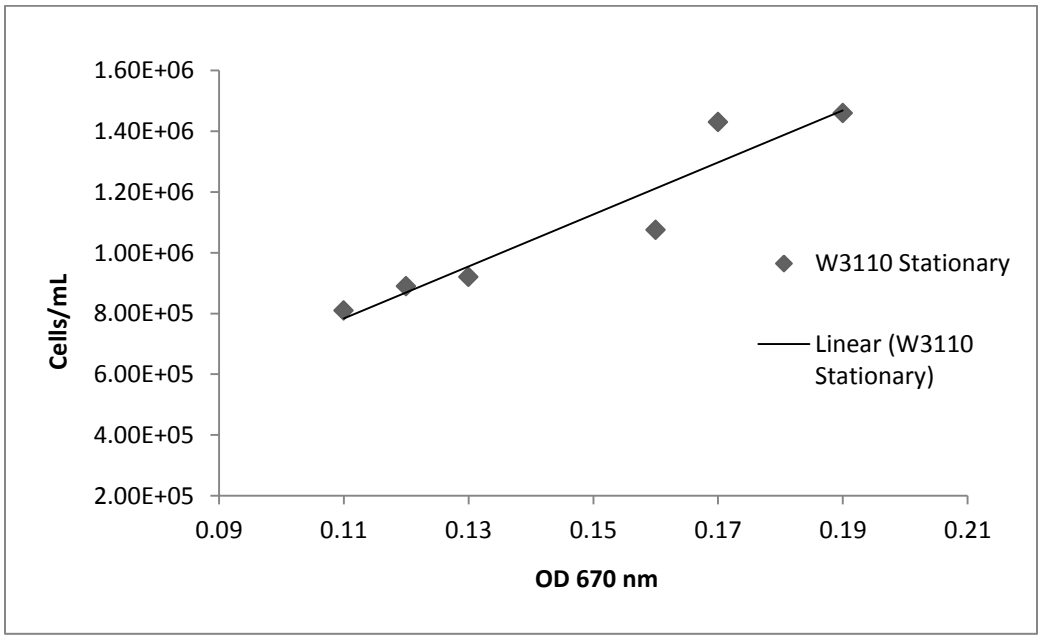

Figure 3. Relationship between the total cell count and optical density at 670 nm for the stationary phase *E. coli* strain W3110. Measurements were taken using a Spec 20, at 670 nm wavelength, at a constant temperature of 37°C. Strains were grown at 37°C in LB prior to the start.

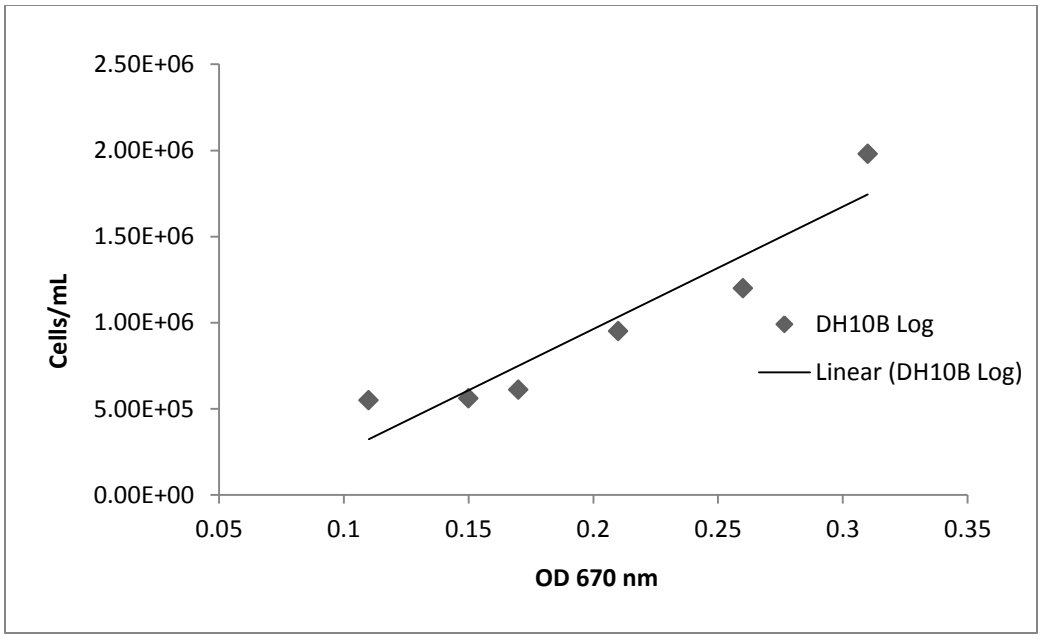

Figure 4. Relationship between the total cell count and optical density at 670 nm for the log phase *E. coli* strain DH10B. Measurements were taken using a Spec 20, at 670 nm wavelength, at a constant temperature of 37°C. Strains were grown at 37°C in LB prior to the start.

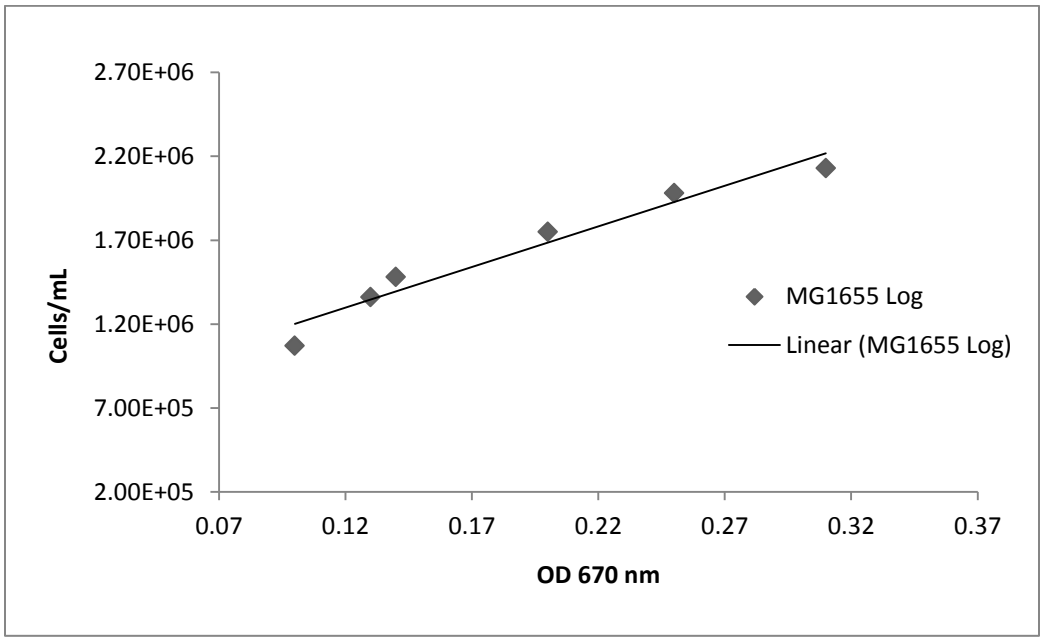

Figure 5. Relationship between the total cell count and optical density at 670 nm for the log phase *E. coli* strain MG1655. Measurements were taken using a Spec 20, at 670 nm wavelength, at a constant temperature of 37°C. Strains were grown at 37°C in LB broth prior to the start.

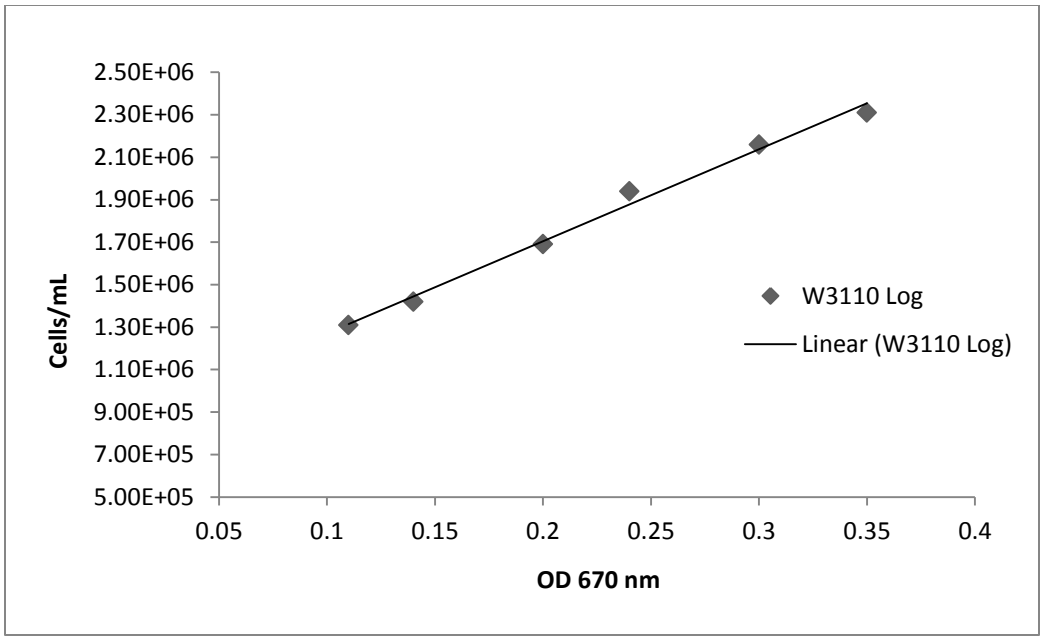

Figure 6. Relationship between the total cell count and optical density at 670 nm for the log phase *E. coli* strain W3110. Measurements were taken using a Spec 20, at 670 nm wavelength, at a constant temperature of 37°C. Strains were grown at 37°C in LB broth prior to the start.

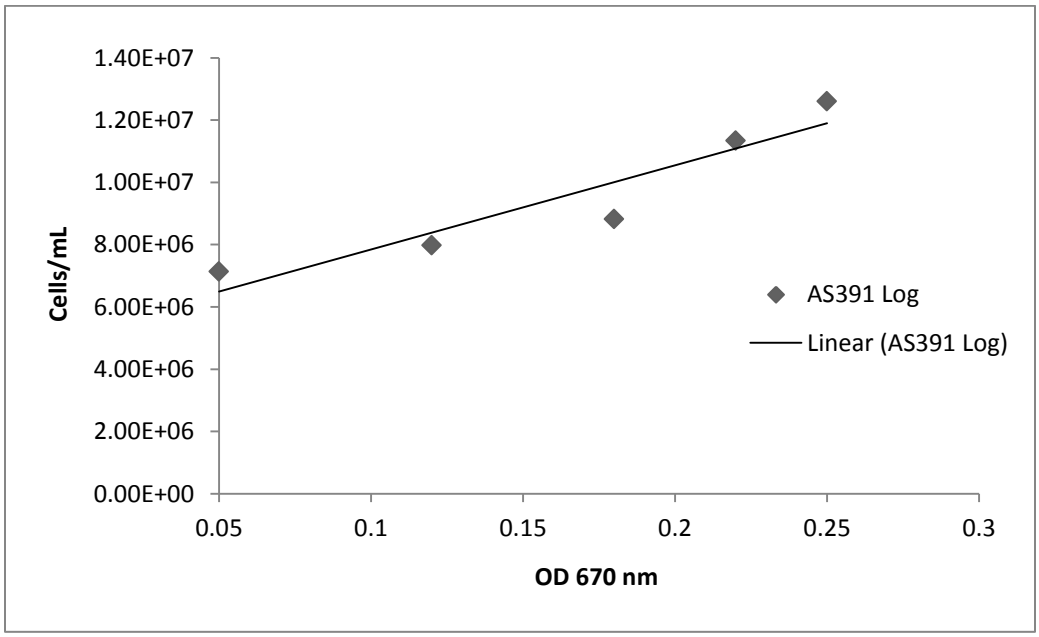

Figure 7. Relationship between the total cell count and optical density at 670 nm for the log phase *E. coli* strain AS391. Measurements were taken using a Spec 20, at 670 nm wavelength, at a constant temperature of 37°C. Strains were grown at 37°C in LB broth supplemented with 0.2% glucose prior to the start.

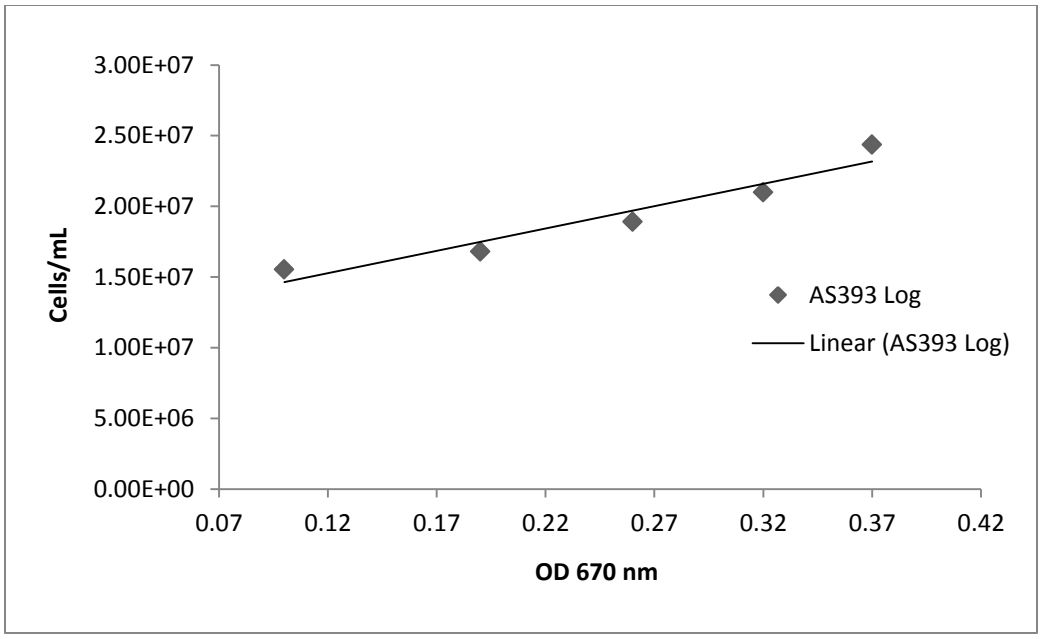

Figure 8. Relationship between the total cell count and optical density at 670 nm for the log phase *E. coli* strain AS393. Measurements were taken using a Spec 20, at 670 nm wavelength, at a constant temperature of 37°C. Strains were grown at 37°C in LB broth supplemented with 0.2% glucose prior to the start.

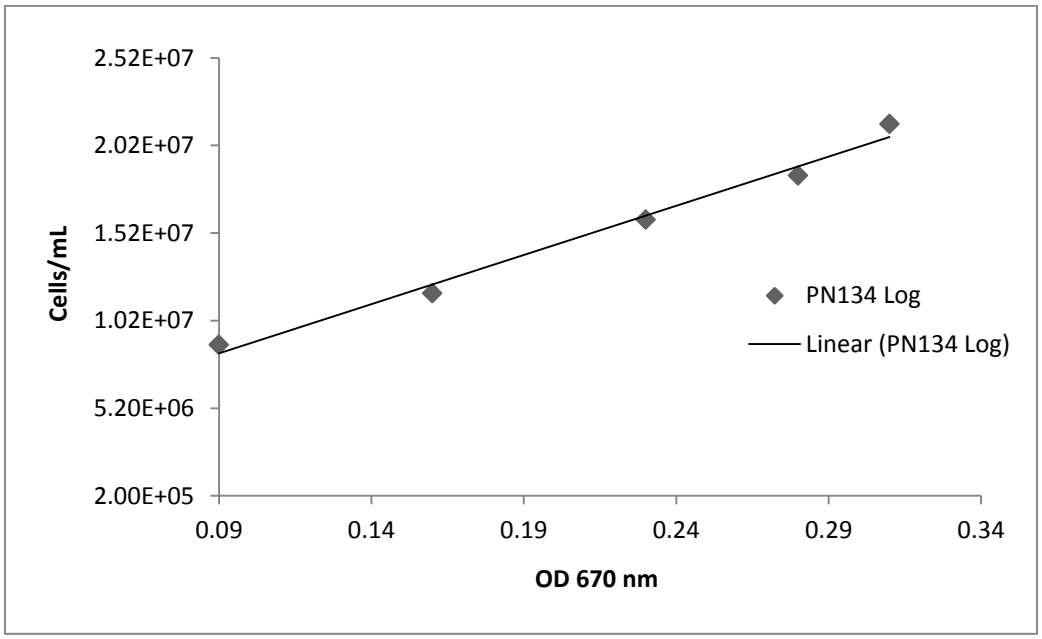

Figure 9. Relationship between the total cell count and optical density at 670 nm for the log phase *E. coli* strain PN134. Measurements were taken using a Spec 20, at 670 nm wavelength, at a constant temperature of 37°C. Strains were grown at 37°C in LB broth supplemented with 0.2% glucose prior to the start.

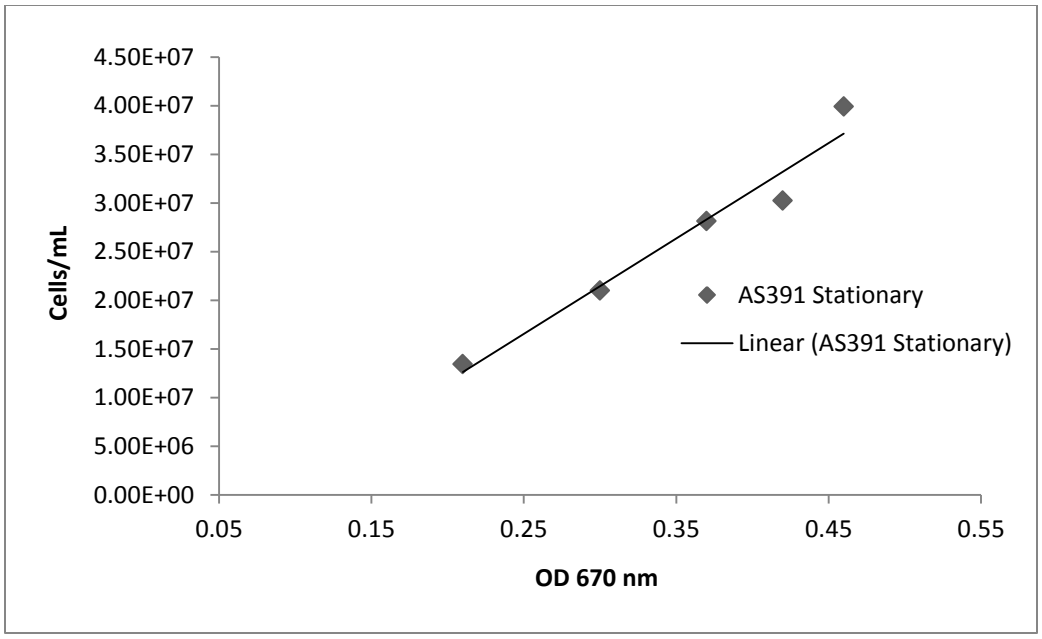

Figure 10. Relationship between the total cell count and optical density at 670 nm for the stationary phase *E. coli* strain AS391. Measurements were taken using a Spec 20, at 670 nm wavelength, at a constant temperature of 37°C. Strains were grown at 37°C in LB broth supplemented with 0.2% glucose prior to the start.

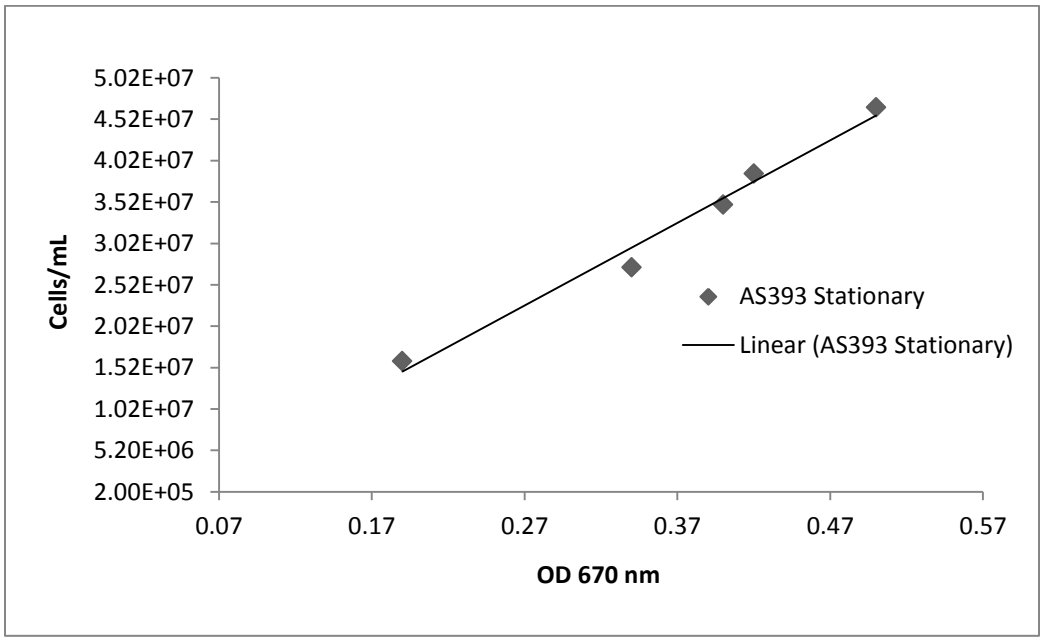

Figure 11. Relationship between the total cell count and optical density at 670 nm for the stationary phase *E. coli* strain AS393. Measurements were taken using a Spec 20, at 670 nm wavelength, at a constant temperature of 37°C. Strains were grown at 37°C in LB broth supplemented with 0.2% glucose prior to the start.

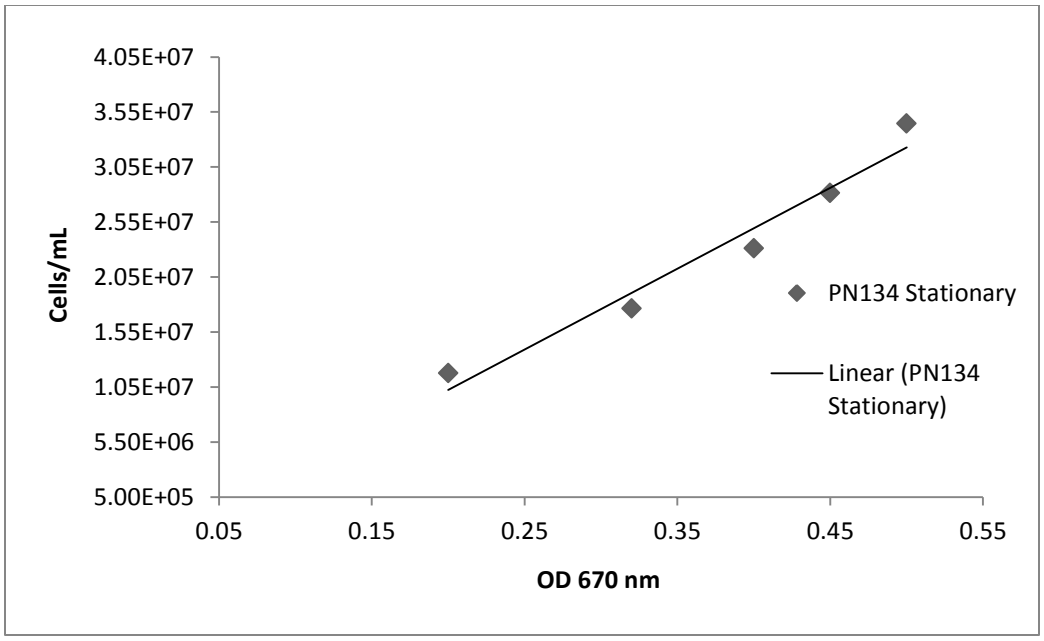

Figure 12. Relationship between the total cell count and optical density at 670 nm for the stationary phase *E. coli* strain PN134. Measurements were taken using a Spec 20, at 670 nm wavelength, at a constant temperature of 37°C. Strains were grown at 37°C in LB broth supplemented with 0.2% glucose prior to the start.

Method of Mixing for SYTO9/PI Calibration for DH10B, MG1655, and W3110

The first method of mixing for cell resuspension was vortexing. When results from the PI calibration did not produce any linear relationship between the fluorescence and the concentrations of the two dyes, a new method of mixing occurred. The second mixing method was simple inversion, which was shown to be the better mixing method (Figures 13-14).

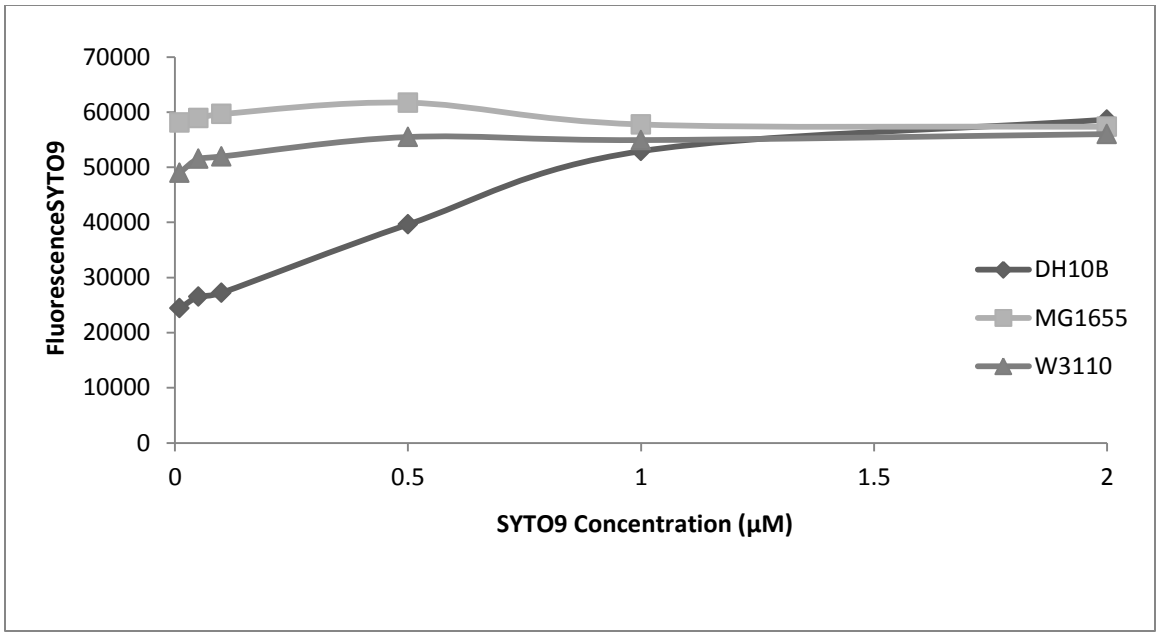

Figure 13. SYTO9 Saturation Curve for the three *E. coli* strains: DH10B, MG1655, and W3110 using vortexing for cell resuspension. Readings were taken using a fluorescence microplate reader with an excitation wavelength of 480 nm and emission of 520 nm. Strains were grown at 37°C in LB glucose prior to the start.

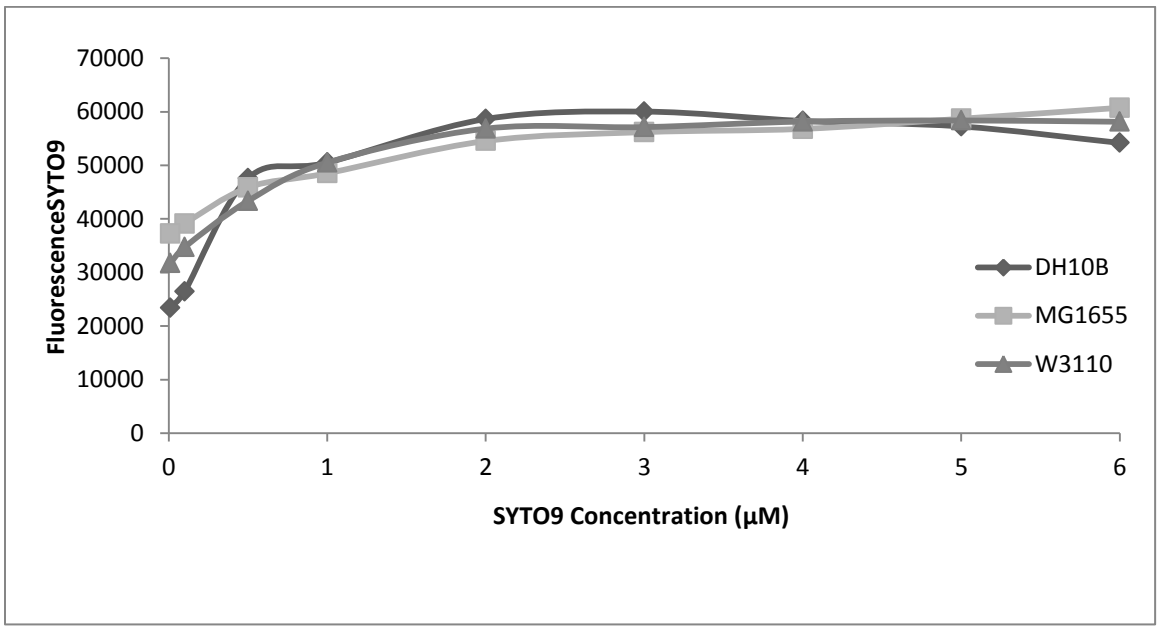

Figure 14. SYTO9 Saturation Curve for the three *E. coli* strains: DH10B, MG1655, and W3110 using gentle inversion for cell resuspension. Readings were taken using a fluorescence microplate reader with an excitation wavelength of 480 nm and emission of 520 nm. Strains were grown at 37°C in LB broth prior to the start.

SYTO9/PI Calibration for DH10B, MG1655, and W3110

SYTO9 and PI were calibrated for the *E. coli* strains DH10B, MG1655, and W3110. The range of dye used for the propidium iodine had to be expanded to a wider range, from 1 to 100 μM, because linearity between the two fluorophores and live to dead ratios had not occurred at the range of 0.01 to 20 μM (Figures 15-17). Using this wider range, the propidium iodine concentration was narrowed down for further experiments.

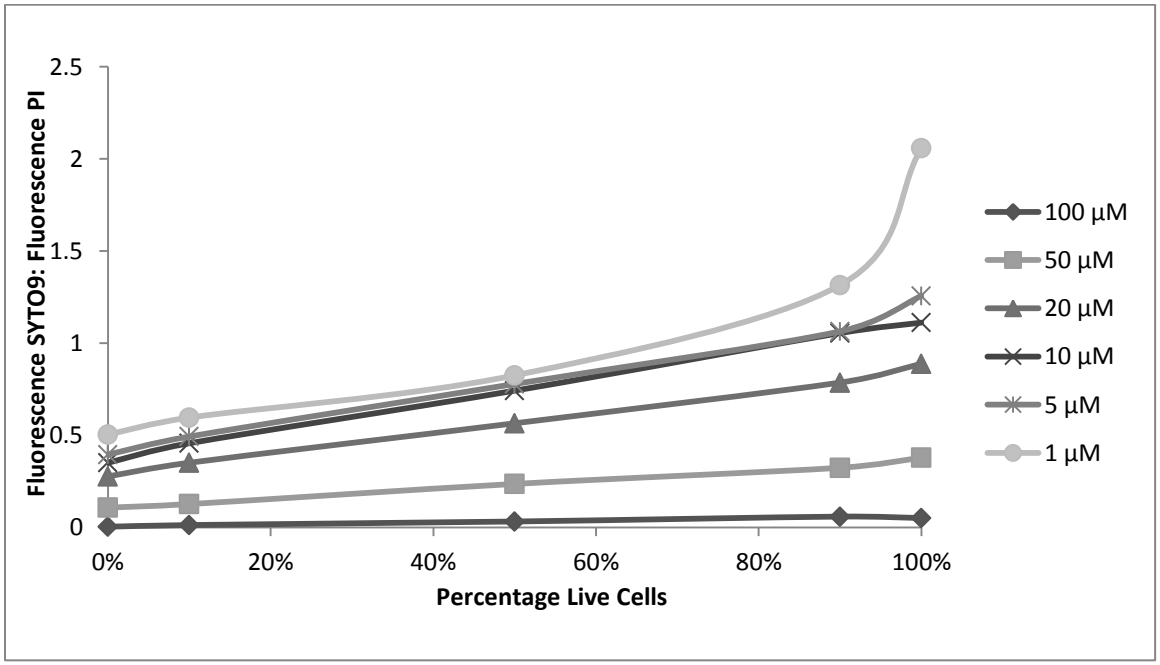

Figure 15. Propidium Iodine Saturation Curve for DH10B. A live: dead assay for the adequate concentration level of propidium iodine fluorophore. The SYTO9 fluorophore was used at a different concentration level for each strain. Strains were grown at 37°C in LB broth prior to the start. The measurements were recorded using a fluorescence microplate reader, using an excitation wavelength of 480 nm and emission of 520 nm for SYTO9 and emission of 612 nm for PI, and the strain was prepared using the 2 nucleic acids from the fluorescence assay.

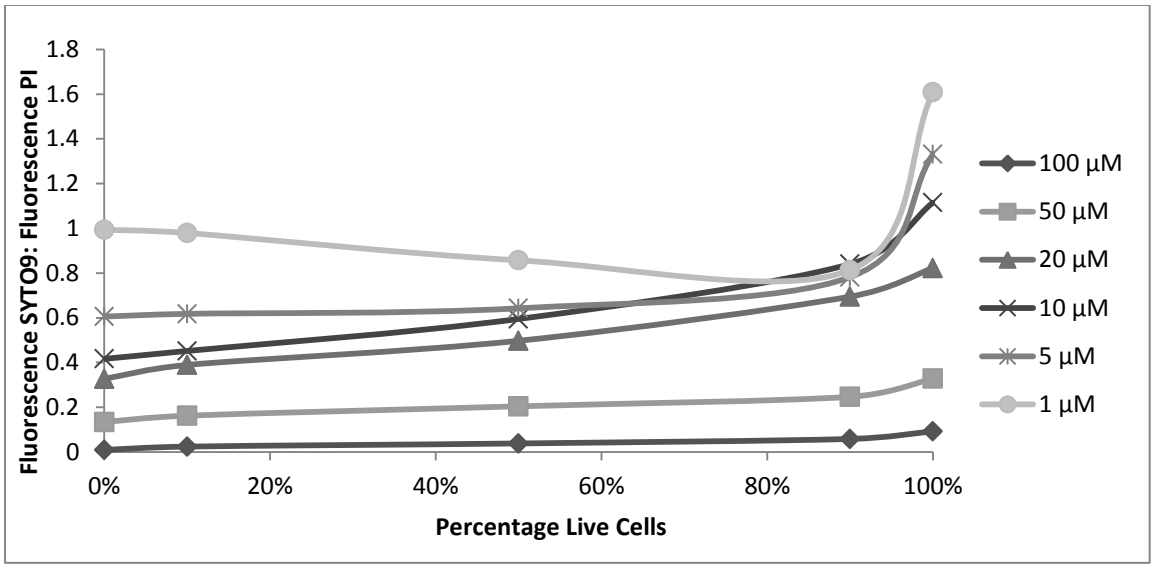

Figure 16. Propidium Iodine Saturation Curve for MG1655. A live: dead assay for the adequate concentration level of propidium iodine fluorophore. The SYTO9 fluorophore was used at a different concentration level for each strain. Strains were grown at 37°C in LB broth prior to the start. The measurements were recorded using a fluorescence microplate reader, using an excitation wavelength of 480 nm and emission of 520 nm for SYTO9 and emission of 612 nm for PI, and the strain was prepared using the 2 nucleic acids from the fluorescence assay.

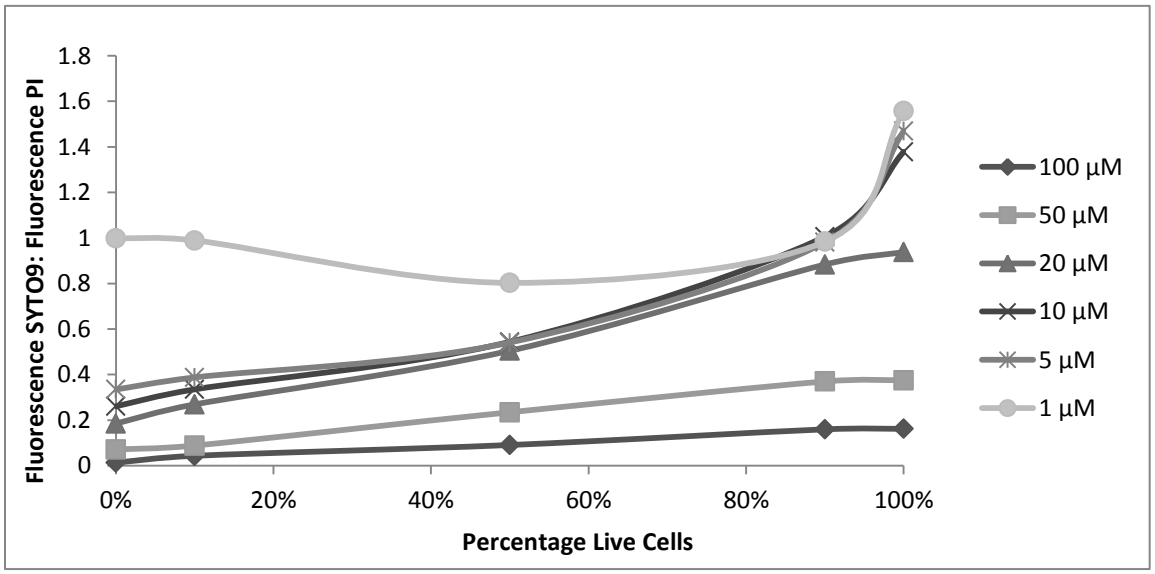

Figure 17. Propidium Iodine Saturation Curve for W3110. A live: dead assay for the adequate concentration level of propidium iodine fluorophore. The SYTO9 fluorophore was used at a different concentration level for each strain. Strains were grown at 37°C in LB broth prior to the start. The measurements were recorded using a fluorescence microplate reader, using an excitation wavelength of 480 nm and emission of 520 nm for SYTO9 and emission of 612 nm for PI, and the strain was prepared using the 2 nucleic acids from the fluorescence assay.

SYTO9/PI Calibration for the Knockout Strains AS391, AS393, and PN134

SYTO9 and PI were calibrated for the *E. coli* strains AS391, AS393, and PN134. For these three strains, like the previous strains, the range of SYTO9 dye concentrations tested was 0.1 to 6 μM. The range of dye used for the propidium iodine for these strains was the same range as before, between 10 to 40 μM (Figure 18-20).

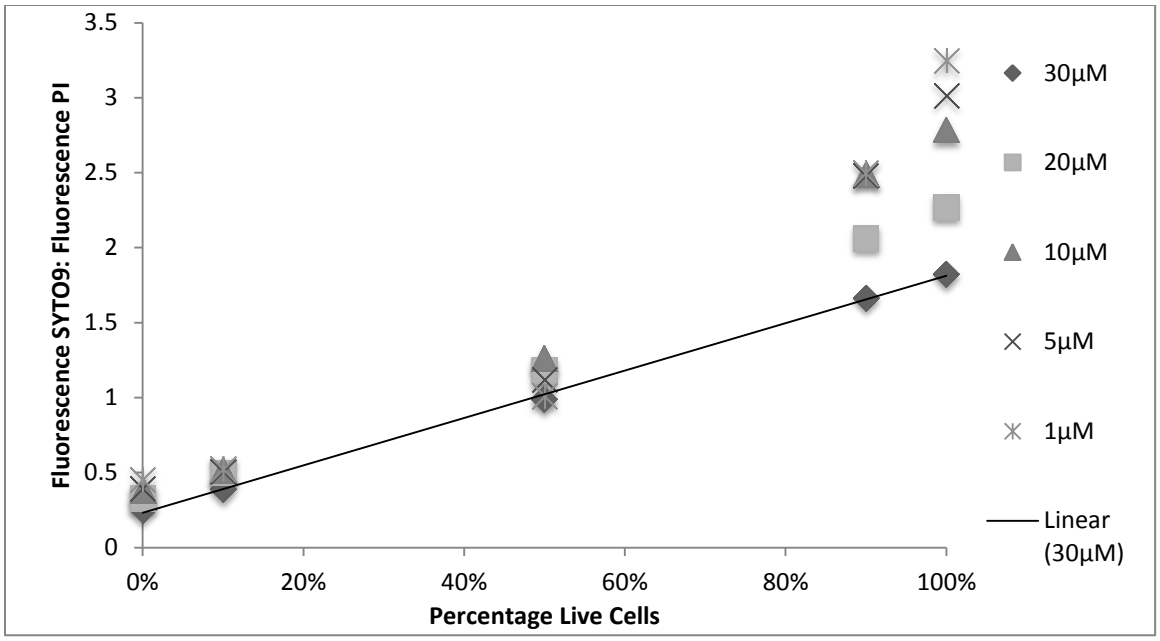

Figure 18. Propidium Iodine Saturation Curve for AS391. A live: dead assay for the adequate concentration level of propidium iodine fluorophore. The SYTO9 fluorophore was used at a different concentration level for each strain. Strains were grown at 37°C in LB broth supplemented with 0.2% glucose prior to the start. The measurements were recorded using a fluorescence microplate reader, using an excitation wavelength of 480 nm and emission of 520 nm for SYTO9 and emission of 612 nm for PI, and the strain was prepared using the 2 nucleic acids from the fluorescence assay.

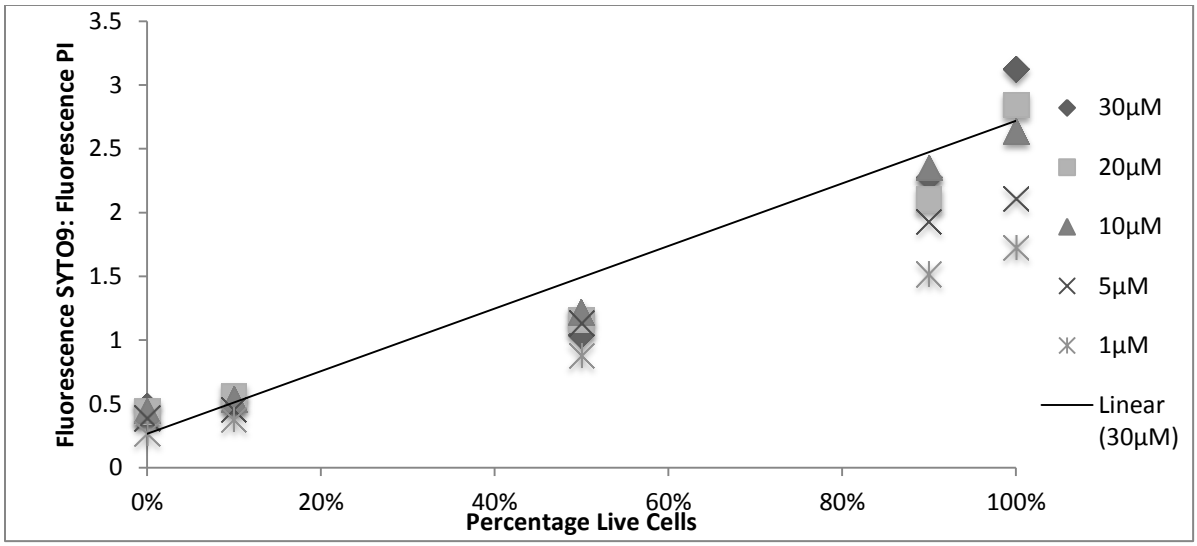

Figure 19. Propidium Iodine Saturation Curve for AS393. A live: dead assay for the adequate concentration level of propidium iodine fluorophore. The SYTO9 fluorophore was used at a different concentration level for each strain. Strains were grown at 37°C in LB broth supplemented with 0.2% glucose prior to the start. The measurements were recorded using a fluorescence microplate reader, using an excitation wavelength of 480 nm and emission of 520 nm for SYTO9 and emission of 612 nm for PI, and the strain was prepared using the 2 nucleic acids from the fluorescence assay.

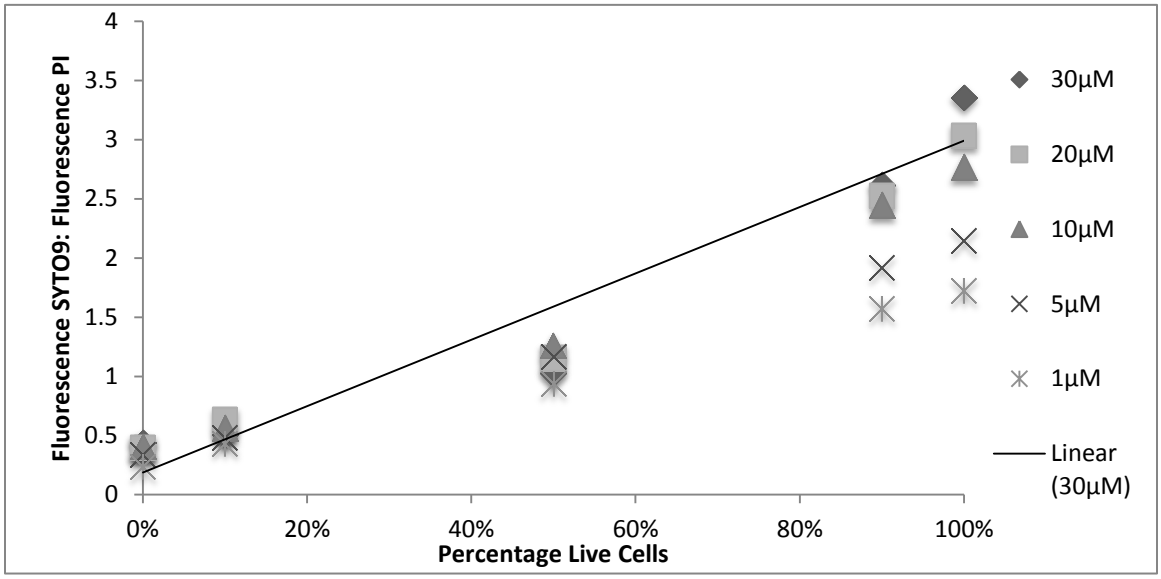

Figure 20. Propidium Iodine Saturation Curve for PN134. A live: dead assay for the adequate concentration level of propidium iodine fluorophore. The SYTO9 fluorophore was used at a different concentration level for each strain. Strains were grown at 37°C in LB broth supplemented with 0.2% glucose prior to the start. The measurements were recorded using a fluorescence microplate reader, using an excitation wavelength of 480 nm and emission of 520 nm for SYTO9 and emission of 612 nm for PI, and the strain was prepared using the 2 nucleic acids from the fluorescence assay.

Paraquat Assay

The effects of 50µM paraquat solution on the three SOD knockout *E. coli* strains were assessed. Samples were allowed to aerate for 15 minute prior to the addition of paraquat. The treated cell samples were mixed by the UV/Vis platereader using various mixing times ranging from 5 seconds to mixing continuously (Figure 21-29).

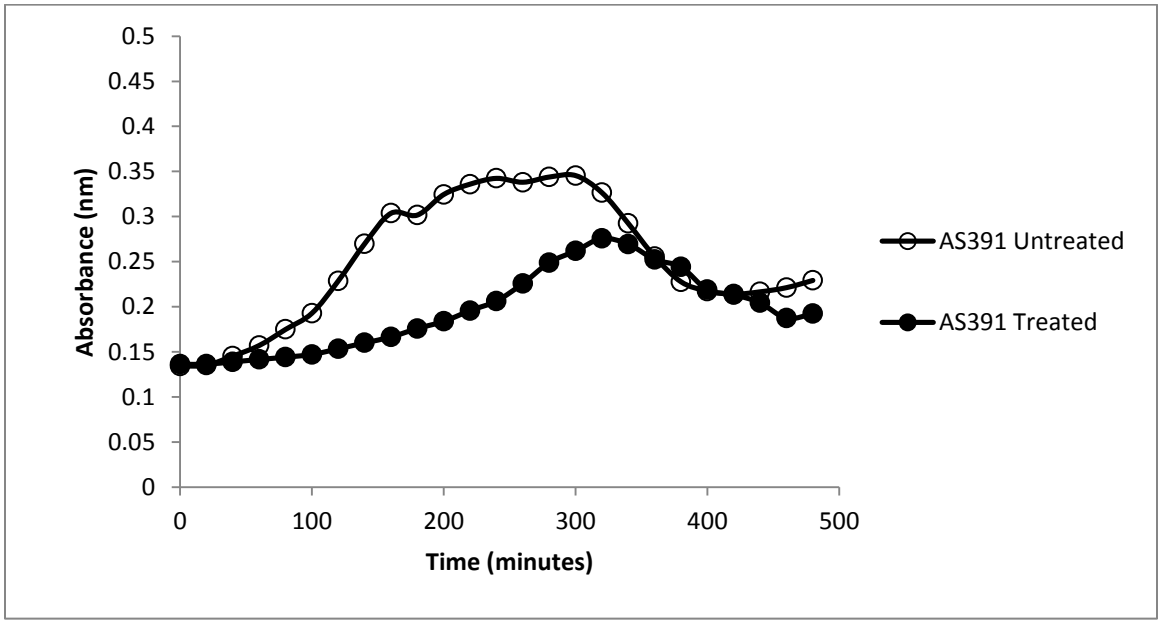

Figure 21. Growth Curve with Paraquat Treatment for the *E. coli* strain: AS391. The strain was grown in an LB media broth and aerated for 15 minutes before starting. Treated received paraquat after the 15 minutes of aeration. Measurements were taken using a UV/Vis platereader, at 670 nm wavelength, at a constant temperature of 37°C and samples were mixed for 5 seconds before each reading.

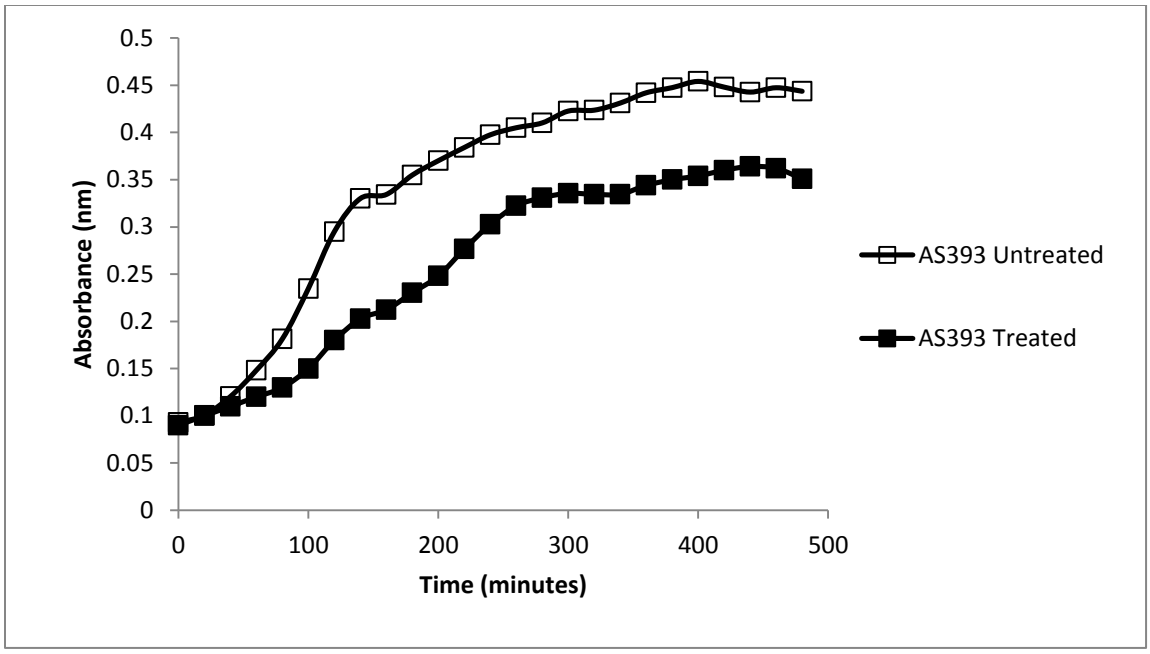

Figure 22. Growth Curve with Paraquat Treatment for the *E. coli* strain: AS393. The strain was grown in an LB media broth and aerated for 15 minutes before starting. Treated received paraquat after the 15 minutes of aeration. Measurements were taken using a UV/Vis platereader, at 670 nm wavelength, at a constant temperature of 37°C and samples were mixed for 5 seconds before each reading.

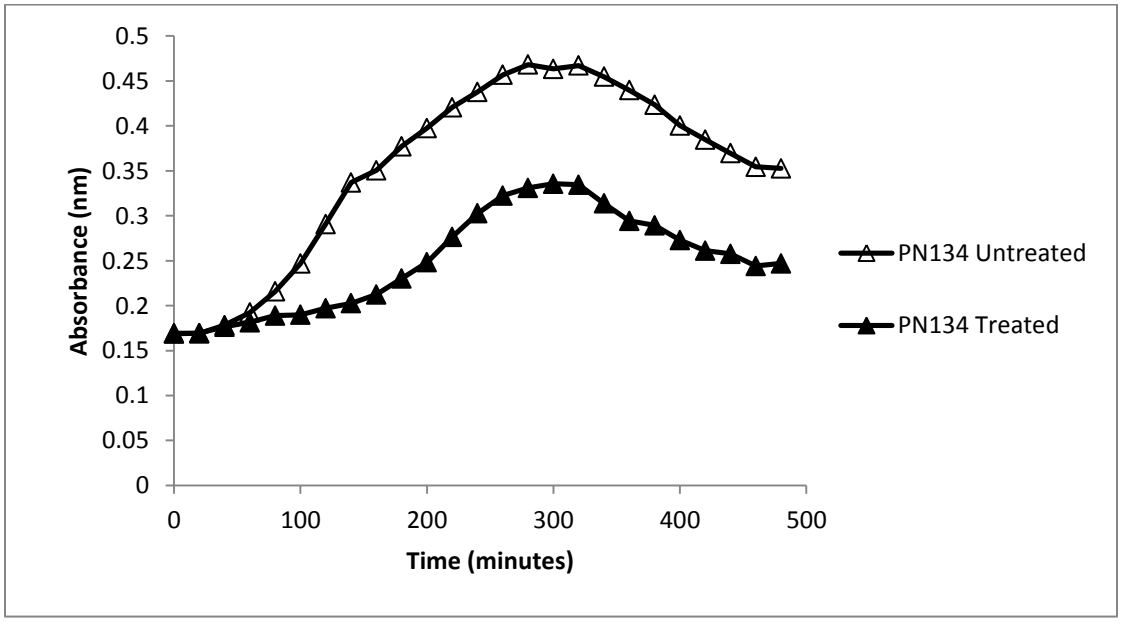

Figure 23. Growth Curve with Paraquat Treatment for the *E. coli* strain: PN134. The strain was grown in an LB media broth and aerated for 15 minutes before starting. Treated received paraquat after the 15 minutes of aeration. Measurements were taken using a UV/Vis platereader, at 670 nm wavelength, at a constant temperature of 37°C and samples were mixed for 5 seconds before each reading.

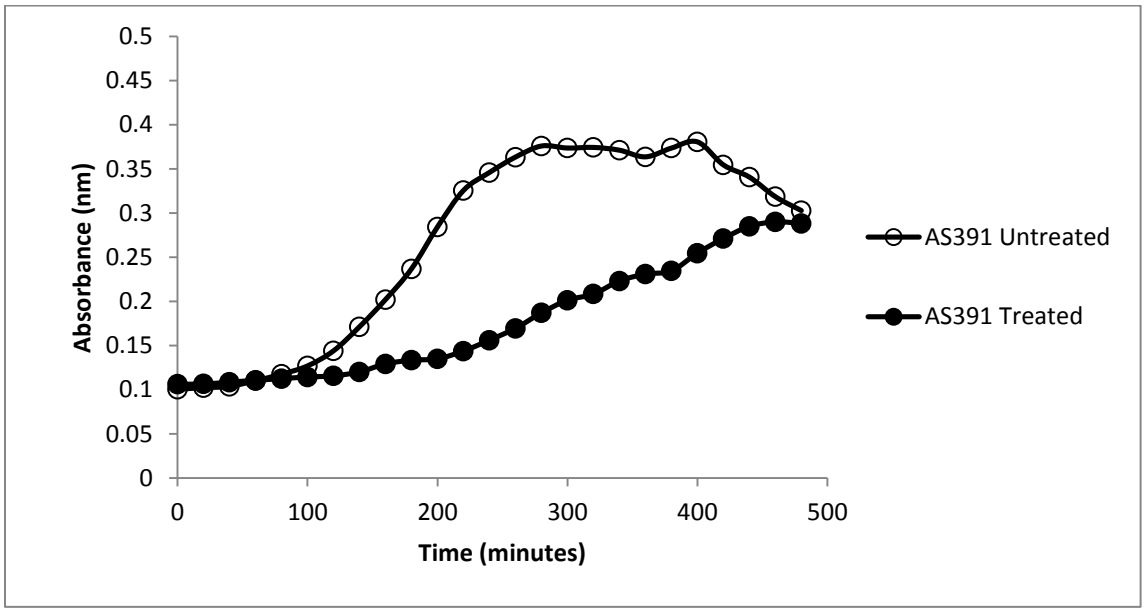

Figure 24. Growth Curve with Paraquat Treatment for the *E. coli* strain: AS391. The strain was grown in an LB media broth and aerated for 15 minutes before starting. Treated received paraquat after the 15 minutes of aeration. Measurements were taken using a UV/Vis platereader, at 670 nm wavelength, at a constant temperature of 37°C and samples were mixed for 5 seconds before each reading.

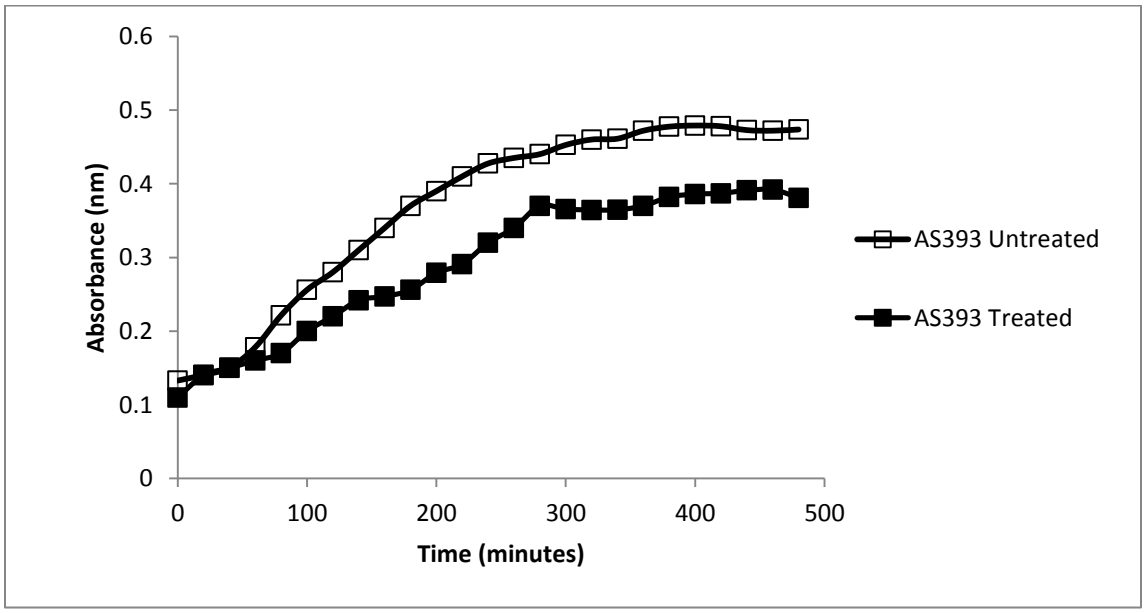

Figure 25. Growth Curve with Paraquat Treatment for the *E. coli* strain: AS393. The strain was grown in an LB media broth and aerated for 15 minutes before starting. Treated received paraquat after the 15 minutes of aeration. Measurements were taken using a UV/Vis platereader, at 670 nm wavelength, at a constant temperature of 37°C and samples were mixed for 5 seconds before each reading.

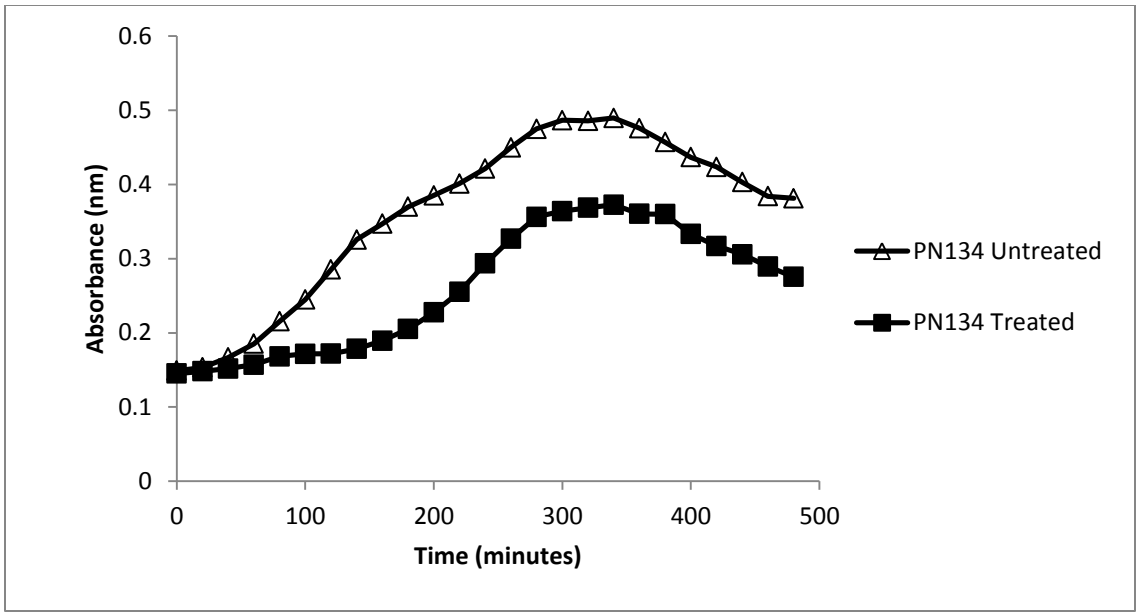

Figure 26. Growth Curve with Paraquat Treatment for the *E. coli* strain: PN134. The strain was grown in an LB media broth and aerated for 15 minutes before starting. Treated received paraquat after the 15 minutes of aeration. Measurements were taken using a UV/Vis platereader, at 670 nm wavelength, at a constant temperature of 37°C and samples were mixed for 5 seconds before each reading.

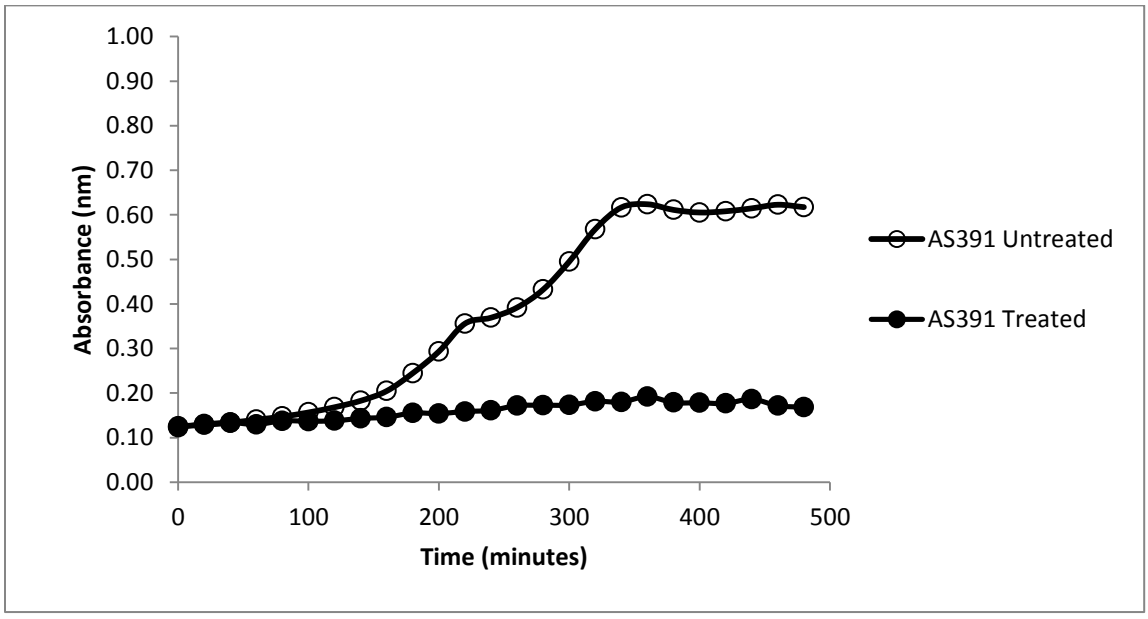

Figure 27. Growth Curve with Paraquat Treatment for the *E. coli* strain: AS391. The strain was grown in an LB media broth and aerated for 15 minutes before starting. Treated received paraquat after the 15 minutes of aeration. Measurements were taken using a UV/Vis platereader, at 670 nm wavelength, at a constant temperature of 37°C and samples were mixed continuously.

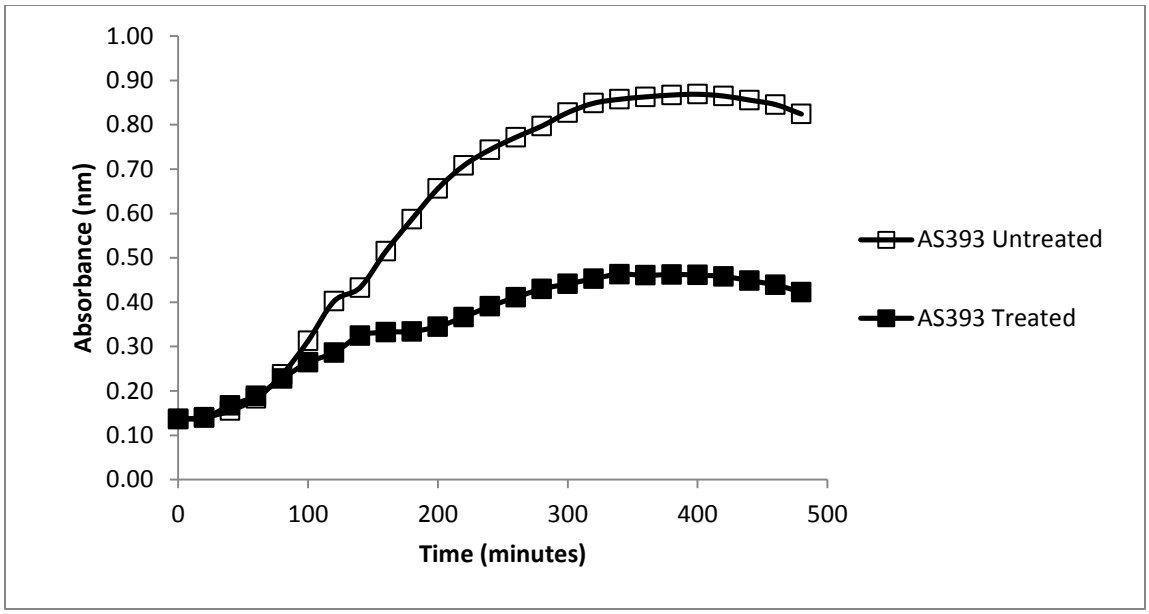

Figure 28. Growth Curve with Paraquat Treatment for the *E. coli* strain: AS393. The strain was grown in an LB media broth and aerated for 15 minutes before starting. Treated received paraquat after the 15 minutes of aeration. Measurements were taken using a UV/Vis platereader, at 670 nm wavelength, at a constant temperature of 37°C and samples were mixed continuously.

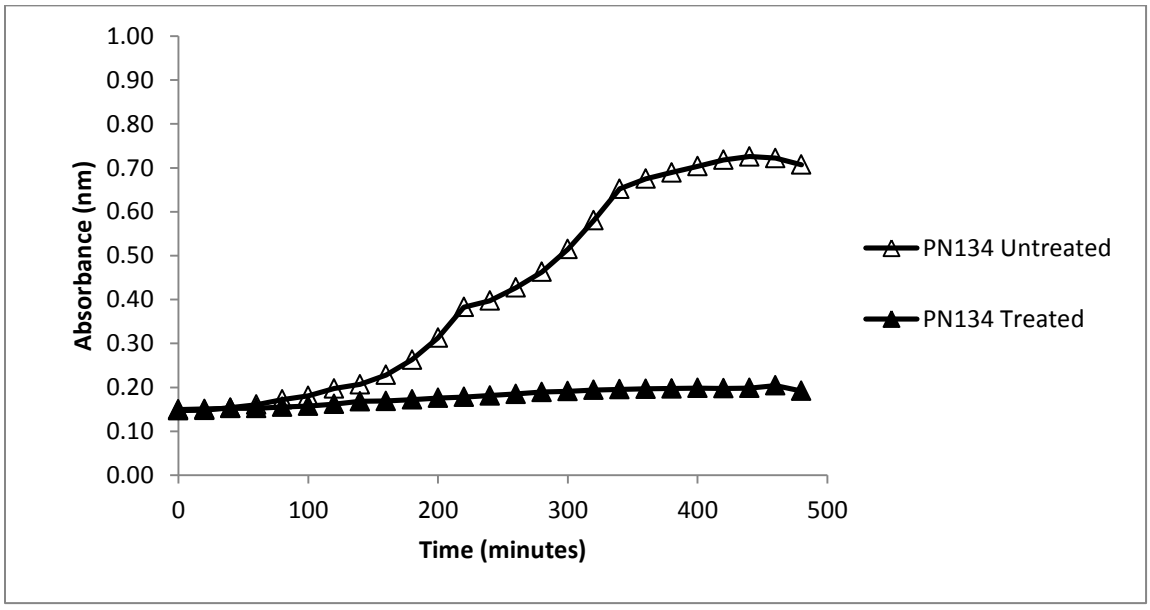

Figure 29. Growth Curve with Paraquat Treatment for the *E. coli* strain: PN134. The strain was grown in an LB media broth and aerated for 15 minutes before starting. Treated received paraquat after the 15 minutes of aeration. Measurements were taken using a UV/Vis platereader, at 670 nm wavelength, at a constant temperature of 37°C and samples were mixed continuously.

Cell viability using xanthine/Xanthine Oxidase at pH 7.5

In order to determine cell viability using the xanthine/xanthine oxidase assay, the SYTO9/ PI fluorescence assay was used. Fluorophore emissions were measured using a fluorescence microplate reader. Certain assay variables were changed to see the effects on cell viability, such as increased treated cell aliquot sizes (increased from 100 µM to 400 µM) (Figure 30-32), temperature changes (increasing the temperature from 4°C to 27°C during centrifuging and increasing xanthine solution storage temperature from 4°C to 27°C), and different centrifuging times (decreased from 9 to 5 minutes) (Figure 33-35).

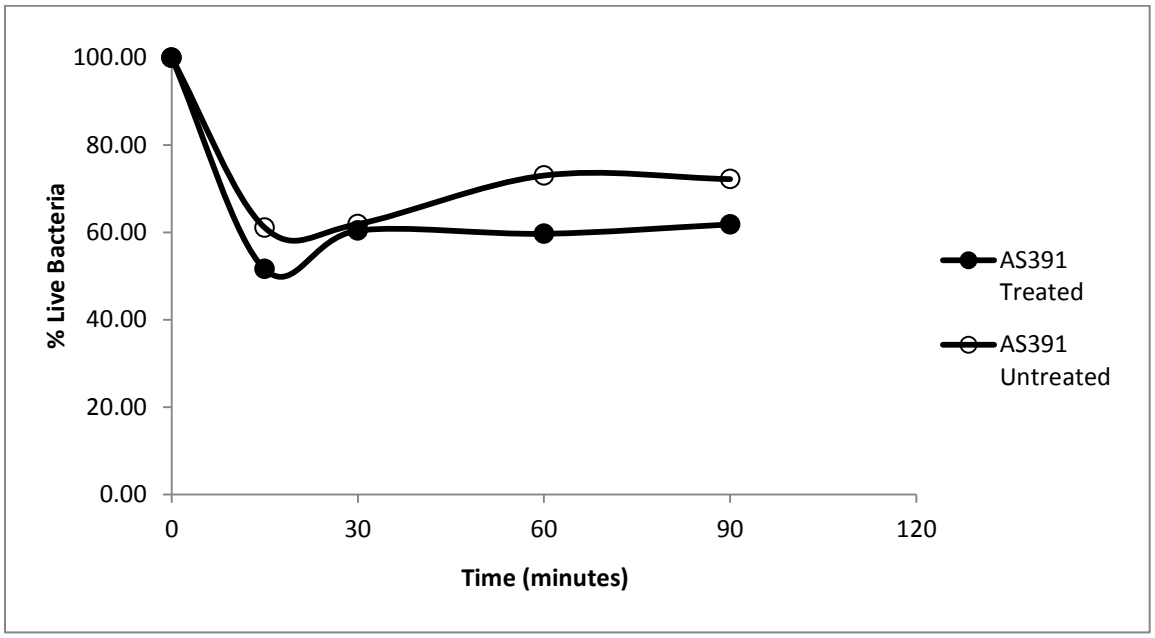

Figure 30. Effect of xanthine/xanthine oxidase treatment on the viability of AS391 at pH 7.5 (aliquot increases). Cells were harvested at stationary phase and resuspended in a potassium phosphate buffer which was adjusted to a pH of 7.5. Untreated and treated cells received 1 mL of xanthine solution. Treated cells received 100 µL xanthine oxidase while untreated received 100 µL H_2O. Viability was tested with the fluorescence assays.

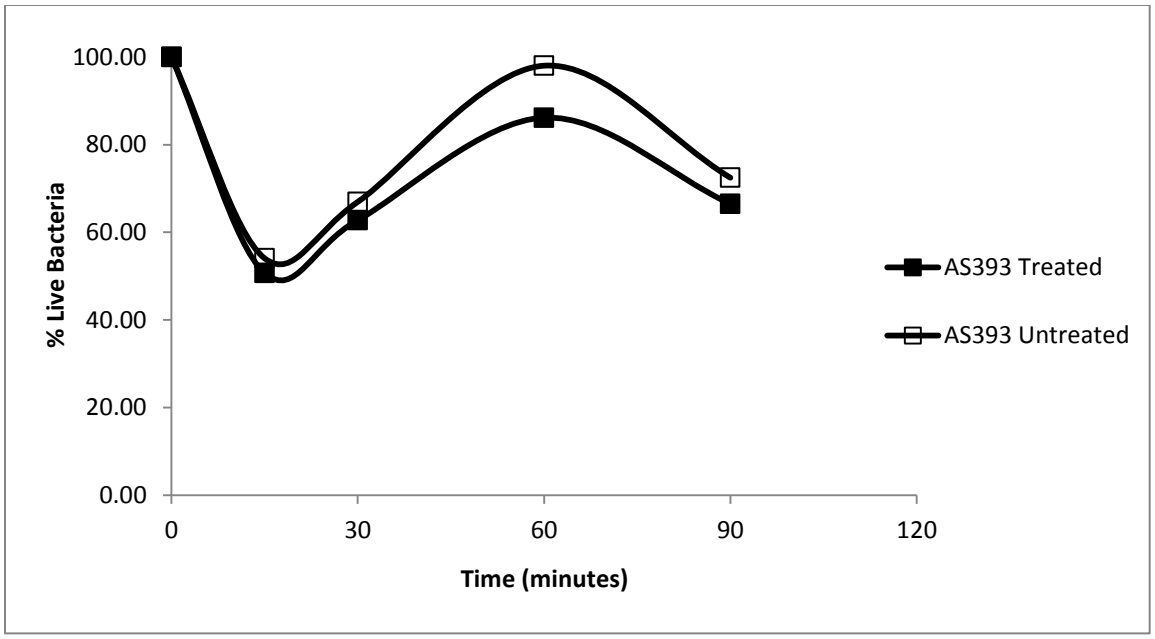

Figure 31. Effect of xanthine/xanthine oxidase treatment on the viability of AS393 at pH 7.5 (aliquot increases). Cells were harvested at stationary phase and resuspended in a potassium phosphate buffer which was adjusted to a pH of 7.5. Untreated and treated cells received 1 mL of xanthine solution. Treated cells received 100 µL xanthine oxidase while untreated received 100 µL H_2O. Viability was tested with the fluorescence assays.

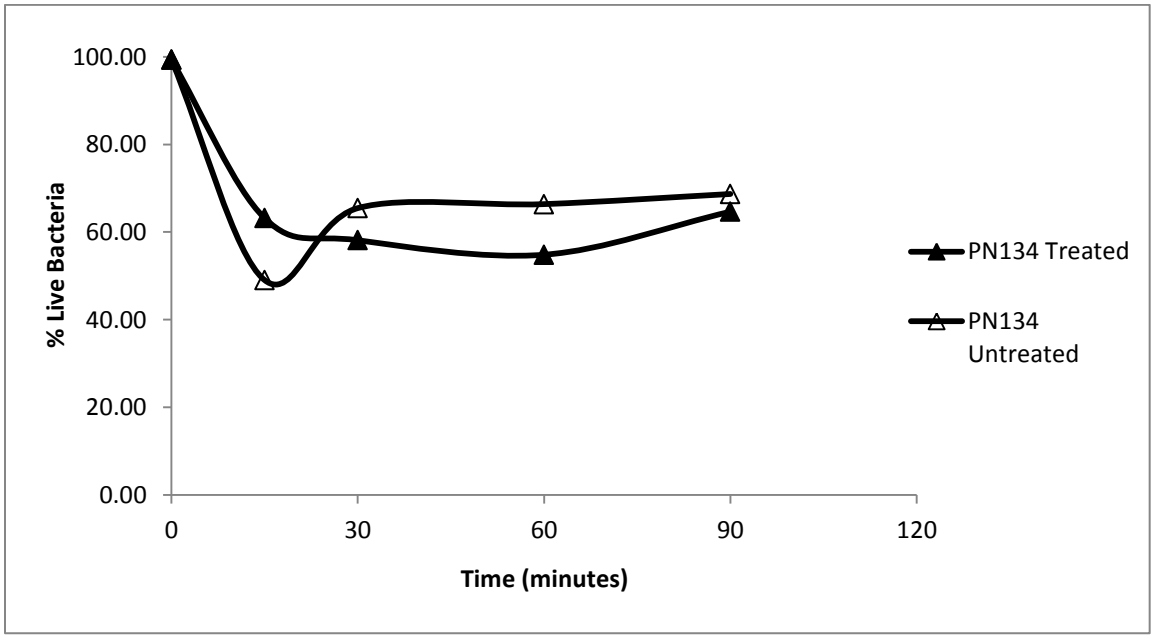

Figure 32. Effect of xanthine/xanthine oxidase treatment on the viability of PN134 at pH 7.5 (aliquot increases). Cells were harvested at stationary phase and resuspended in a potassium phosphate buffer which was adjusted to a pH of 7.5. Untreated and treated cells received 1 mL of xanthine solution. Treated cells received 100 µL xanthine oxidase while untreated received 100 µL H_2O. Viability was tested with the fluorescence assays.

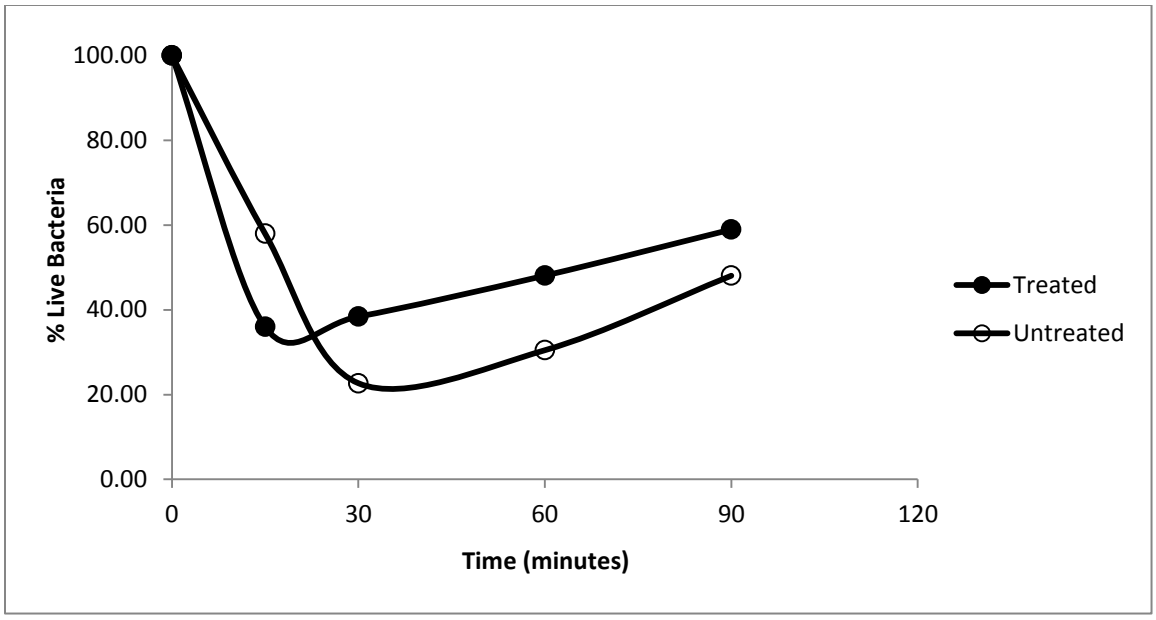

Figure 33. Effect of xanthine/xanthine oxidase treatment on the viability of AS391 at pH 7.5 (temperature/centrifuge changes). Cells were harvested at stationary phase and resuspended in a potassium phosphate buffer which was adjusted to a pH of 7.5. Untreated and treated cells received 1 mL of xanthine solution. Treated cells received 100 µL xanthine oxidase while untreated received 100 µL H_2O. Viability was tested with the fluorescence assays.

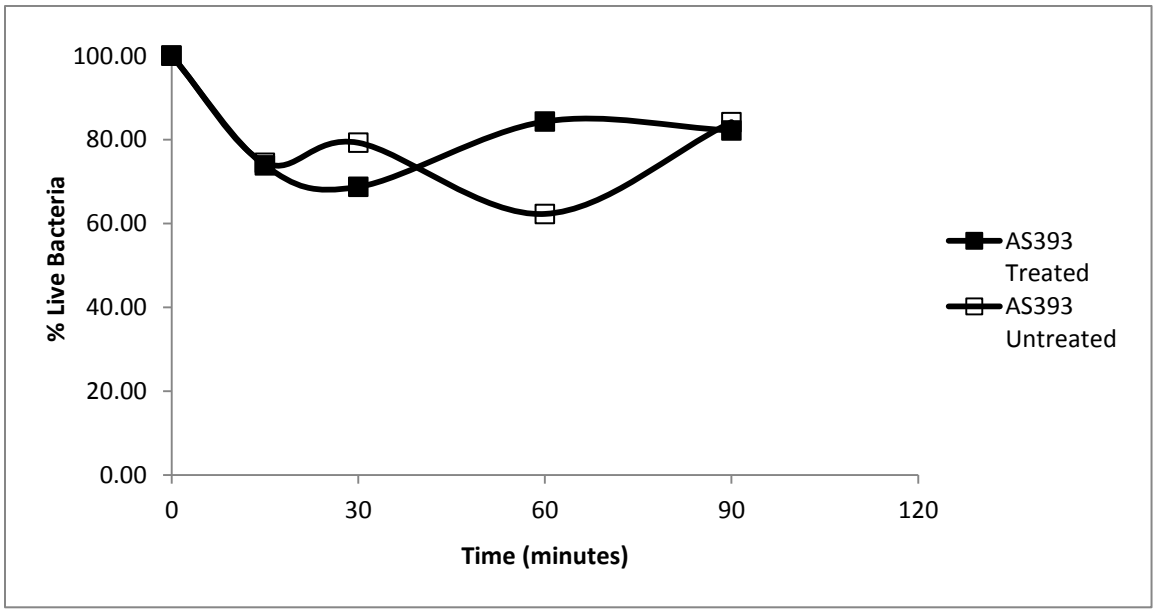

Figure 34. Effect of xanthine/xanthine oxidase treatment on the viability of AS393 at pH 7.5 (temperature/centrifuge changes). Cells were harvested at stationary phase and resuspended in a potassium phosphate buffer which was adjusted to a pH of 7.5. Untreated and treated cells received 1 mL of xanthine solution. Treated cells received 100 µL xanthine oxidase while untreated received 100 µL H_2O. Viability was tested with the fluorescence assays.

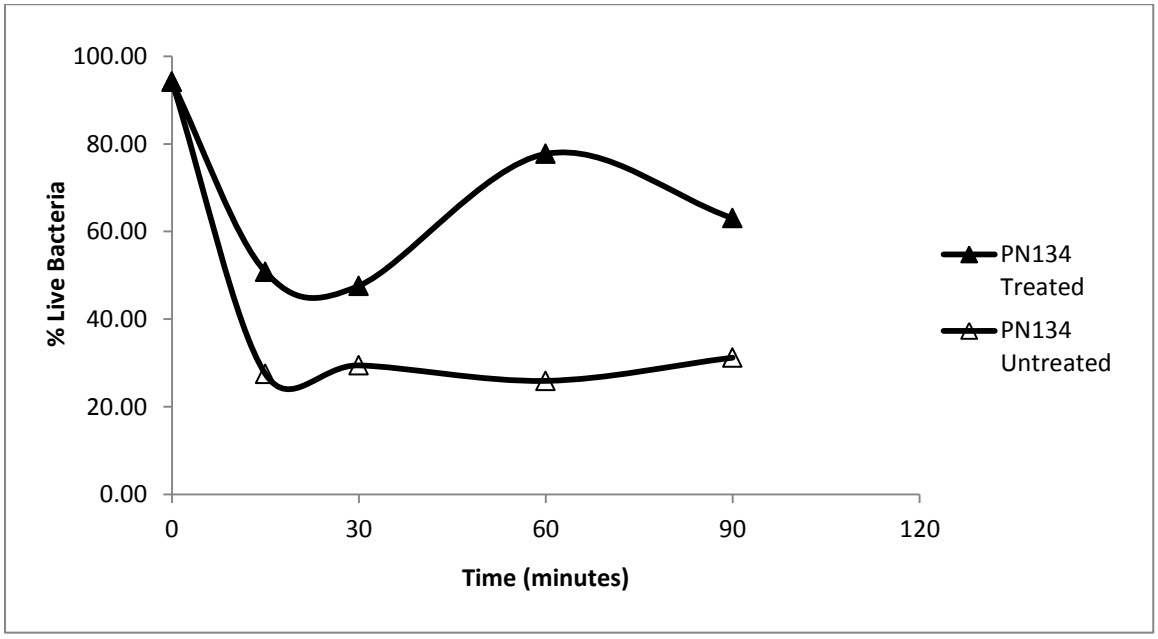

Figure 35. Effect of xanthine/xanthine oxidase treatment on the viability of PN134 at pH 7.5 (temperature/centrifuge changes). Cells were harvested at stationary phase and resuspended in a potassium phosphate buffer which was adjusted to a pH of 7.5. Untreated and treated cells received 1 mL of xanthine solution. Treated cells received 100 μL xanthine oxidase while untreated received 100 μL H_2O. Viability was tested with the fluorescence assays.

Cell viability of xanthine/Xanthine Oxidase at pH 6.5

Since the cell viability did not vary significantly at pH 7.5, the pH of the buffer solution was decreased to 6.5. The assay was performed several times with different results each time (Figures 36-38). To assess whether the cells were growing, the absorbance for each sample before the fluorophore emissions was measured (Figures 39-41).

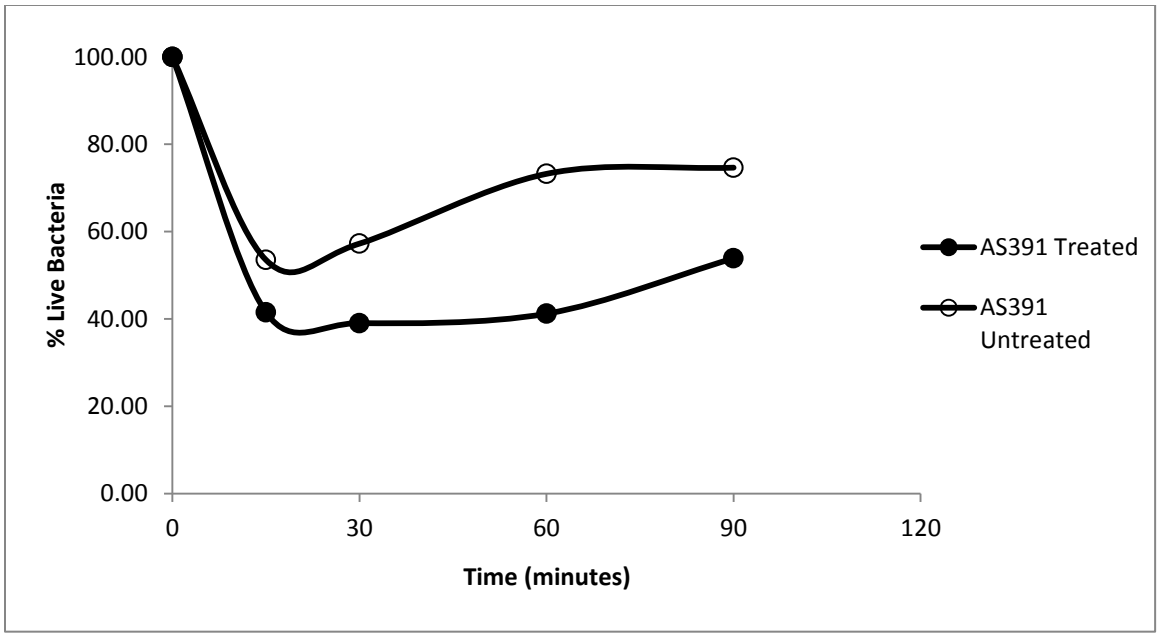

Figure 36. Effect of xanthine/xanthine oxidase treatment on the viability of AS391 at pH 6.5. Cells were harvested at stationary phase and resuspended in a potassium phosphate buffer which was adjusted to a pH of 6.5. Untreated and treated cells received 1 mL of xanthine solution. Treated cells received 100 µL xanthine oxidase while untreated received 100 µL H_2O. Viability was tested with the fluorescence assay.

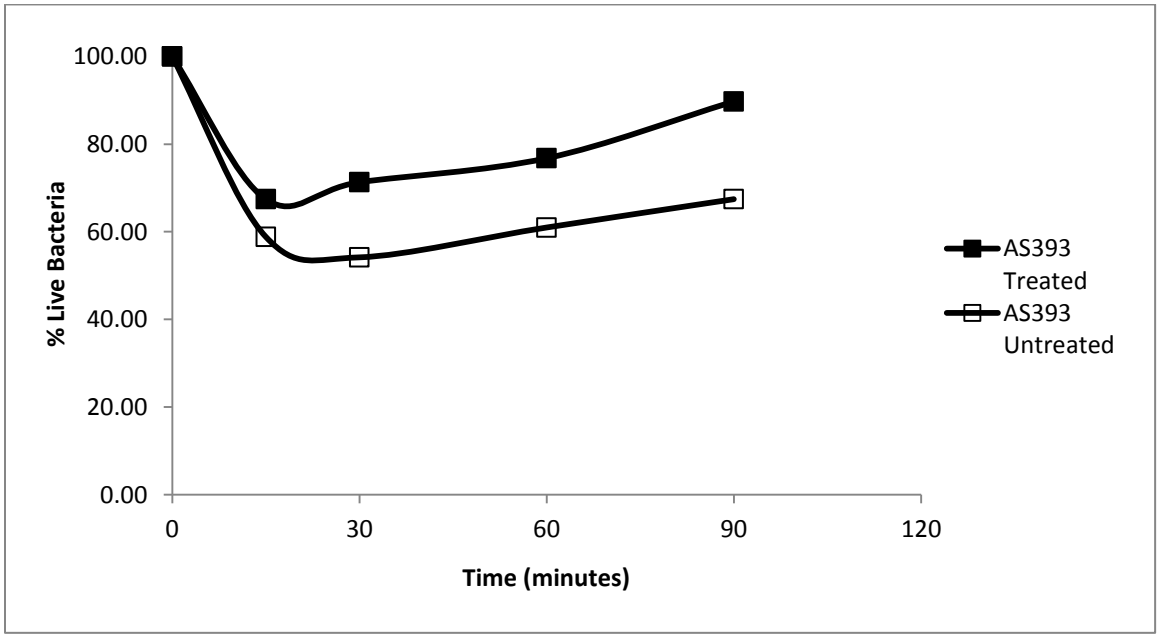

Figure 37. Effect of xanthine/xanthine oxidase treatment on the viability of AS393 at pH 6.5. Cells were harvested at stationary phase and resuspended in a potassium phosphate buffer which was adjusted to a pH of 6.5. Untreated and treated cells received 1 mL of xanthine solution. Treated cells received 100 µL xanthine oxidase while untreated received 100 µL H_2O. Viability was tested with the fluorescence assays.

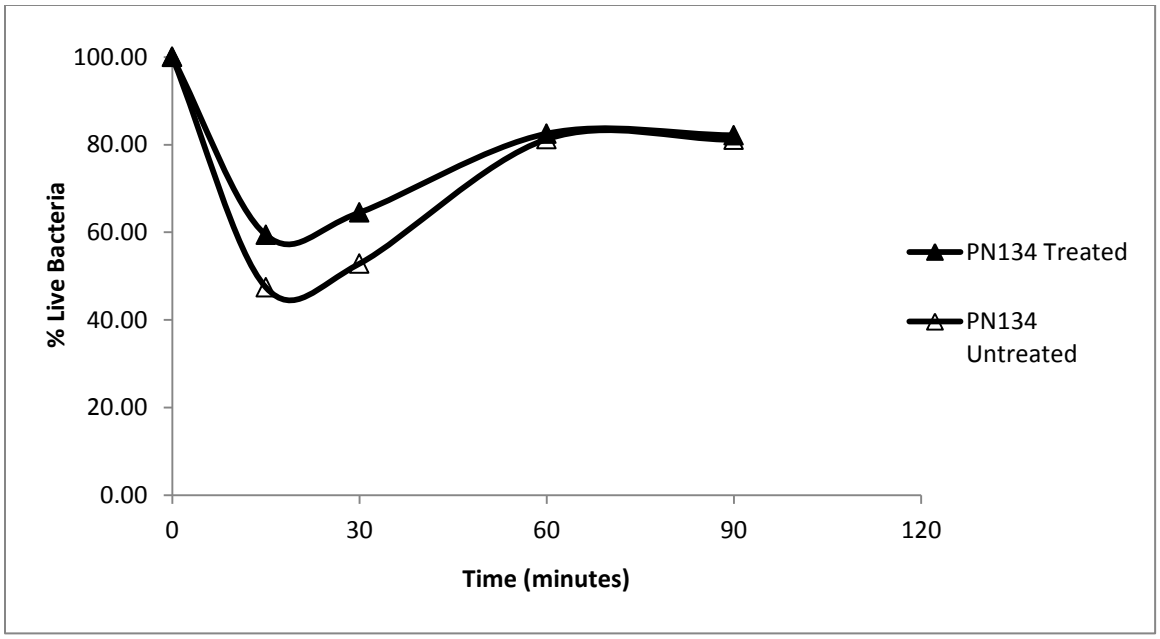

Figure 38. Effect of xanthine/xanthine oxidase treatment on the viability of PN134 at pH 6.5. Cells were harvested at stationary phase and resuspended in a potassium phosphate buffer which was adjusted to a pH of 6.5. Untreated and treated cells received 1 mL of xanthine solution. Treated cells received 100 µL xanthine oxidase while untreated received 100 µL H_2O. Viability was tested with the fluorescence assays.

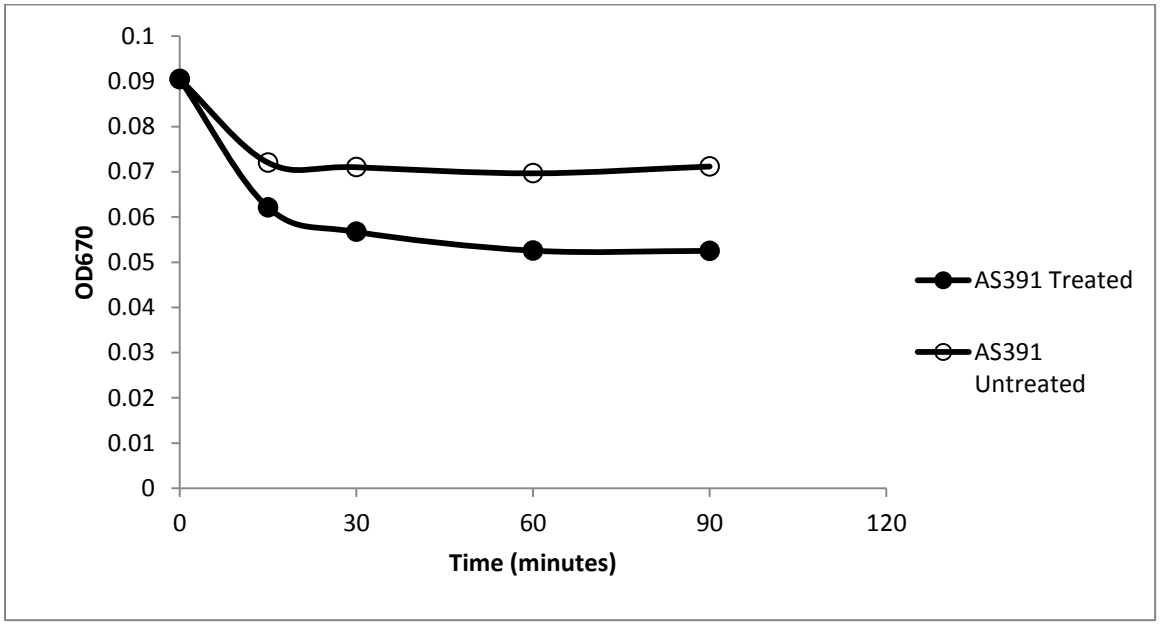

Figure 39. Optical Density for the *E. coli* strain AS391, prior to xanthine oxidase assay measurements. The strains were started 1 ½ hours after the start of the first strains and were grown for the appropriate time frame in an LB media broth at 37°C before use. The measurements were taken using a UV Vis microplate reader at the wavelength of 670 nm. Samples were taken from the xanthine oxidase reaction tubes and measured before undergoing centrifugation for the fluorescence assays.

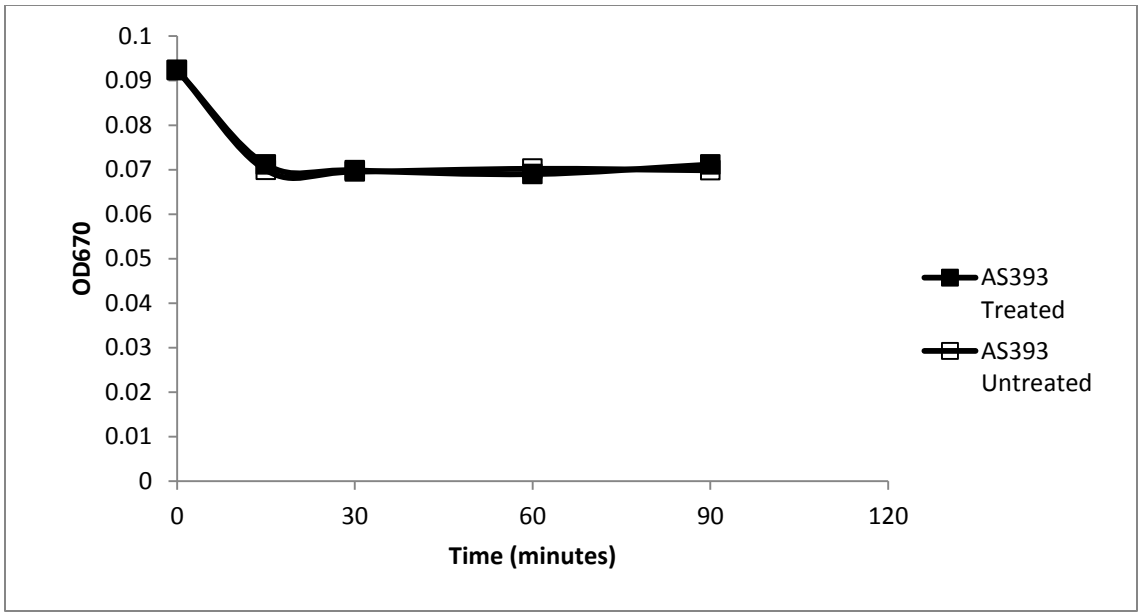

Figure 40. Optical Density for the *E. coli* strain AS393, prior to xanthine oxidase assay measurements. The strains were started 1 ½ hours after the start of the first strains and were grown for the appropriate time frame in an LB media broth at 37°C before use. The measurements were taken using a UV Vis microplate reader at the wavelength of 670 nm. Samples were taken from the xanthine oxidase reaction tubes and measured before undergoing centrifugation for the fluorescence assays.

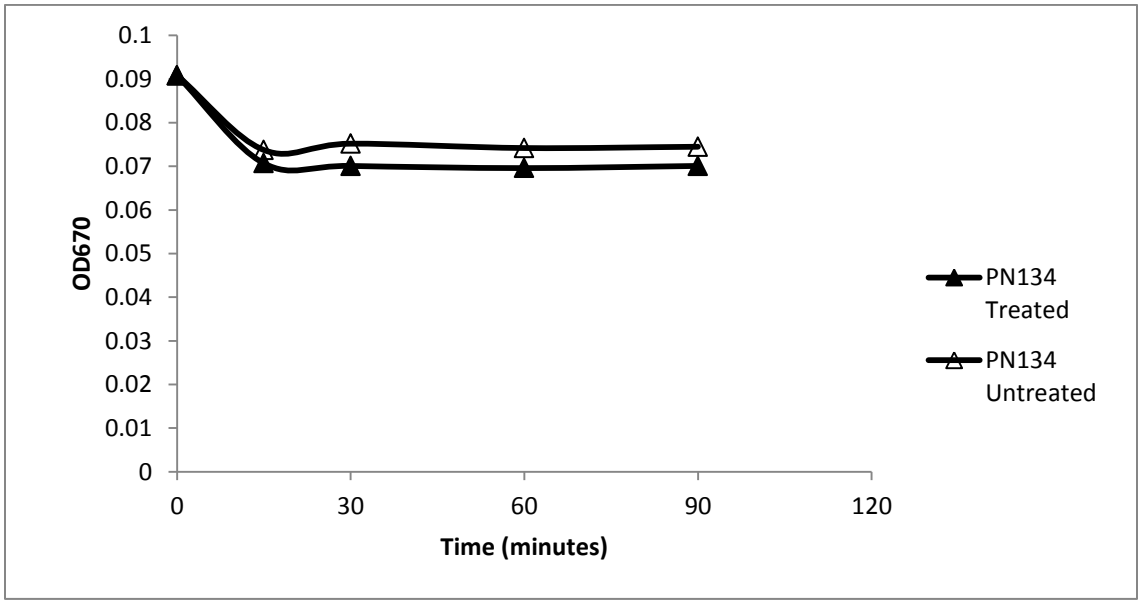

Figure 41. Optical Density for the *E. coli* strain PN134, prior to xanthine oxidase assay measurements. The strains were started 1 ½ hours after the start of the first strains and were grown for the appropriate time frame in an LB media broth at 37°C before use. The measurements were taken using a UV Vis microplate reader at the wavelength of 670 nm. Samples were taken from the xanthine oxidase reaction tubes and measured before undergoing centrifugation for the fluorescence assay.

APPENDIX B

Recipes:

Luria-Bertani Broth (LB)
Per Liter
Tryptone 10 g
Yeast extract 5 g
NaCl 5 g
H_2O to 1 L

Adjusted pH to 7.2 with 1 M NaOH

Luria-Bertani Plate Media (LB)
Per Liter
Tryptone 10 g
Yeast extract 5 g
NaCl 5 g
H_2O to 1 L
Agar 15 g

Adjusted pH to 7.2 with 1 M NaOH

Luria-Bertani Broth (LB) with Glucose
Per Liter
Tryptone 10 g
Yeast extract 5 g
NaCl 5 g
H_2O to 1 L
Supplemented with 0.2% (w/v) Glucose

Adjusted pH to 7.2 with 1 M NaOH

Luria-Bertani Plate Media (LB) with Glucose
Per Liter
Tryptone 10 g
Yeast extract 5 g
NaCl 5 g
H_2O to 1 L
Agar 15 g
Supplemented with 0.2% (w/v) Glucose

Adjusted pH to 7.2 with 1 M NaOH

Stab Agar
Per Liter
Tryptone 10 g
Yeast Extract 5 g
NaCl 5 g
Agar 6 g
Cysteine 10 mg
H_2O to 1 L

Adjusted pH to 7.2 with 1 M NaOH

Phosphate Buffered Saline (PBS)
Per Liter
NaCl 8 g
KCl 0.2 g
Na_2HPO_4 1.44 g
KH_2PO_4 0.24 g
H_2O to 1 L

Adjusted pH to 7.4 with 1 M NaOH

0.85% NaCl Solution
Per Liter
NaCl 8.5g
H_2O to 1 L

50 mM Potassium Phosphate Buffer
KH_2PO_4 3.4 g
H_2O to 500 mL

Adjust pH to 7.5 with 1 M KOH or pH 6.5 with 1 M HCl